REPORT DOCUMENTATION PAGE

AFRL-SR-AR-TR-02-

0254

1. AGENCY USE ONLY *(Leave blank)*	2. REPORT DATE	3. REPO
	23 JULY 2002	FINAL REPORT (15 JUN 1998 TO 29 DEC 2001)

4. TITLE AND SUBTITLE
POLYAZETES - TOWARDS HIGH ENERGY DENSITY MATERIALS

5. FUNDING NUMBERS
F49620-98-1-0483
62702E
G611/09

6. AUTHOR(S)
J. George Radziszewski

7. PERFORMING ORGANIZATION NAME(S) AND ADDRESS(ES)
Colorado School of Mines
Chemical Engineering & Petroleum Refining Dept.
Golden, CO 80401-1887

8. PERFORMING ORGANIZATION REPORT NUMBER

9. SPONSORING/MONITORING AGENCY NAME(S) AND ADDRESS(ES)
AFOSR/NL
801 N. Randolph Street Room 732
Arlington VA 22203-1977

10. SPONSORING/MONITORING AGENCY REPORT NUMBER

11. SUPPLEMENTARY NOTES

12a. DISTRIBUTION AVAILABILITY STATEMENT
Approved for public release; distribution is unlimited

12b. DISTRIBUTION CODE

13. ABSTRACT *(Maximum 200 words)*

We have investigated several ways to prepare and characterize spectroscopically novel compounds of pure nitrogen: tetrazete N4 and pentazole anion N5. They are of interest to DARPA/AFOSR as potential new high energy density materials (HEDM)s and attractive propellants. Results of earlier, extensive theoretical work (quantum mechanical computations) consistently suggest that tetrazete should be a metastable compound with decomposition barrier of 60 kcal/mol, and it should contain 180 kcal/mol of energy with respect to the two dinitrogen molecules. We have carefully scrutinized several methods to prepare tetrazete and for its subsequent detection we have employed a number of spectroscopic techniques. Microwave, electrical discharge of gaseous nitrogen or fast atom bombardment of nolid N2 (at 10 K) produces highly reactive neutral and charged nitrogen fragments: N-atoms, N3 radicals and variety of ions. Majority of them recombine among themselves to form back dinitrogen or react with always-present trace amounts of impurities (mostly oxygen atoms) to produce nitrogen oxides.

20020903 048

14. SUBJECT TERMS

15. NUMBER OF PAGES

16. PRICE CODE

17. SECURITY CLASSIFICATION OF REPORT	18. SECURITY CLASSIFICATION OF THIS PAGE	19. SECURITY CLASSIFICATION OF ABSTRACT	20. LIMITATION OF ABSTRACT

PREPARATION OF NOVEL POLYAZETES
FINAL TECHNICAL REPORT
PATENT AND FISCAL REPORT

Project funded by DARPA (*via* AFOSR)

Grant No. F49620-98-1-0483

Project duration: 06/01/1998 – 12/31/2001

Principal Investigator: J. George Radziszewski

Colorado School of Mines (and National Renewable Energy Laboratory)

Golden, CO 80401

Phone: (303) 275-3833; Fax: (303) 275-2905

E-mail: jradzisz@mines.edu

I. FINAL TECHNICAL REPORT

PREPARATION OF NOVEL POLYAZETES

SUMMARY

We have investigated several ways to prepare and characterize spectroscopically novel compounds of pure nitrogen: tetrazete N_4 and pentazole anion N_5^-. They are of interest to DARPA/AFOSR as potential new high energy density materials (HEDM)s and attractive propellants. Results of earlier, extensive theoretical work (quantum mechanical computations) consistently suggest that tetrazete should be a metastable compound with decomposition barrier of 60 kcal/mol, and it should contain 180 kcal/mol of energy with respect to the two dinitrogen molecules. We have carefully scrutinized several methods to prepare tetrazete and for its subsequent detection we have employed a number of spectroscopic techniques. Microwave, electrical discharge of gaseous nitrogen or fast atom bombardment of solid N_2 (at 10 K) produces highly reactive neutral and charged nitrogen fragments: N-atoms, N_3 radicals and variety of ions. Majority of them recombine among themselves to form back dinitrogen or react with always-present trace amounts of impurities (mostly oxygen atoms) to produce nitrogen oxides. In our experiments we have condensed such mixtures on the low-temperature (5.6 –20 K) spectroscopic targets (salt windows or Pt-plated cupper). We have observed in IR absorption and Raman spectroscopy many lines characteristic for such compounds. In addition, we have detected absorption lines in the positions that are highly compatible with signals predicted by high-level quantum mechanical calculations for tetrazete. Due to the high symmetry of N_4 only one IR absorption should be observable for a pure $^{14}N_4$ or $^{15}N_4$ isotopomers, making the convincing and unambiguous proof difficult on the basis of such observation alone. So far, we have not able to prepare samples of pure isotopomers concentrated enough for obtaining the clear-cut, reproducible Raman spectrum (that should contain 3 lines), nor samples of mixed $^{14\text{-}15}N_4$ isotopomers that should consist of multiple IR absorptions. The spectra that we were able to record although very encouraging suffer from lack of reproducibility and low signal-to-noise ratio. These basic findings were described in detail in our article in *Chem. Phys. Lett.* **2000**, *328*, 227. The by-product of these attempts: the detailed spectroscopy of all twelve possible isotopomers of N_2O (consisting of ^{14}N, ^{15}N, ^{16}O, ^{17}O, and ^{18}O atoms) has been published in *J. Chem. Phys.* **2001,** *115*, 1757.

Our extensive synthetic work aiming at the preparation of pentazole anion (N_5^-)did not yet produced desired compound. The work is still in progress. The results of our initial attempts were published this year in two papers: *Tetrahedron*, **2002**, *58*, 2085, and *J. Org. Chem.* **2002**, *67*, 1354. The third paper is in final stages of preparation and we intend to submit it to *JACS*.

I. FINAL TECHNICAL REPORT

PREPARATION OF NOVEL POLYAZETES

Below we describe our activities and present results of our effort during the 31/2 years of the project. Preparation of the new pure nitrogen compounds is excidingly difficult. We believe that we had made the first successful steps towards this goal. In the two main technical sections below we will describe separately work towards the tetrazete (N_4), and pentazole anion (N_5^-).

A. "Tetrazete - N_4" (Tetrazatricyclo[1.1.0.0]^{2,4}butane)

1. Background

Progress in the preparation of neutral, pure nitrogen compounds is measured in centuries. In 1890, 118 years after the original discovery of molecular dinitrogen,[1] the azide anion N_3^- was added to the short list of known pure polynitrogen species.[2] Subsequently, the N_3 radical and several ions like N_3^+, N_4^+ have been observed and characterized.[3-5] They play important roles in atmospheric chemistry, but they are all short living intermediates. Recent synthetic preparation[6] of N_5^+ promises to revitalize this seemingly stagnant area and is raising expectations for other startling discoveries.

Despite of ubiquitous presence of nitrogen in the atmosphere and in the vast majority of biological molecules, the early name for molecular nitrogen, *azote*, emphasizes its low reactivity and chemical inertness. The N≡N triple bond is one of the most stable chemical bonds, with a bond dissociation enthalpy of 228 kcal/mol. There are very few reactions in which nitrogen participates in its native and most abundant molecular form. In contrast, the only other known forms of neutral nitrogen, atomic N and N_3 radicals, are quite reactive.[7] Nitrogen atoms can be prepared in high yield (10^{19} atoms/(sr s)) by subjecting gaseous N_2 to electrical or microwave discharge.[8] However, the most common way of natural generation of reactive nitrogen is neither conductive coupling

(microwave irradiation) nor purely electrical ionization (atmospheric discharges) but the direct or multi-photon solar photolysis and electron impact dissociation of N_2.[9] The most frequent reactions of N atoms in the atmosphere are with oxygen, leading to the formation of NO, N_2O, NO_2, or higher oxides.

The results of advanced quantum mechanical calculations suggest that several additional neutral compounds of pure nitrogen are conceivable, such as the polyazetes N_4, N_6, and N_8.[10-16] In the last decade these species have been the object of intense computational scrutiny. Apart from purely cognitive curiosity, the motivation for these investigations undoubtedly lies in the potential utility of such compounds as highly energetic materials. The most advanced quantum chemical methods estimate tetrazete, N_4, to be a metastable tetrahedral molecule containing 185 kcal/mol of energy relative to two isolated N_2 molecules but residing in a potential well with a 60 kcal/mol barrier.[13] The energy diagram is presented in the figure below.

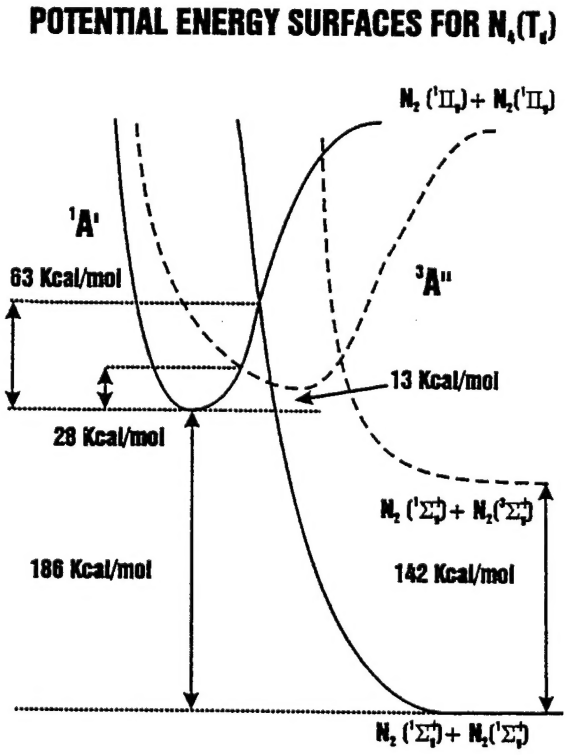

Figure. Energy diagram for tetrahedral (T_d) tetrazete N_4.

The predicted proximity of a dissociative triplet state may result in restricted utility of N_4 but it also could rule out the possibility of its preparation at all if the singlet-triplet crossing occurs deep in the well.[17] Still, the level of optimism generated by quantum chemists fuels experimental search for N_4 despite of such possible complications. The number of ways that might lead to N_4 is limited: in principle, for example, it can be assembled from reactions of N atoms with N_2 or the N_3 radical or fusion of two molecules of N_2; perhaps it could be extruded in excited state from larger polycyclic systems, in analogy with photochemical reactions observed for hydrocarbons.[18] The polyazete N_6 may be prepared by coupling of two N_3 radicals, and N_8 (azidopentazole) perhaps by reaction of yet unknown lithium pentazole with iodo azide.[19] They combine the promise of being attainable synthetic goals and highly energetic materials. The recent report of synthetic preparation of N_5^+ ion[6] by using delicate "wet" synthetic methods lends fresh credence for this effort.

The optimism among experimentalists with respect to the possible synthesis of N_4 was lately largely based on the theoretical prediction that the species should be sufficiently kinetically stable for experimental observation. Perhaps it is formed naturally during atmospheric electrical discharges, but is never accumulated, either due to low photochemical stability, or to the expected extremely high sensitivity towards moisture and oxygen, leaving virtually no traces of its intermediacy. This brings the question of how N_4 could actually be detected, if it is ever prepared in the laboratory. Before absolute proof for its existence can be produced by classical identification methods (NMR, elemental analysis, or X-Ray or neutron diffraction), experimental detection and initial recognition will have to relay on optical spectroscopy observations. Theoreticians tend to agree that N_4 in its lowest, metastable state will prefer tetrahedral geometry (point group T_d). Hence, it will have only one (t_2) vibrational mode weakly active in infrared absorption and three (e, t_2, a_1) vibrations active in Raman spectroscopy. The comparison of group theory and computational predictions for IR and Raman is presented below.

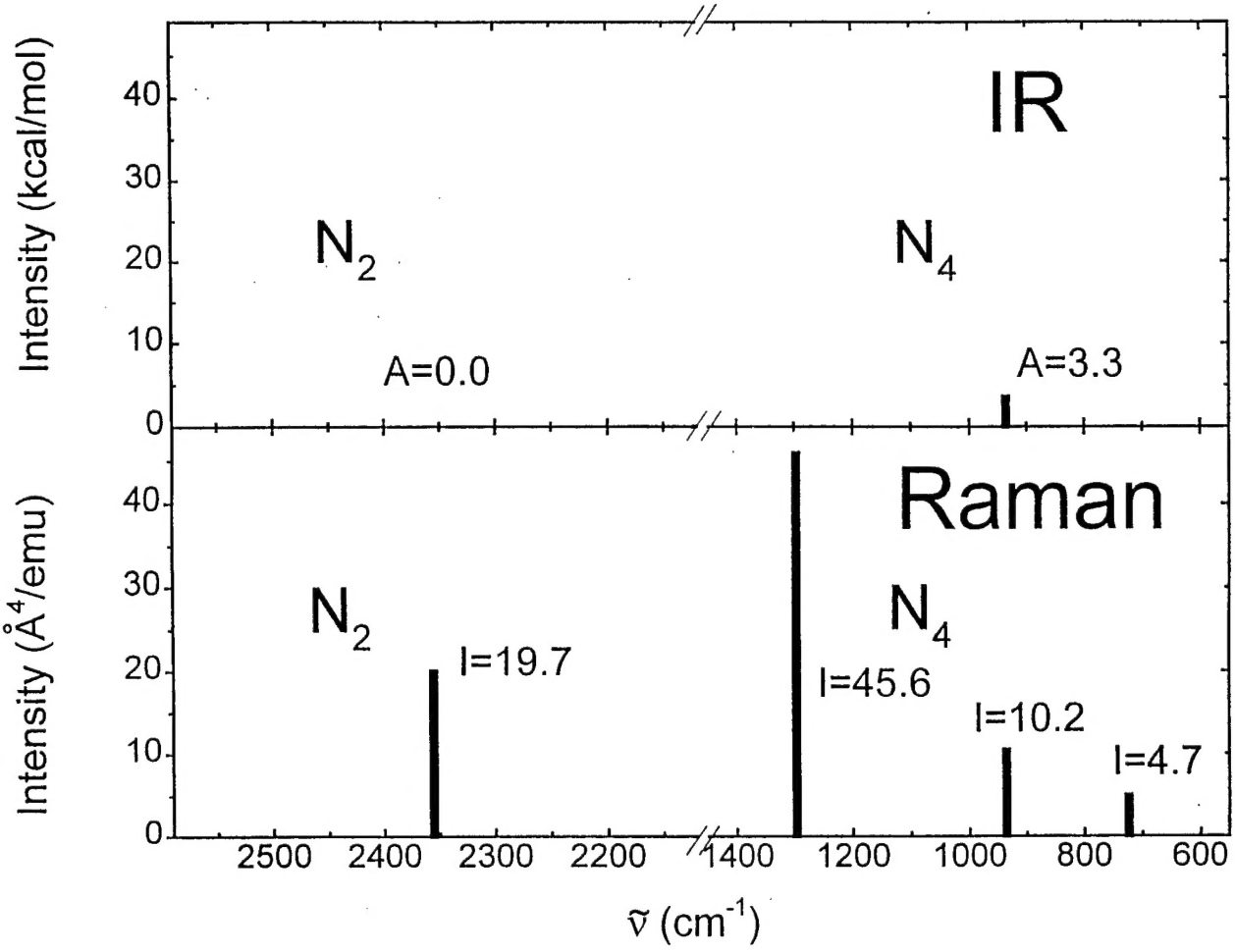

Figure. Comparison of calculated spectral activity in Raman scattering and infrared absorption for tetrahedral (T_d) tetrazete N_4.

Since the lowest optically allowed, excited electronic states are calculated about 10 eV above the ground state,[20, 21] electronic absorption or emission do not look very promising as initial detection methods.

2. Results and Discussion (Infrared absorption spectroscopy)

Attempts to produce N_4 by breaking the bond between the nitrogen atoms in the N_2 molecule have used the combination of photodissociation, microwave and electrical discharge techniques, performed in the gas and solid (low temperature matrix) phases for pure $^{14}N_2$, $^{15}N_2$, and for mixtures of the two isotopic species. The ensuing products were analyzed by their IR, Raman scattering, electronic absorption, luminescence and ESR spectra, recorded on the samples before, during and after N_2 dissociation. Unequivocal evidence for the production of neutral nitrogen atoms (N) was obtained directly from electron spin resonance (ESR) spectra, from the appearance of chemiluminescence from recombination of atomic nitrogen, and from the detection of various molecules, such as NO, N_2O, NO_2,N_3 and hydrazoic acid, HN_3. Analysis of the distribution of various isotopomers of the latter, obtained for the $^{14}N_2/^{15}N_2$ mixtures, revealed that the mechanism of HN_3 formation involves an attack of atomic nitrogen on the N_2 molecule. This may be the first step towards obtaining N_4. Indeed, a weak line was observed in the IR spectra at 937 cm^{-1} (903 cm^{-1} for $^{15}N_2$ substrate). Both the absolute position and isotopic shift are in excellent agreement with recent calculations for N_4 by Bartlett *et al.* However, these lines are often on the verge of the detection limit and, therefore, are not always reproducible. The low efficiency of the production of the species associated with the IR transition at 937 cm^{-1} is in line with the expected multi step nature of N_4 formation.

In our attempts to prepare N_4 we subject gaseous dinitrogen to microwave irradiation (see Experimental Section below). The resulting atomization of N_2 is followed by additional gas phase reactions involving atomic N, possibly including reactions induced by VUV photons emitted by the plasma. The reaction mixture is finally quenched on a

cold spectroscopic window (6.2-35 K). Nitrogen-matrix isolation of the products provides several useful advantages: Long lifetimes of the trapped species, ability to perform secondary photochemistry in a medium transparent for VUV radiation, as well as high simplicity of the well-resolved spectrum.

Apart from the inevitable lines due to the common impurities (CO_2, CO, H_2O, etc.) and trace amounts of nitrogen oxides (NO, N_2O, NO_2, etc., as compiled in the list below),

Spectral Features of Reference Compounds

H_2O	IR: 1597.1, 3634.9, 3727.3 (cm^{-1})
CO_2	IR: 667.2, 2349.1 (cm^{-1})
CO	2139.8 (cm^{-1})
NO	1874.9 (cm^{-1})
NH_3	971.4, 1632,2, 3332.7, 3440 (cm^{-1})
HN_3	607.1, 1291.4, 2235.6, 2575.9, 3493.4 (cm^{-1})
NO_2	746.7, 1314.2, 1615.7 (cm^{-1})
N_2O	585.8, 1281.2, 2217.2, 2557.6, 3471.4 (cm^{-1})
NH_2	IR: 1499.2, 3220.4, (cm^{-1}); UV: 343.8 nm
N_3	IR: 472.7, 1287.0, 1657.5 (cm^{-1}); UV: 273 nm
N_2	2328.3 (cm^{-1})
O_2	1548.9 (cm^{-1})
N atoms	emission: 523 nm ($^2D \rightarrow {}^4S$)
O atoms	emission: 556 nm ($^1S \rightarrow {}^1D$)

Figure. Partial list of the most prominent infrared absorptions of common impurities encountered in our work with nitrogen plasma.

careful inspection of the IR spectra recorded with the highest sensitivity arrangement available to us reveals a line at 936.7 cm^{-1} when $^{14}N_2$ is used in experiment (Fig. 1, bottom). No other absorption in the IR or UV-Vis spectra can be correlated with this line. On ^{15}N labeling 936.7 cm^{-1} line undergoes a shift to 900.0 cm^{-1} (Fig. 1, top of the lower part).

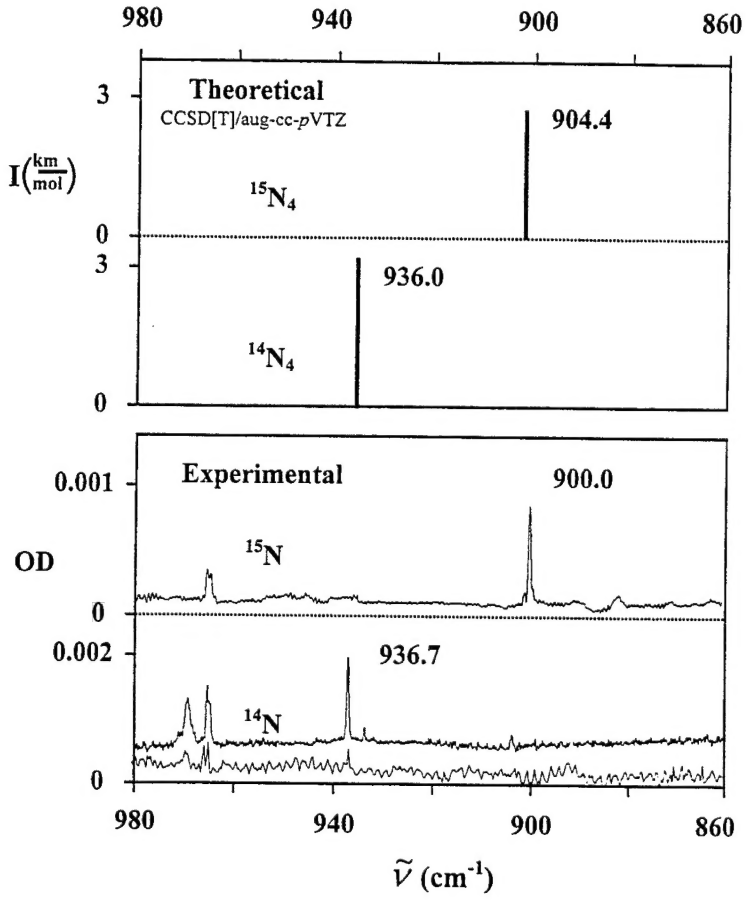

Figure. Observed IR absorption (lower set) from sample containing separately: $^{14}N_2$ (two separate experiments) and $^{15}N_2$ quenched plasma, and respective theoretical predictions (upper set). The peak at 969 cm^{-1} (bottom spectrum) belongs to NH_3 impurity and the unresolved doublet at 965 cm^{-1} (in both spectra) originates in O_4^-.

The calculated IR spectrum of $^{14}N_4$ (T_d) consists of a single line at 936.0 cm^{-1} with intensity equal to 3.4 km/mol (harmonic approximation; triply degenerate asymmetric NN stretch, t_2 symmetry species).[22] The line is predicted at 904.4 cm^{-1} in the $^{15}N_4$ species, with almost no change in intensity (Fig. 1, upper part). The theoretical predictions evidently support the assignment of the peaks observed at 936.7 cm^{-1} and 900.0 cm^{-1} to the IR active t_2 levels of tetrahedral $^{14}N_4$ and $^{15}N_4$. Unfortunately, this is not exactly a very fingerprint-like type of evidence. The visually very convincing evidence presented in figure above is by no means absolute. The observed lines are extremely weak, and there are many compounds with possible vibrations occurring in this spectral region. Our spectra can be reproduced only with great difficulty. In a few dozen of experiments with $^{14}N_2$ we were able to observe the 936.7 cm^{-1} absorption only 3 times, and only after very long spectral averaging (the recorded intensities were less than 0.01 optical density units). We have reproduced the $^{15}N_4$ line only once, and have so far been unable to observe $^{15}N^{14}N$ multiplets expected in experiments with $^{15}N/^{14}N$ mixtures. In spite of numerous attempts, we have so far been unable to correlate the intensity changes of the 937 cm^{-1} signal with any of the simple adjustable experimental parameters (N_2 flow rate, microwave power, deposition window temperature, amount of direct sample illumination by plasma emissions, etc.).

The 937 cm^{-1} line is apparently split into a doublet (Figure above). The splitting can possibly be explained by the trapping of N_4 in two different sites. Removal of a pair of neighboring N_2 molecules from solid state α-N_2 (the allotrope prevailing at low temperature) produces a cavity with two diastereomerically different sites. The difference vanishes by transition to the β-N_2 allotrope, which would explain the disappearance of the splitting on heating.

Assignment of the 937 and 900 cm^{-1} lines to $^{14}N_4$ and $^{15}N_4$ implies a very large isotope effect. Might these line be due to ^{14}N and ^{15}N isotopomers of another

compound than tetrazete? An isotopic shift from 937 to 900 cm^{-1} would imply that the nitrogen atom in the unknown compound participates strongly in the vibration (as, for instance, a shift from 918 to 907 cm^{-1} in S=Si=S upon $^{28}Si \rightarrow {}^{29}Si$ substitution is considered[23] as evidence of a large involvement of silicon in the vibration). If we treat our unknown species as a pseudo-diatomic molecule, consisting of a vibrating nitrogen atom and a pseudo-atom of mass *s*, the ratio of the reduced masses upon $^{14}N \rightarrow {}^{15}N$

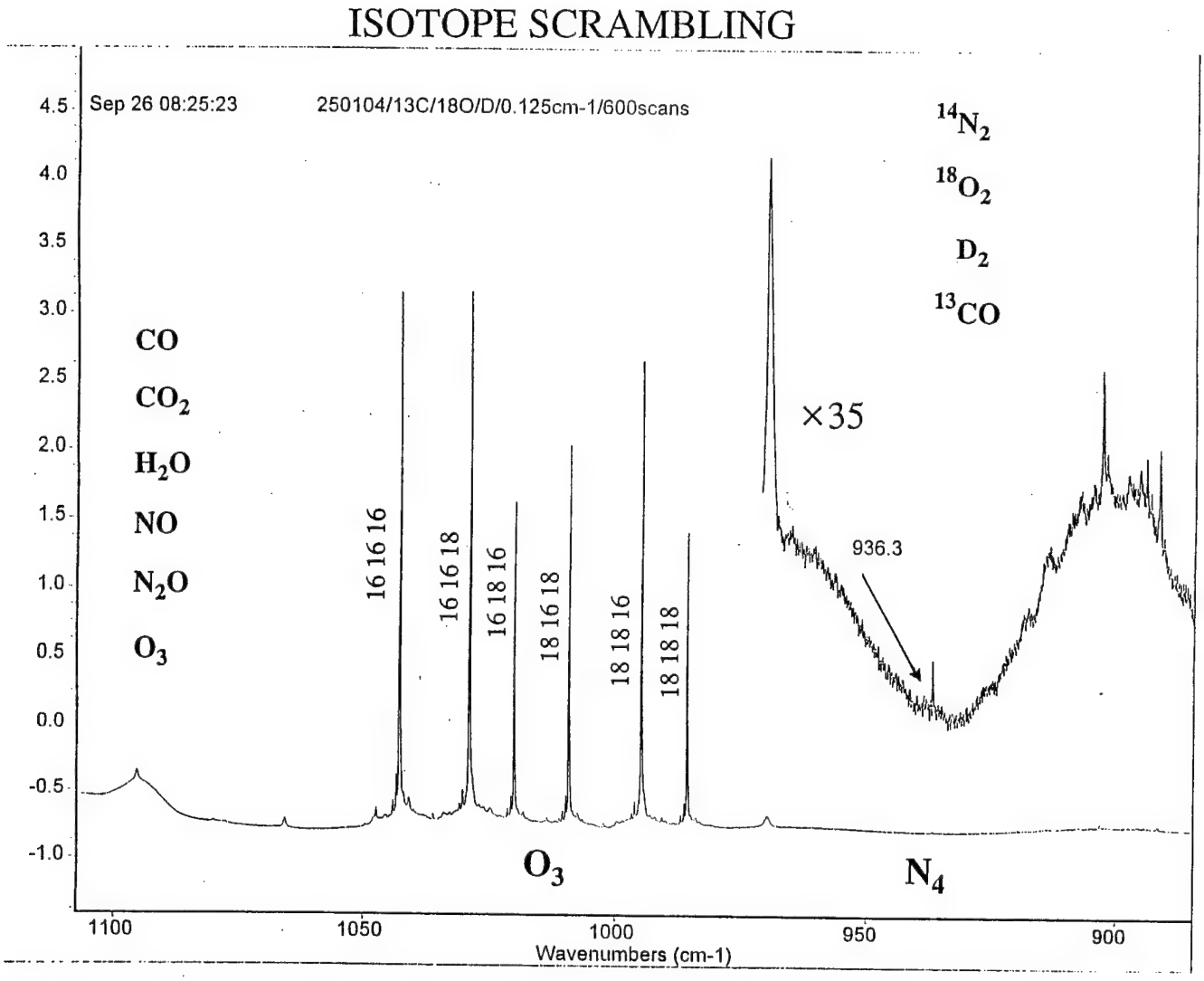

Figure. Isotopic scrambling by microwave discharge.

substitution would be equal to $\mu_2/\mu_1 = (1/s + 1/14)/(1/s + 1/15)$. This ratio can be experimentally estimated as $\left(\tilde{\nu}_1 / \tilde{\nu}_2\right)^2$, where $\tilde{\nu}_1$ and $\tilde{\nu}_2$ are the wavenumbers for the ^{14}N- and the ^{15}N-containing compounds. Solving the equation for $\left(\tilde{\nu}_1 / \tilde{\nu}_2\right)^2 = (937/900)^2 = 1.084$ yields a negative s value without physical meaning. On the other hand, if the molecule is built entirely of nitrogen atoms, the value of s changes after $^{14}\text{N} \rightarrow {}^{15}\text{N}$ substitution from 42 to 45 and the ratio μ_2/μ_1 is now equal to 15/14 = 1.071, which close to the observed value $\left(\tilde{\nu}_1 / \tilde{\nu}_2\right)^2 = 1.084$. This strongly supports the assignment of the 937 cm^{-1} line to tetrazete. In addition, the assignment is supported by the experimental observation of a lack of isotopic shift upon adding ^{18}O (from $H_2{}^{18}O$) or ^{13}C (from ^{13}CO) to the sample, which makes the presence of oxygen or carbon in the molecule very improbable. The figure on the previous page presents a part of the spectrum when such isotopic species were intentionally introduced , and were "scrambled" by microwaves into the products.

As discussed above, the experiments reveal a vibrational line at 937 cm^{-1} which is best explained as originating in N_4, especially because the observed shift for ^{15}N is in excellent agreement with theoretical predictions. Conclusive arguments for the assignment may be provided by using mixtures of ^{14}N and ^{15}N. A total of five different isotopomers are possible: $^{14}N_4$, $^{14}N_3{}^{15}N$, $^{14}N_2{}^{15}N_2$, $^{14}N{}^{15}N_3$, and $^{15}N_4$.

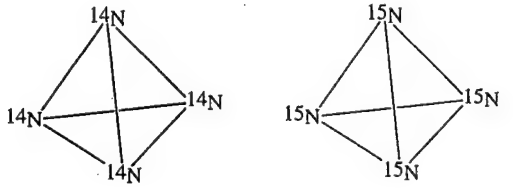

T_d (1 band; t_2)

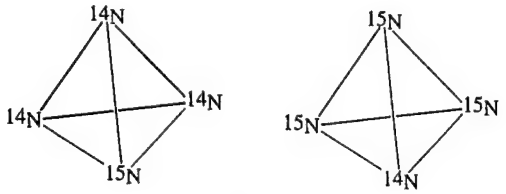

C_{3v} (2 bands; a_1, e)

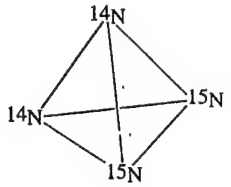

C_{2v} (3 bands; a_1, b_1,b_2)

The triple degeneracy will be lifted for the three mixed species, leading to characteristic multiplet patterns in the IR spectrum. For $^{14}N_3{}^{15}N$ and $^{14}N^{15}N_3$species we will have: $T_d \rightarrow C_{3v} \Rightarrow\ t_2 \rightarrow a_1 + e$, and for $^{14}N_2{}^{15}N_2$ species: $T_d \rightarrow C_{2v} \Rightarrow t_2 \rightarrow a_1 + b_1 + b_2$. In the ensuing analysis we shall assume that the relative IR intensities of the split components are 1:2 and 1:1:1, respectively.

Let us consider three possible cases, each leading to the production of N_4. Let us assume that the substrate is a mixture of $^{14}N_2$ (molar fraction f) and $^{15}N_2$ (molar fraction $1-f$).

Case 1. N_4 is formed from two nitrogen molecules: $N_2 + N_2 \rightarrow N_4$. In this case, three different species could be formed: $^{14}N_4$, $^{14}N_2{}^{15}N_2$, $^{15}N_4$. A general formula for the ratios of reaction yields (φ) is:

$$\varphi(^{14}N_4) : \varphi(^{14}N_2{}^{15}N_2) : \varphi(^{15}N_4) = f^2 : 2f(1-f) : (1-f)^2$$

For a 1:1 mixture of $^{14}N_2$ and $^{15}N_2$ ($f = 1\text{-}f = 0.5$) a 1:2:1 population ratio is expected. In the IR spectrum not three, but five lines should be observed. This is due to the fact that in $^{14}N_2{}^{15}N_2$ the vibration is no longer degenerate because of lower symmetry. Thus, for a 1:1 mixture of $^{14}N_2$ and $^{15}N_2$, the expected pattern of IR peaks for the product mixture is a quintet with intensity ratios: 1:(2/3):(2/3):(2/3):1, as indicated in the diagram below.

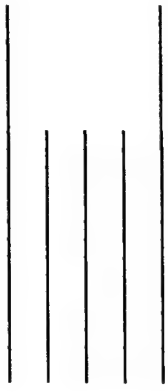

Case 2. N_4 is produced from one nitrogen molecule and two N atoms: $N_2 + N + N \rightarrow N_4$. All five different isotopomers can now be formed: $^{14}N_4$, $^{14}N_3{}^{15}N$, $^{14}N_2{}^{15}N_2$, $^{14}N^{15}N_3$, and $^{15}N_4$. The ratio of reaction yields (φ) is:

$$\varphi(^{14}N_4) : \varphi(^{14}N_3{}^{15}N) : \varphi(^{14}N_2{}^{15}N_2) : \varphi(^{14}N^{15}N_3) : \varphi(^{15}N_4) =$$
$$f^3 : 2f^2(1-f) : \{f(1-f)^2 + f^2(1-f)\} : 2f(1-f)^2 : (1-f)^3$$

The specific case of a 1 : 1 mixture should lead to a 1:2:2:2:1 pattern. Symmetry lowering in $^{14}N_3{}^{15}N$, $^{14}N^{15}N_3$ leads to the splitting of a triply degenerate vibration into a non-degenerate and a doubly degenerate one. The expected pattern of IR peaks is now a nonet, with intensity ratios: 1:(4/3): (2/3): (2/3): (2/3): (2/3): (2/3): (4/3):1. This is obtained under assumption, based on the results of calculations, that the doubly degenerate vibration is higher in energy in $^{14}N_3{}^{15}N$ than the non-degenerate one, while it is lower in energy for $^{14}N^{15}N_3$. For the opposite situation, the two (4/3): (2/3) ratios in positions 2 and 4 and 6 and 8 should be inverted.

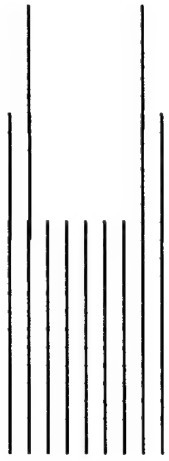

Case 3. Now we assume that N_4 is formed from nitrogen atoms: $N + N + N + N \rightarrow N_4$. As in the previous case, five species should be detected: $^{14}N_4$, $^{14}N_3{}^{15}N$, $^{14}N_2{}^{15}N_2$, $^{14}N^{15}N_3$, $^{15}N_4$, with relative yields:

$$\varphi(^{14}N_4) : \varphi(^{14}N_3{}^{15}N) : \varphi(^{14}N_2{}^{15}N_2) : \varphi(^{14}N^{15}N_3) : \varphi(^{15}N_4) =$$

$$f^4 : 4f^3(1-f) : 6f^2(1-f)^2 : 4f(1-f)^3 : (1-f)^4$$

For a 1:1 mixture this leads to: 1:4:6:4:1 yield ratios. As in case 2, a nonet is expected in the IR spectrum, this time, however, with different intensity ratios:
1: (8/3): 2 : (4/3) : 2: (4/3) :2: (8/3) : 1 (the same assumption as in the previous case was made regarding the energy ordering in $^{14}N_3{}^{15}N$ and $^{14}N^{15}N_3$).

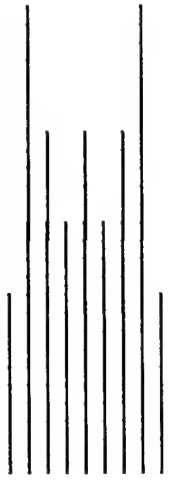

It can be seen from the above that a large difference is to be expected for the isotopic mixtures of $^{14}N_2$ and $^{15}N_2$ with respect to a "simple" behavior predicted for pure isotopes. In reality, the experimental pattern observed in the mixtures may be even more complex, due to possible accidental degeneracies, and site splittings and to the fact that the reaction may proceed according to more than just one mechanism. Therefore, while the observation of the splitting should provide a very convincing argument for the presence of tetrazete, the definitive conclusions regarding the mechanism of its formation may be much harder to reach.

Recently, we were able to prepare a sample "microwaved" from 1:1 mixture of $^{14}N_2$ and $^{15}N_2$. It clearly exhibits complex multiplex in the expected spectral region

between 937 cm^{-1} and 900 cm^{-1}(see figure below). The spectrum is very week and has not yet been reproduced. We are still continuing searching for the ways to acquire this critical piece of information.

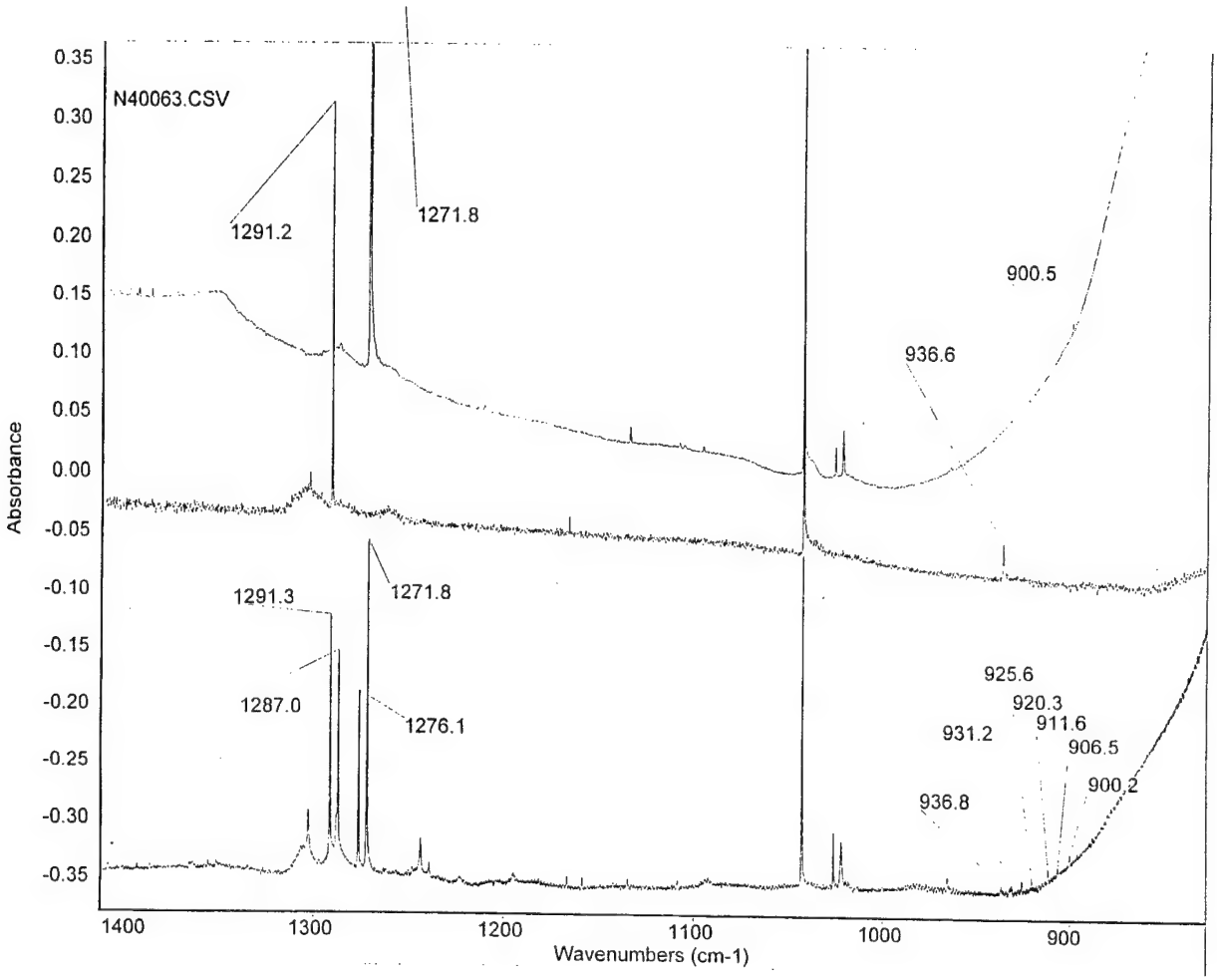

Figure. Experimental infrared absorption patterns from plasma produced by microwave discharge) from 1:1 mixture of $^{14}N_2$ and $^{15}N_2$ and quenched at 6.7K (bottom trace). Similar spectra obtained from pure $^{14}N_2$ (middle trace) and from pure $^{15}N_2$ (top trace).

3. Fast Atom Bombardment (FAB) Experiments

The N_4: we have investigated broad range of varying experimental conditions of generation of nitrogen fragments using Fast Atom Bombardment (FAB), mostly of solid nitrogen substrate bombarded by N atoms but we have also looked at nitrogen matrices bombarded with Ar, Ne, Kr and Xe. In some experiments we have combined FAB with uv-irradiations. Various charged and neutral species were generated and observed. Unfortunately, not even traces of the signals previously assigned to N_4 were detected. The by-product of these attempts: the detailed spectroscopy of all twelve possible isotopomers of N_2O (consisting of ^{14}N, ^{15}N, ^{16}O, ^{17}O, and ^{18}O atoms) has been published [*J. Chem. Phys.* **2001,** *115*, 1757].

4. Other attempts to prepare and collect tetrazete

We have investigated several other ways to obtain larger quantities (or concentrations) of N_4. We have made several attempts at purely photochemical ways utilizing resonance vacuum ultraviolet radiation from Kr lamp or from other noble gasses (Xe, Ne) discharge to illuminated solid nitrogen. No N_4 was observed in these experiments.

In other approach, the microwave set-up was attached to the helium cryostat operating at temperatures above the melting point of dinitrogen, in the recirculating arrangement. There was a small pump in the loop, attached next to the cryostat, and pumping the nitrogen back to the plasma discharge zone. The cryostat was fitted with the salt window (BaF2), and kept in the FTIR to allow the constant monitoring of the condensed on the cold window products. We made several runs of this setup lasting between 4 and 60 hours. Despite of using all kinds of provisions (baking under high vacuum, additional liquid nitrogen traps, commercial highly efficient oxygen and water absorbers, we were not able to remove the traces of water from the setup and end up with condensing on our window water and various oxides of nitrogen, but never detecting N_4.

In a modified set-up, where we used high current electrical discharge in the old Kr laser tube (rather than microwave discharge), also in re-circulating mode we have obtained similar results.

5. Raman Spectroscopy of N_4

We put a serious effort into the application of Raman spectroscopy for detection of tetrazete. We have acquired (with the help of DURIP funds) components of Raman setup, designed and built a unique instrument for cryogenic Raman work. Despite of the general weakness of Raman effect this spectroscopy is a method of choice for scrutinizing highly symmetrical, homonuclear species, like N_4 since they exhibit large changes of polarizibility along the normal coordinates directly related to Raman activity. For the tetrahedral (T_d) N_4 three vibrational transitions [at 724 cm^{-1} (e, I = 9.4 $Å^4$/amu), 936 cm^{-1} (t_2, I = 30.6 $Å^4$/amu) and 1296 cm^{-1} (a_1, I = 45.7 $Å^4$/amu)] are predicted to be active in Raman [*vs.* one in IR, calculated at 936 cm^{-1}(t_2, I = 3.3 km/mol)]. Raman spectra thus could provide independent confirmation for IR findings and should allow unique fingerprinting and definitive identification of N_4.

We were hoping that very short wavelength excitation at 227, 244, 257 (intracavity-doubled Ar-ion laser fundamentals), or at 356 nm (Ar-ion fundamental) would lead to greatly enhanced strength of Raman signal (ν^4 advantage; nearly **two orders** of magnitude for 356 nm in comparison with 1064 nm!), and provide a shift from obstructive luminescence in visible (towards its red end). Both fluorescence and phosphorescence (from ever present traces of impurities) should appear at much longer wavelength than Raman signals.

In our laboratory we use the best, ultrahigh sensitivity UV enhanced, back-thinned CCD detector chip (4080 by 800 pixels) and large solid angle light collection. We have substantial experience with measuring very difficult cryogenic matrix Raman of reactive intermediates (carbon analogues of N_4: cyclobutadiene and tetrahedranes).

In this project we devoted the major fraction of available resources to utilize this technique. We did sensitivity testing using natural abundance on ^{15}N in our dinitrogen samples. The figure below clearly demonstrates that quite small quantities of the nitrogen species can be recorded with our setup.

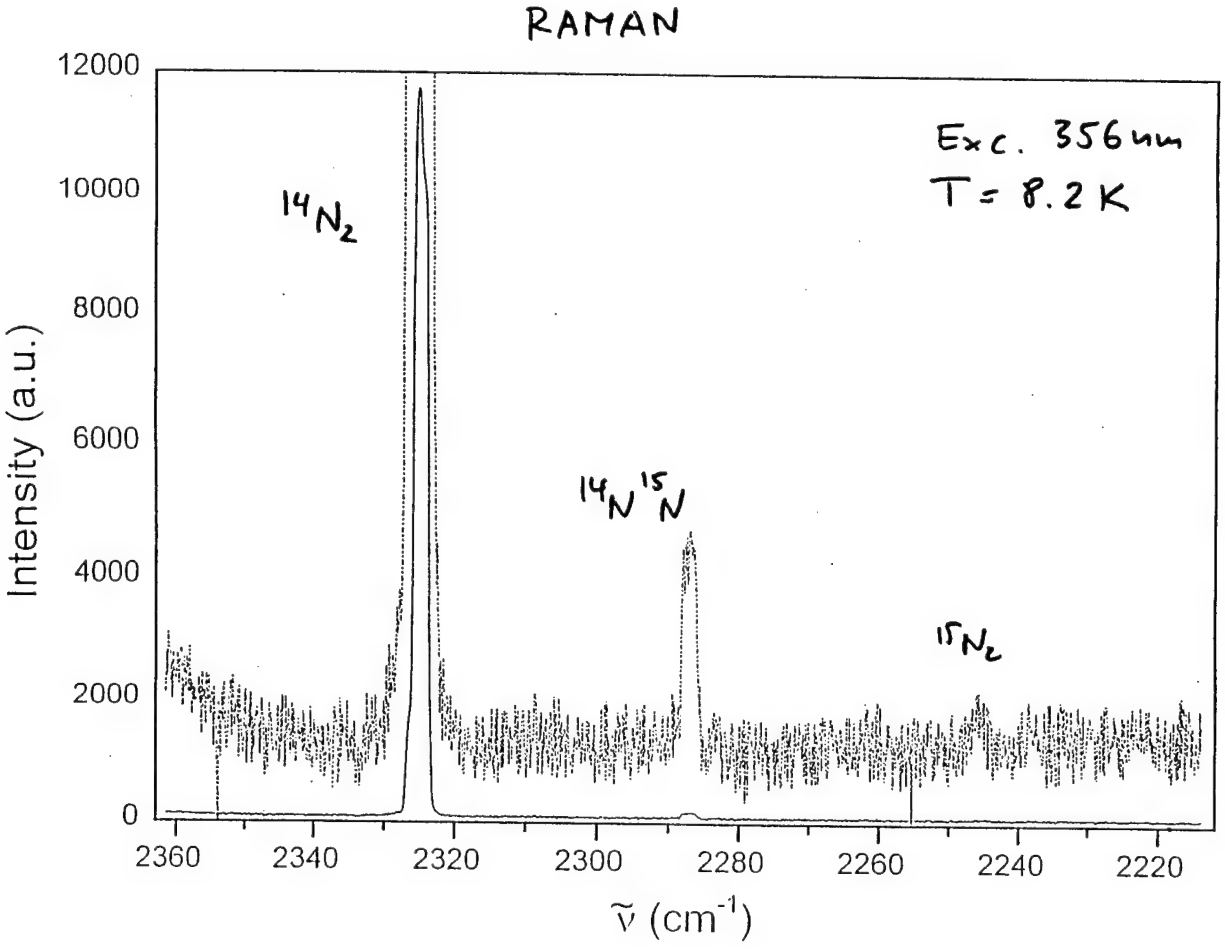

Figure. Segment of the Raman spectrum in the region of symmetric stretch of dinitrogen $^{14}N_2$ at 2326 cm^{-1} (solid line). The dotted line presents the same spectrum magnified 50 times. Now the natural abundance of ^{15}N in the Raman line at 2288 cm^{-1} of dinitrogen $^{15}N^{14}N$ is clearly visible as is most likely the line from $^{15}N2$ at 2247 cm^{-1}. Excitation is at 356 nm (Ar-ion laser). The solid sample at 8.2K is kept on a cold tip attached to closed-cycle helium cryostat

But despite of this high sensitivity available it was very difficult to make the convincing assignments of the lines from our samples containing exceedingly small amounts of species presumed to be N_4. We had recorded several weak signals in the positions expected (calculated) for N_4, and some representative traces are shown below.

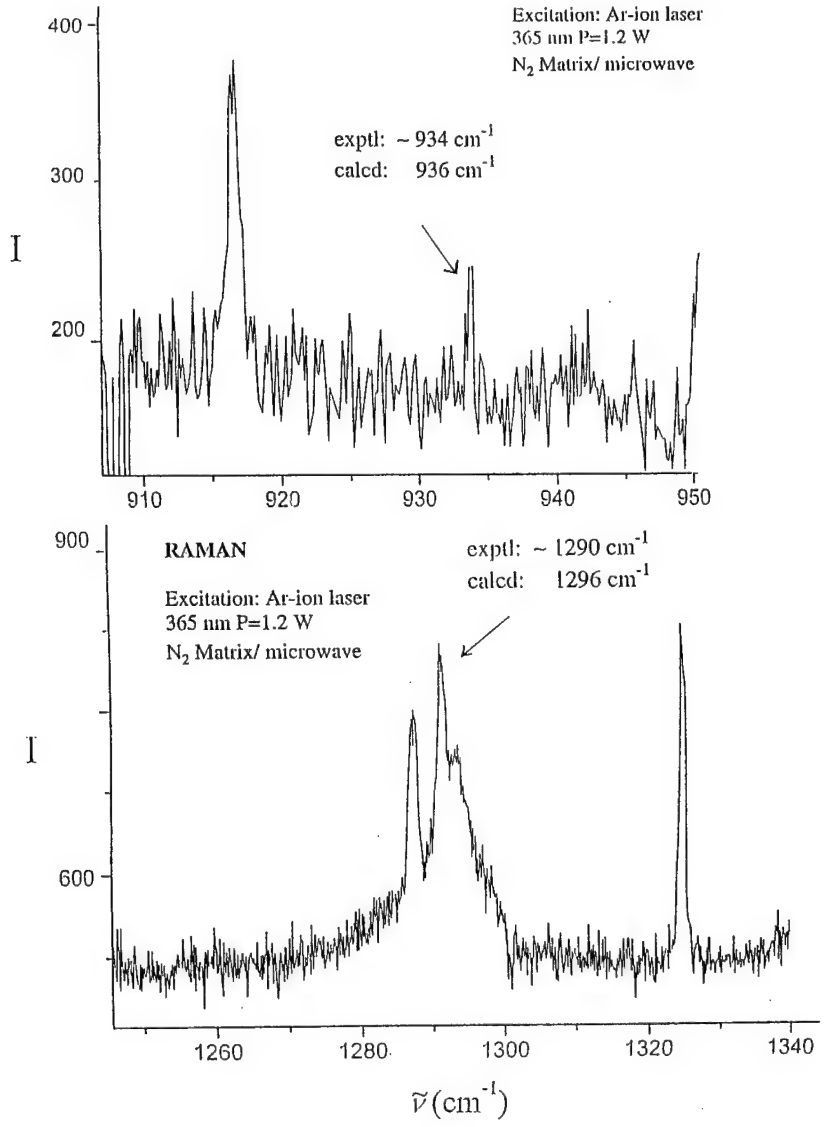

Figure. Raman spectra obtained from the solid (mostly dinitrogen) after condensation of the plasma prepared with the microwave discharge. Excitation at 365 nm (Ar-ion laser); power 1.2 W.

At present, mostly due to the lack of reproducibility, low correlation between their simultaneous appearance in the spectra, unexplained lack of isotopic shift(s) on ^{15}N labeling we cannot justify their assignment to N_4 species.

6. Experimental

In our work we use standard matrix isolation set-up consisting of high vacuum station and closed-cycle helium cryostat equipped with vacuum shroud suited for optical spectroscopy. The 2450 MHz microwave cavity is inserted on the quartz tube (bent at right angle to change the level of direct sample illumination by photons emitted from plasma) either on a segment directly pointing towards deposition window or perpendicular to it (figure below). A container coated with potassium mirror is inserted

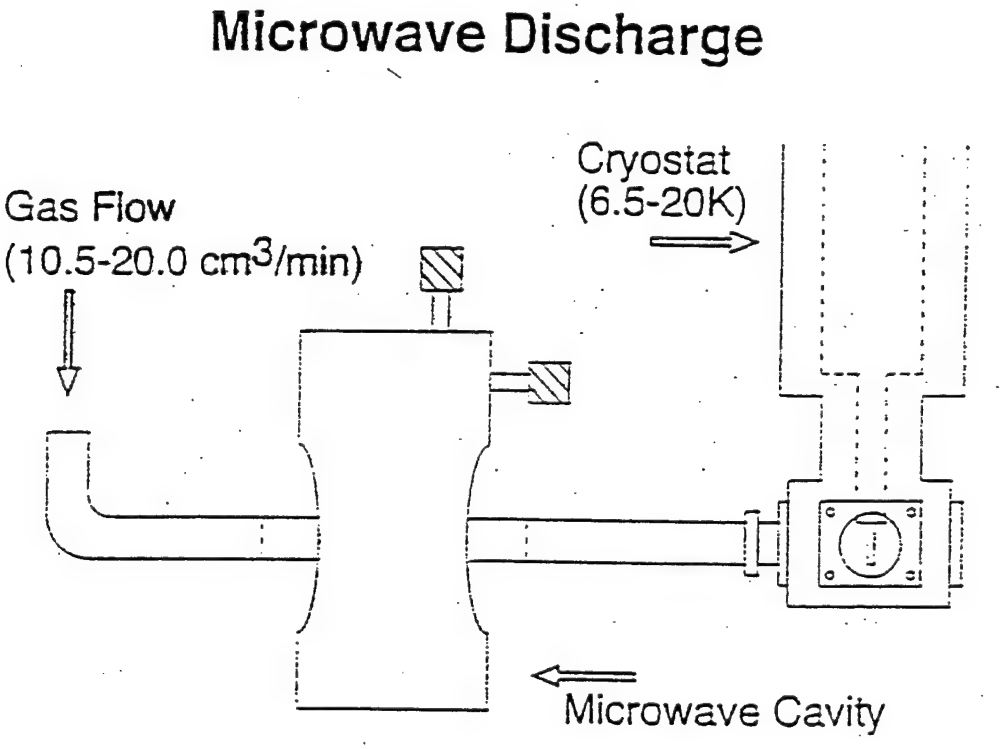

Figure. Schematics of arrangement for the discharge with microwave cavity.

prior to the quartz tube in the deposition line to keep residual water from the gaseous nitrogen. Most of the CO_2 and some H_2O is removed by the liquid nitrogen trap. The minute amounts of oxygen are removed by the commercial oxygen absorber (to 20 ppb level). This experimental set-up, after usual baking at 250 °C and 450 °C, allows us to reduce the total amount of impurities to less than 100 ppb. The grounded metal mesh placed between the end of quartz tube and cold window helps to keep our sample electrically neutral. Typically, we used flow rate of 0.04- 2 ml/min. Deposition target (CsI or BaF_2) was kept at 6.2 –35 K. The microwave forward power was between 15 W and 90 W. Our IR absorption spectra were measured on Nicolet Magna 560 FTIR with resolution 0.12 cm^{-1}; UV-Vis spectra recorded simultaneously with IR using Shimadzu 3101 spectrophotometer and home-built interface. Samples for Raman spectroscopy were collected on specially made holders mounted on modified cryostat and were excited with cw-Ar-ion laser lines: 356 nm, 488nm, and 514.5 nm and scattered light was analyzed using double monochromator and photon-counting detection.

8. References to preparation of "tetrazete"

(1) Molecular nitrogen was discovered by D. Rutherford, in 1772. Also, several other scientists (Cavendish, Priestley, Scheele and others) isolated it independently from air about that time.

(2) Curtius, T. *Ber. Deutsch. Chem. Ges.* **1890**, *23*, 3023.

(3) Tian, R.; Facelli, J. C.; Michl, J. *J. Phys. Chem.* **1988**, *92*, 4073.

(4) Guathrie, J. A.; Chaney, R. C.; Cunningham, A. J. *J. Chem. Phys.* **1991**, *95*, 930.

(5) Thompson, E. W.; Jacox, M. E. *J. Chem. Phys.* **1990**, *93*, 3856.

(6) Christe, K. O.; Wilson, W. W.; Sheehy, J. A.; Boatz, J. A. *Angew. Chem. Int. Ed.* **1999**, *38,* 2004.

(7) Among radicals the N_3 radical is often classified as not an especially reactive radical (i.e., Hewett, K. B.; Setser, D. W. *J. Phys. Chem. A* **1998**, *102*, 6274).

(8) Xu, N.; Du, Y-C.; Ying, Z.; Ren, Z. M.; Li, F. M. *Rev. Sci. Instrum.* **1997**, *68*, 2994.

(9) Strobel, D. F.; Meier, R. R.; Summers, M. E.; Strickland, D. J. *Geophys. Res. Lett.* **1991**,*18*, 689.

(10) Larson, A.; Larsson, M.; Ostmark, H. *J. Chem. Soc., Faraday Trans.* **1997**, *93*, 2963.

(11) Leininger, M. L.; Van Huis, T. J.; Schaefer, H. F., III. *J. Phys. Chem. A* **1997**, *101,* 4460.

(12) Glukhovtsev, M. N.; Jiao, H.; Schleyer, P. v. R. *Inorg. Chem.* **1996**, *35,* 7124.

(13) Frankcl, M. M.; Chesick, J. P. *J. Phys. Chem.* **1990**, *94*, 526.

(14) Korkin, A. A.; Balkova, A.; Bartlett, R. J.; Boyd, R. J.; von Schleyer, P. *J. Phys. Chem.* **1996**, *100,* 5702.

(15) Glukhovtsev, M. N.; Laiter, S. *J. Phys. Chem.* **1996**, *100,* 1569.

(16) Dunn, K. M.; Morokuma, K. *J. Chem. Phys.* **1995**, *102,* 4904.

(17) Yarkony, D. R. *J. Am. Chem. Soc.* **1992**, *114*, 5406.

(18) Littmann, D. *Dissertation*, Justus Liebig Univ. Giessen, **1985**.

(19) Dehnicke, K. *Angew. Chem.* **1967**, *76*, 253.

(20) Hada, M.; Nakatsuji, H., *unpublished results*.

(21) Perera, S. A.; Bartlett, R. J., *private communication*.

(22) Perera, S. A.; Bartlett, R. J. Chem. Phys. Lett., *in press*.

(23) Schnoeckel, H.; Koeppe, R. *J. Am. Chem. Soc.* **1989**, *111*, 4583.

B. Synthetic Preparation of Pentazole Anion (N_5^-)

Our extensive synthetic work aiming at the preparation of pentazole anion (N_5^-)did not yet produced desired compound. Most of the synthetic work was performed at Vanderbilt University in collaboration with synthetic group of Prof. P. Kaszynski. The work is still in progress. The results of our initial attempts were published this year in

two papers: *Tetrahedron*, **2002**, *58*, 2085, and *J. Org. Chem.* **2002**, *67*, 1354. The third paper is in final stages of preparation and we intend to submit it to *JACS*. Below, we describe briefly several of our synthetic attempts. The detailed accounts are provided in the mentioned above papers, which we published earlier this year.

In this area the goal was to prepare pentazole anion (N_5^-). We have been exploring azacarboxylates **1** as potential precursors to pentazole (Scheme 1). Unlike the azodicarboxylates **1a** (L=COOR), compounds with L being a good leaving group, such as sulfonyl (**1b**) or sulfonate (**1c**), are virtually unknown and are believed to be unstable. The success of this approach hinges upon addressing the following two key problems:

1. Generation of sufficiently stable **1** to serve as an effective intermediate to pentazole

2. Displacement of L by a nucleophile according to the addition-elimination mechanism

The first represents a virtually class of compounds, while the second an unknown class of reactions.

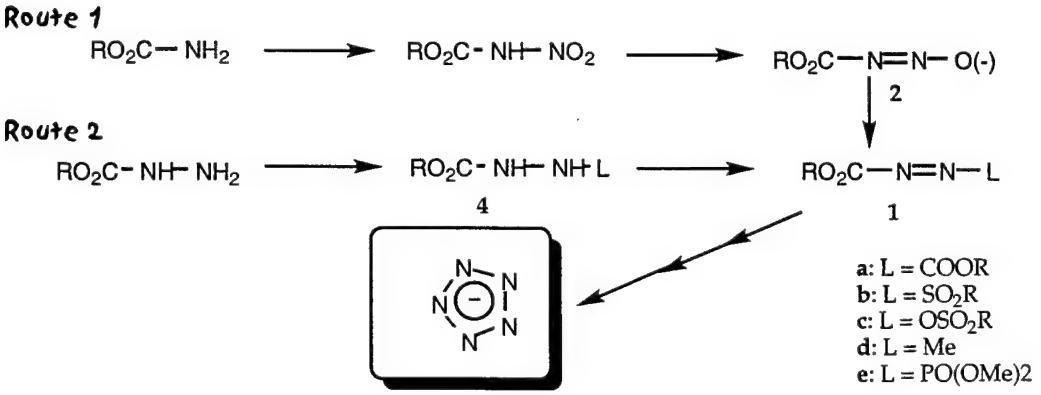

Scheme 1

In our initial approach to **1**, we successfully reproduced the preparation of nitrosourethane anion (**2**) an unstable compound described only once in the literature in the early 1900s (Route 1 in Scheme 1). In contrary to the previous report, we found that the silver salt of the anion **2** could not be O-methylated to give **1d** and the tetrabutylammonium salt gave predominantly or exclusively the highly mutagenic N-methylnitrosourethane **3** (Scheme 2). Although we cannot exclude the possibility of preparing the desired intermediate **1c** using this route, the prospect is bleak at this point. These results will be described in a short paper, currently in preparation for publication.

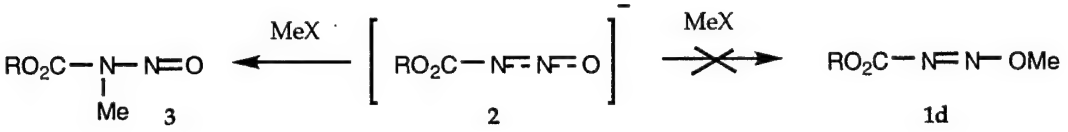

Scheme 2

Lack of success in Route 1 prompted us to focus on **1b** which is a dinitrogen analog of the sulfonoacrylate well known to undergo the desired nucleophilic substitution reaction. Initial attempts at oxidation of hydrazide **4c** were promising, but no stable product could be obtained. Soon we discovered that azosulfones, such as **1b**, have been proclaimed to be unstable for isolation and a handful of earlier reports on these compounds were disproved.

We speculated that the low stability of the $-SO_2-N=N-$ link might be related to the environment rather than to its inherent chemical instability. Recently, we found conditions under which we could generate and ISOLATE good yields of **1c** and also $ArSO_2-N=N-SO_2-Ar$ (**5**).. Our initial studies shows that **1b** decomposes with an appreciable rate only at >45 °C, which is 100 °C higher that previously estimated. We plan to provide detailed kinetic and structural studies for **1b** and **5**.

These results demonstrate once again that compounds perceived to be unstable may be stable enough for isolation and manipulation if properly handled. This also includes the target pentazole.

With the azosulfone **1c** in hand, we began studying its reactions. Preliminary results show that **1c** reacts with a nucleophile under low temperature conditions and a complex mixture of products is formed.

II. PATENT AND FISCAL REPORT

There was no intellectual property developed in this project. All our findings were published in peer-reviewed journals and presented at conferences:

- Zheng, J.-P.; Blake, D. M.; Waluk, J.; Spanget-Larsen, J.; and Radziszewski, J. G. "Tetrazaete (N_4). Can It Be Prepared and Observed?"*Chem. Phys. Lett.* **2000**, *328*, 227-233.

- Andrzej Łapinski, Jens Spanget-Larsen, Jacek Waluk, and J. George Radziszewski, "Vibrations of Nitrous Oxide: Matrix-Isolation FTIR Spectroscopy of Twelve N_2O Isotopomers" *J. Chem. Phys.* **2001**, *115*, 1757-1764.

- Vladimir Benin, Piotr Kaszynski, and J. George Radziszewski, "*N*-Chloro-*N,N',N'*-tris(ethoxycarbonyl)hydrazine and *N,N*-Dichloro-bis(ethoxycarbonyl)hydrazine: Synthesis, Stability and Reactions with Nucleophiles" *Tetrahedron*, **2002**, *58*, 2085-2090.

- Vladimir Benin, Piotr Kaszynski, and J. George Radziszewski "Arylpentazoles Revisited: Experimental and Theoretical Studies of 4-Hydroxypentazole and 4-Oxophenylpentazole Anion" *J. Org. Chem*, **2002**, *67*, 1354-1358.

- Vladimir Benin, Piotr Kaszynski, and J. George Radziszewski "The Ambident Ethyl N-Nitrosocarbamate Anion: Experimental and Computational Stydies of Alkylation and Thermal Stability" *J. Am. Chem. Soc.* June **2002**, submitted for publication.

- J. George Radziszewski, Jun-Ping Zheng, Daniel M. Blake, Andrzej Łapinski, Jens Spanget-Larsen, Jacek Waluk "Novel HEDM: Tetrazaete (N_4). Can It Be Prepared and Observed?" *26th International Symposium on Free Radicals*, Assisi, Italy, September **2001**.

FINANCIAL, STAFFING, and PROJECT MANAGEMENT

The grant was awarded as a one year funding with options for agency to extend it twice, each time for additional year. While such arrangement is quite usual and understandable it did cause some logistic hurdles for the PI with hiring and retaining project stuff. In addition to a few one- or multi- year appointments we had to relay on several much shorted arrangements. While we were able to save some money on specialized equipment (instead of purchases as originally planned we have used the loaned equipment) we had to spent more funds on personnel than originally intended. With the prior approval of funding agency we have re-directed some funds initially planed to cover consulting and special fees for laboratory usage (these were waived)

towards the cost of 2-year subcontract with synthetic group in Department of Chemistry at Vanderbilt University.

All the awarded funds were expended and detailed accounting of the expended funds was provided to Agency as a Final Financial Status Report by the Colorado School of Mines Accounting Office.

22 September 2000

Chemical Physics Letters 328 (2000) 227–233

CHEMICAL PHYSICS LETTERS

www.elsevier.nl/locate/cplett

Tetrazete (N_4). Can it be prepared and observed?

Jun Ping Zheng [1], Jacek Waluk [2], Jens Spanget-Larsen [3], Daniel M. Blake [1], J. George Radziszewski *

Department of Chemical Engineering and Petroleum Refining, Colorado School of Mines, and National Renewable Energy Laboratory, Golden, CO 80401, USA

Received 10 April 2000; in final form 8 August 2000

Abstract

The nitrogen plasma generated by microwave or electrical discharge in gaseous N_2 was quenched on a cold window (6.2–35 K) and resulting matrix was examined by IR and UV–Vis absorption spectroscopies. In samples prepared with $^{14}N_2$ we observe a weak infrared transition at 936.7 cm^{-1}. It shifts to 900.0 cm^{-1} when $^{15}N_2$ is used. Both peaks do not correlate with any other features in the spectra and are best explained as originating from tetrahedral tetrazetes (N_4). Their positions are compatible with quantum chemical estimates for $^{14}N_4$, at 936.0 cm^{-1} and $^{15}N_4$, at 904.4 cm^{-1}.

1. Introduction

Progress in the preparation of pure nitrogen compounds is measured in centuries. In 1890, 118 years after the original discovery of molecular dinitrogen [4], the azide anion N_3^- was added to the short list of known pure polynitrogen species [1]. Subsequently, the N_3 radical and several ions like N_3^+, N_4^+ have been observed and characterized [2–4]. They play important roles in atmospheric chemistry, but they are all short-lived intermediates. There are no literature reports on attempts to prepare tetrazete [5], (N_4), although the experimental evidence for other cyclic all-nitrogen species has been reported [5]. Recent synthetic preparation [6] of N_5^+ promises to revitalize this seemingly stagnant area and is raising expectations for other startling discoveries.

Despite the ubiquitous presence of nitrogen in the atmosphere and in the vast majority of biological molecules, the early name for molecular nitrogen, *azote*, emphasizes its low reactivity and chemical

* Corresponding author. Fax: +303-275-2905; e-mail: jradzisz@mines.edu

[1] Colorado School of Mines and National Renewable Energy Laboratory.

[2] Visiting from Inst. Phys. Chem., Polish Academy of Sciences, Kasprzaka 44, 01-224 Warsaw, Poland.

[3] Visiting from Dept. of Life Sciences and Chemistry, Roskilde University, DK-4000 Roskilde, Denmark.

[4] Molecular nitrogen was discovered by D. Rutherford, in 1772. Also, several other scientists (Cavendish, Priestley, Scheele and others) isolated it independently from air about that time.

[5] In this Letter we have adopted traditional name for tetrahedral N_4: tetrazete, used in the majority of the earlier computational reports, although according to the IUPAC nomenclature this compound should be called tetrazatricyclo[1.1.0.$0^{2,4}$]butane.

0009-2614/00/$ - see front matter
PII: S0009-2614(00)00926-X

inertness. The N ≡ N triple bond is one of the most stable chemical bonds, with a bond dissociation enthalpy of 228 kcal/mol. There are very few reactions in which nitrogen participates in its native and most abundant molecular form. In contrast, the only other known forms of neutral nitrogen, atomic N and N_3 radicals, are quite reactive [6]. Nitrogen atoms can be prepared in high yield (10^{19} atoms/(sr s)) by subjecting gaseous N_2 to electrical or microwave discharge [8]. However, the most common way of natural generation of reactive nitrogen is neither conductive coupling (microwave irradiation) nor purely electrical ionization (atmospheric discharges), but the direct or multi-photon solar photolysis and electron impact dissociation of N_2 [9]. The most frequent reactions of N atoms in the atmosphere are with oxygen, leading to the formation of NO, N_2O, NO_2, or higher oxides.

Results of intense computational scrutiny during last decade suggest that several additional neutral compounds of pure nitrogen are conceivable, such as the polyazetes N_4, N_6, and N_8 [10–18]. Apart from purely cognitive curiosity, the motivation for these investigations undoubtedly lies in the potential utility of such compounds as highly energetic materials. The quantum chemical methods estimate for tetrazete, N_4, to be a metastable tetrahedral molecule containing 185 kcal/mol of energy relative to two isolated N_2 molecules but residing in a potential well with a 60 kcal/mol barrier [11,12,15–17]. The proximity of a dissociative triplet state predicted by calculations may result in restricted utility of N_4 but it also could rule out the possibility of its preparation at all if the singlet–triplet crossing occurs deep in the potential well. Still, the level of optimism generated by quantum chemists stimulates experimental search for N_4 despite this and other possible complications. The availability of precise theoretical estimates of spectral characteristics of N_4 (in particular vibrational frequencies) and experimental sensitivity improvements make presently such undertaking more promising. The number of ways that might lead to N_4 is limited: in principle, for example, it can be assembled from reactions of N atoms with N_2 or the N_3 radical or fusion of two molecules of N_2; perhaps it could be 'extruded' in an excited state from larger polycyclic systems, in analogy with photochemical reactions observed for hydrocarbons [19]. The polyazete N_6 may be prepared by coupling of two N_3 radicals, and N_8 (azidopentazole) perhaps by reaction of yet unknown lithium pentazole with iodo azide [20]. These species combine the promise of being attainable synthetic goals and highly energetic materials. The recent report of synthetic preparation of N_5^+ ion [6] by using delicate 'wet' synthetic methods lends fresh credence for this effort.

The optimism among experimentalists with respect to the possible synthesis of N_4 is largely based on the theoretical prediction that the species should be sufficiently kinetically stable for experimental observation. Perhaps it is formed naturally during atmospheric electrical discharges, but is never accumulated, either due to low photochemical stability, or to the expected extremely high sensitivity towards moisture and oxygen, leaving virtually no traces of its intermediacy. This brings the question of how N_4 could actually be detected, if it is ever prepared in the laboratory. Before absolute proof for its existence can be produced by classical identification methods (NMR, elemental analysis, or X-ray or neutron diffraction), experimental detection and initial recognition will have to rely on optical spectroscopy observations. Theoreticians tend to agree that N_4 in its lowest, metastable state will prefer tetrahedral geometry (point group T_d). Hence, it will have only one (t_2) vibrational mode weakly active in infrared absorption and three (e, t_2, a_1) vibrations active in Raman spectroscopy. Since the lowest optically allowed, excited electronic states are calculated at about 10 eV above the ground state [21,22], electronic absorption or emission do not look very promising as initial detection methods.

Recently reported mass-spectrometric detection of presumably tetrahedral N_3O^+ ion [23] further reinforces the notion that it may be possible to prepare N_4.

2. Experimental

In our attempts to prepare N_4 we subject gaseous dinitrogen to microwave irradiation. The resulting

[6] Among radicals, the N_3 radical is often classified as not an especially reactive radical (i.e., Ref. [7]).

atomization of N_2 is followed by additional gas phase reactions involving atomic N, possibly including reactions induced by vacuum ultraviolet (VUV) photons emitted by the plasma. The reaction mixture is condensed on a cold spectroscopic window (6.2–35 K). Nitrogen-matrix isolation of the products provides several useful advantages: long lifetimes of the trapped species, ability to perform secondary photochemistry in a medium transparent to VUV radiation, as well as the simplicity of the well-resolved spectrum.

Classical VUV photolysis experiments were also performed, using a krypton lamp (Resonance Ltd., KrLM-1) for irradiation of both, gaseous deposition mixtures and solid nitrogen matrices. We use a standard matrix isolation set-up consisting of high vacuum station and closed-cycle helium cryostat equipped with vacuum shroud suited for optical spectroscopy. The 2450 MHz microwave cavity is inserted on the quartz tube (bent at right angle to change the level of direct sample illumination by photons emitted from plasma) either on a segment directly pointing towards the deposition window or perpendicular to it. A container coated with a potassium mirror is inserted prior to the quartz tube in the deposition line to keep residual water from the gaseous nitrogen. Most of the CO_2 and H_2O are removed by the liquid nitrogen trap. The minute amounts of oxygen are removed by the commercial oxygen scrubber (HP-3150-0414). This experimental set-up, after usual baking at 250°C and 450°C, allows us to reduce the total amount of impurities to less than 100 ppb. The grounded metal mesh placed between the end of the quartz tube and cold window helps to keep our sample electrically neutral. Typically, we used a flow rate of 0.04–2 ml/min. The gases used in these experiments: $^{14}N_2$ (purity – 99.995%), and $^{15}N_2$ (isotopic purity – 98% +) were purchased from Air Products and Cambridge Isotope Laboratories. The deposition target (CsI or BaF_2) was kept at 6.2–35 K. The microwave forward power was between 15 W and 90 W. Our IR absorption spectra were measured on a Nicolet Magna 560 FTIR with resolution 0.125 cm^{-1}. UV–Vis spectra were recorded simultaneously with the IR spectra using a Shimadzu 3101 spectrophotometer and home-built interface. Samples for Raman spectroscopy were excited with cw Ar-ion laser lines: 356 nm, 488 nm, and 514.5 nm and scattered light was analyzed using a double monochromator and CCD detection.

3. Results and discussion

The IR spectra of nitrogen matrices obtained after microwave or electrical discharges or after VUV photolysis reveal traces of nitrogen oxides (NO, N_2O, NO_2, etc.) and common impurities (CO_2, CO, H_2O, etc.). An example is presented in Fig. 1. The use of $^{15}N_2$ and $^{18}O_2$ allowed us to obtain complete characterization of vibrational patterns of various isotopomers of nitrogen oxides. Here, we focus on a single line at 936.7 cm^{-1}, recorded when $^{14}N_2$ was used in experiments utilizing the highest sensitivity arrangement (Fig. 2, bottom). No other absorption peaks in the IR or UV–Vis spectra can be correlated with this line (on the basis of selective thermal and photochemical response of all other detectable bands in the spectrum). On ^{15}N labeling the 936.7 cm^{-1} line undergoes a shift to 900.0 cm^{-1} (Fig. 2, top of the lower part). When ^{13}C, ^{2}H, ^{18}O are introduced simultaneously to the initial load of ^{14}N-dinitrogen (from $^{13}C^{16}O_2$, $^{1}H_2{}^{18}O$ and $^{2}H^{16}O$) and passed through microwave discharge zone we observe a full isotopic scrambling in side-products and in the common impurities (nitrogen oxides, ammonia, CO, CO_2, H_2O, etc.) but there is no influence on the 936.7 cm^{-1} line.

The calculated IR spectrum of $^{14}N_4$ (T_d) consists of a single line at 936.0 cm^{-1} with intensity equal to 3.4 km/mol (harmonic approximation; triply degenerate asymmetric NN stretch, t_2 symmetry species) [10]. Within the harmonic approximation, the ratio of the wavenumbers for the absorption of isotopomers $^{14}N_4$ and $^{15}N_4$ is determined entirely by the ratio of the isotope masses. The line for $^{15}N_4$ is thus predicted at 904.4 cm^{-1} [$= (14.003/15.000)^{1/2} \times 936.0$ cm^{-1}], (Fig. 2, upper part). The theoretical predictions support the assignment of the peaks observed at 936.7 cm^{-1} and 900.0 cm^{-1} to the IR active t_2 levels of tetrahedral $^{14}N_4$ and $^{15}N_4$. Unfortunately, this is not exactly a very fingerprint-like type of evidence. The visually very convincing evidence presented in Fig. 2 is by no means absolute. The observed lines are extremely weak, and there are

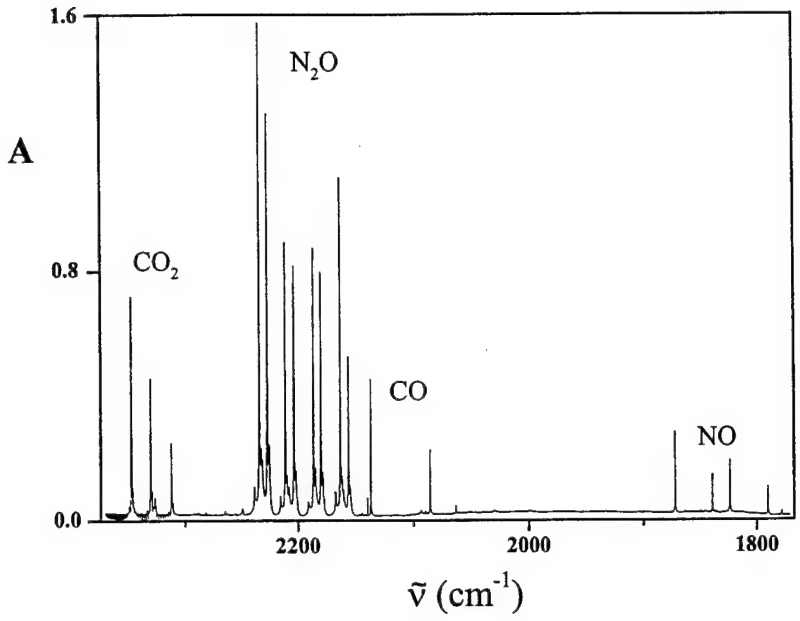

Fig. 1. Portions of IR absorption spectra from samples containing mixtures of $^{14}N_2{}^{15}N_2$, $^{16}O_2$ and $^{18}O_2$. The lines are due to various isotopomers of N_2O, NO, CO, and CO_2.

many compounds with possible vibrations occurring in this spectral region. Our spectra can be reproduced with great difficulty (the recorded intensities in the 900 cm^{-1} region were less than 0.01 optical density units). We have so far been unable to observe $^{15}N^{14}N$ multiplets expected in experiments with $^{15}N/^{14}N$ mixtures. In spite of numerous attempts, we have yet not correlated the intensity changes of the 936.7 cm^{-1} signal with any of the simple adjustable experimental parameters (N_2 flow rate, microwave power, deposition window temperature, level of direct sample illumination by plasma emissions, etc.).

It may be a paradox that the elusive presence of the 936.7 cm^{-1} line can be an argument for its assignment to N_4. A mechanism of tetrazete formation in the gas phase must involve at least two steps, and therefore the concentration of the product in the matrix should be very small, even compared to the concentration of products formed (in one step) from impurities, such as oxygen or water. Since, by definition, the concentration of impurities cannot be strictly controlled, this would explain the absence of the 936.7 cm^{-1} line in many experiments.

The 936.7 cm^{-1} line is apparently split into a doublet (Fig. 2). The splitting can possibly be explained by the trapping of N_4 in two different sites. Removal of a pair of neighboring N_2 molecules from solid state α-N_2 (the allotrope prevailing at low temperature) produces a cavity with two diastereomerically different sites. The difference vanishes by transition to the β-N_2 allotrope, which would explain the disappearance of the splitting on heating.

Application of Raman spectroscopy might provide strong additional evidence for the presence of N_4. Our attempts have failed so far, most likely due to exceedingly small amounts of the compound in the samples and interfering emission from traces of impurities upon strong visible laser excitation of our low-temperature samples. The extremely weak Raman signal from the highly diluted matrix sample is likely buried in stronger and superimposed emissions.

The isotopic shift from 936.7 cm^{-1} to 900.0 cm^{-1} is quite large. Might these lines be due to ^{14}N and ^{15}N isotopomers of another compound than tetrazete? This shift from 937 cm^{-1} to 900 cm^{-1} implies that the nitrogen atom in the unknown compound participates strongly in the vibration (for instance, a shift from 918 cm^{-1} to 907 cm^{-1} in S = Si = S upon $^{28}Si \rightarrow {}^{29}Si$ substitution is consid-

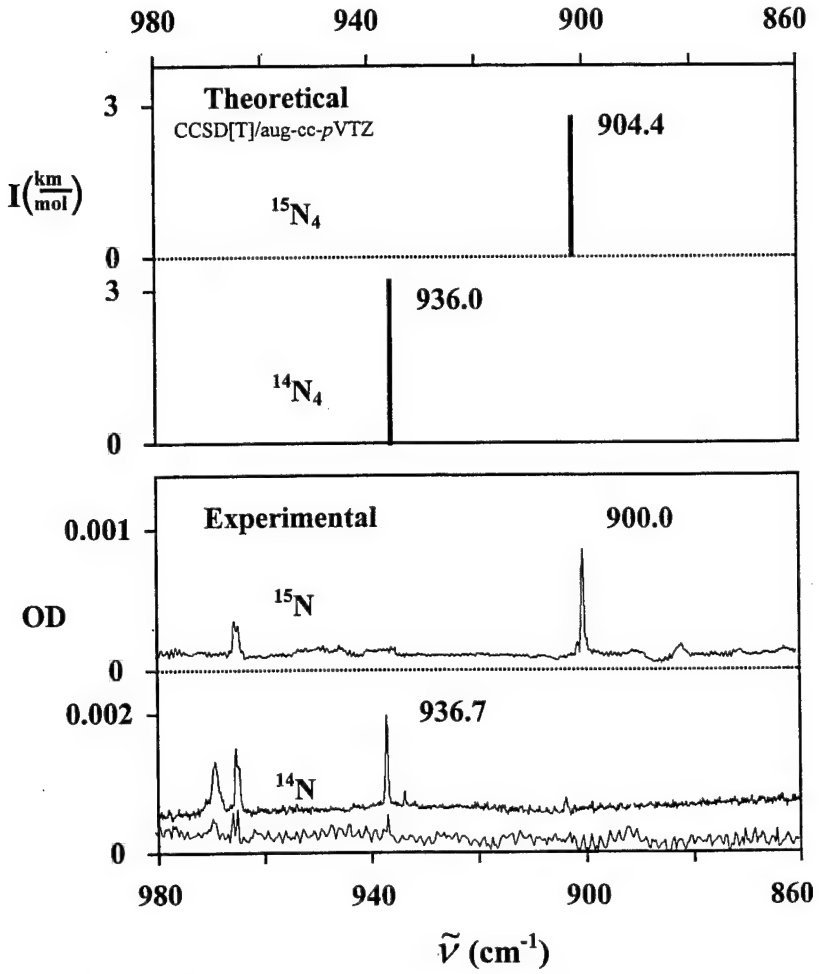

Fig. 2. Observed IR absorption (lower set) from sample containing separately: $^{14}N_2$ (two separate experiments) and $^{15}N_2$ quenched plasma, and respective theoretical predictions (upper set) [10]. The peak at 969 cm^{-1} (bottom spectrum) belongs to NH_3 impurity and the unresolved doublet at 965 cm^{-1} (in both spectra) originates in O_4^- [25].

ered [24] as evidence of a large involvement of silicon in the vibration). If we treat our unknown species as a pseudo-diatomic molecule, consisting of a vibrating nitrogen atom and a pseudo-atom of mass s, the ratio of the reduced masses upon $^{14}N \rightarrow {}^{15}N$ substitution would be equal to $\mu_2/\mu_1 = (1/s + 1/14)/(1/s + 1/15)$. Within the harmonic approximation this ratio can be experimentally estimated as $\mu_2/\mu_1 = (\tilde{\nu}_1/\tilde{\nu}_2)^2$, where $\tilde{\nu}_1$ and $\tilde{\nu}_2$ are the wavenumbers for the ^{14}N- and the ^{15}N-containing compounds. Solving the equation for $(\tilde{\nu}_1/\tilde{\nu}_2)^2 = (937/900)^2 = 1.084$ yields a negative s value without physical meaning. On the other hand, if the molecule is built entirely of nitrogen atoms, the value of s changes after $^{14}N \rightarrow {}^{15}N$ substitution from 42 to 45 and the ratio μ_2/μ_1 is now equal to $15/14 = 1.071$, which is close to the observed value $(\tilde{\nu}_1/\tilde{\nu}_2)^2 = 1.084$. This agreement strongly supports the assignment of the 936.7 cm^{-1} line to tetrazete. Such assignment is additionally strengthened by the experimental observation of no isotopic shift for the 936.7 cm^{-1} band upon adding ^{18}O and ^{2}H (from $H_2{}^{18}O$ and $^{2}H^{16}O$) or ^{13}C (from $^{13}CO_2$) to the sample. The complete random migration of these isotopic labels in the N_2O, H_2O, or CO_2, after atomization in the plasma zone, makes the presence

of oxygen, hydrogen or carbon in the molecule highly improbable.

The experiments discussed above reveal a vibrational line at 936.7 cm^{-1} which is best explained as originating in N_4, particularly due to the fact that observed ^{15}N shift is in excellent agreement with theoretical predictions. Conclusive arguments for the assignment may be provided by using mixtures of ^{14}N and ^{15}N. A total of five different isotopomers are possible: $^{14}N_4$, $^{14}N_3{}^{15}N$, $^{14}N_2{}^{15}N_2$, $^{14}N^{15}N_3$, and $^{15}N_4$. The triple degeneracy will be lifted for the three mixed species, leading to characteristic multiplet patterns in the IR spectrum. For $^{14}N_3{}^{15}N$ and $^{14}N^{15}N_3$ species we will have $T_d \rightarrow C_{3v} \Rightarrow t_2 \rightarrow a_1 + e$, and for $^{14}N_2{}^{15}N_2$ species: $T_d \rightarrow C_{2v} \Rightarrow t_2 \rightarrow a_1 + b_1 + b_2$. In the ensuing analysis we shall assume that the relative IR intensities of the split components are 1:2 and 1:1:1, respectively.

One may consider three possible cases, each leading to the production of N_4. Let us assume that the substrate is a mixture of $^{14}N_2$ (molar fraction f) and $^{15}N_2$ (molar fraction $1-f$). In the first case, N_4 is formed from two nitrogen molecules: $N_2 + N_2 \rightarrow N_4$. Three different species could be formed: $^{14}N_4$, $^{14}N_2{}^{15}N_2$, $^{15}N_4$. A general formula for the ratios of reaction yields (φ) is:

$$\varphi(^{14}N_4):\varphi(^{14}N_2{}^{15}N_2):\varphi(^{15}N_4) = f^2:2f(1-f):(1-f)^2.$$

For a 1:1 mixture of $^{14}N_2$ and $^{15}N_2$ ($f = 1-f = 0.5$) a 1:2:1 population ratio is expected. In the IR spectrum not three, but five lines should be observed. This is due to the fact that in $^{14}N_2{}^{15}N_2$ the vibration is no longer degenerate because of lower symmetry. Thus, for a 1:1 mixture of $^{14}N_2$ and $^{15}N_2$, the expected pattern of IR peaks for the product mixture is a quintet with intensity ratios: $1:(2/3):(2/3):(2/3):1$.

In the second case, N_4 is produced from one nitrogen molecule and two N atoms: $N_2 + N + N \rightarrow N_4$. All five different isotopomers can now be formed: $^{14}N_4$, $^{14}N_3{}^{15}N$, $^{14}N_2{}^{15}N_2$, $^{14}N^{15}N_3$, and $^{15}N_4$. Symmetry lowering in $^{14}N_3{}^{15}N$, $^{14}N^{15}N_3$ leads to the splitting of a triply degenerate vibration into a non-degenerate and a doubly degenerate one. For the 1:1 mixture, the expected pattern of IR peaks is now a nonet, with intensity ratios: $1:(4/3):(2/3):(2/3):(2/3):(2/3):(4/3):1$. This is obtained under the assumption, based on the results of calculations, that the doubly degenerate vibration has higher energy in $^{14}N_3{}^{15}N$ than the non-degenerate one, while it is lower in energy for $^{14}N^{15}N_3$. For the opposite situation, the $(4/3):(2/3)$ ratio in positions 2 and 4 and the $(2/3):(4/3)$ ratio in positions 6 and 8 should be inverted.

In the third case, N_4 is formed from nitrogen atoms: $N + N + N + N \rightarrow N_4$. Again, five species should be detected: $^{14}N_4$, $^{14}N_3{}^{15}N$, $^{14}N_2{}^{15}N_2$, $^{14}N^{15}N_3$, $^{15}N_4$. As in case 2, a nonet is expected in the IR spectrum of a 1:1 mixture, this time, however, with different intensity ratios: $1:(8/3):2:(4/3):2:(4/3):2:(8/3):1$ (the same assumption as in the previous case was made regarding the energy ordering in $^{14}N_3{}^{15}N$ and $^{14}N^{15}N_3$).

It can be seen from the above that a large difference is to be expected for the isotopic mixtures of $^{14}N_2$ and $^{15}N_2$ with respect to a 'simple' behavior predicted for pure isotopes. The experiments with isotopic mixtures should therefore be crucial for the definitive assignment. It should be noted, however, that the intensities of the lines produced in such experiments should be much lower than the intensity of a single line produced for one isotopic species only. Since our observation of the latter was already near the instrumental sensitivity limit ($> 10^{-4}$ optical density units), this would explain our present inability to detect multiplet lines in the 1:1 mixtures of $^{14}N_2$ and $^{15}N_2$. In reality, the experimental pattern observed in the mixtures may be even more complex, due to possible accidental degeneracies and the matrix site splittings and to the fact that the reaction may proceed according to more than just one mechanism. Therefore, while the observation of the splitting would provide a very convincing argument for the presence of tetrazete, the conclusions regarding the mechanism of its formation may be much harder to reach.

4. Conclusions

We have obtained noteworthy experimental evidence for the isolation of tetrazete, a hitherto unobserved, neutral polynitrogen compound, N_4. The ob-

served and predicted IR spectra, including the ^{15}N-isotopic shift for the fully labeled species, are in excellent agreement, but conclusive assignment of the spectral features will require further experimentation.

Acknowledgements

This project is supported by the grant from DARPA/AFOSR (F49620-98-1-0483). Part of the instrumentation used in this project was obtained by funds from a DURIP grant. We also thank Dr. David Funk (LANL) for stimulating discussions and loan of equipment. We would like to thank to Prof. Rodney Bartlett (QTP) and Prof. Hiroshi Nakatsuji (Kyoto University) for sharing unpublished results and Dr. M. Berman (AFOSR) and Dr. A. Morrish (DARPA) for continuing encouragement and support.

References

[1] T. Curtius, Ber. Deutsch. Chem. Ges. 23 (1890) 3023.
[2] R. Tian, J.C. Facelli, J. Michl, J. Phys. Chem. 92 (1988) 4073.
[3] J.A. Guathrie, R.C. Chaney, A.J. Cunningham, J. Chem. Phys. 95 (1991) 930.
[4] E.W. Thompson, M.E. Jacox, J. Chem. Phys. 93 (1990) 3856.
[5] R. Tian, V. Balaji, J. Michl, J. Am. Chem. Soc. 110 (1988) 7225.
[6] K.O. Christe, W.W. Wilson, J.A. Sheehy, J.A. Boatz, Angew. Chem. Int. Ed. 38 (1999) 2004.
[7] K.B. Hewett, D.W. Setser, J. Phys. Chem. A 102 (1998) 6274.
[8] N. Xu, Y.-C. Du, Z. Ying, Z.M. Ren, F.M. Li, Rev. Sci. Instrum. 68 (1997) 2994.
[9] D.F. Strobel, R.R. Meier, M.E. Summers, D.J. Strickland, Geophys. Res. Lett. 18 (1991) 689.
[10] S.A. Perera, R.J. Bartlett, Chem. Phys. Lett. 314 (1999) 381.
[11] T.J. Lee, J.E. Rice, J. Chem. Phys. 94 (1991) 1215.
[12] A. Larson, M. Larsson, H. Östmark, J. Chem. Soc. Faraday Trans. 93 (1997) 2963.
[13] M.L. Leininger, T.J. Van Huis, H.F. Schaefer III, J. Phys. Chem. A 101 (1997) 4460.
[14] M.N. Glukhovtsev, H.P. Jiao, P. von Schleyer, Inorg. Chem. 35 (1996) 7124.
[15] M.M. Frankel, J.P. Chesick, J. Phys. Chem. 94 (1990) 526.
[16] M.N. Glukhovtsev, S. Laiter, J. Phys. Chem. 100 (1996) 1569.
[17] K.M. Dunn, K. Morokuma, J. Chem. Phys. 102 (1995) 4904.
[18] D.R. Yarkony, J. Am. Chem. Soc. 114 (1992) 5406.
[19] D. Littmann, Dissertation, Justus Liebig Univ. Giessen, 1985.
[20] K. Dehnicke, Angew. Chem. 18 (1979) 507.
[21] M. Hada, H. Nakatsuji, unpublished results.
[22] S.A. Perera, R.J. Bartlett, private communication.
[23] R. Engelke, N.C. Blais, R.K. Sander, J. Phys. Chem. A 103 (1999) 5611.
[24] H. Schnoeckel, R. Koeppe, J. Am. Chem. Soc. 111 (1989) 4583.
[25] M.E. Jacox, D.E. Milligan, Chem. Phys. Lett. 14 (1972) 518.

Vibrations of nitrous oxide: Matrix isolation Fourier transform infrared spectroscopy of twelve N_2O isotopomers

Andrzej Łapiński
Department of Chemical Engineering, Colorado School of Mines, Golden, Colorado 80401 and National Renewable Energy Laboratory, Golden, Colorado 80401

Jens Spanget-Larsen
Department of Chemical Engineering, Colorado School of Mines, Golden, Colorado 80401; National Renewable Energy Laboratory, Golden, Colorado 80401; and Department of Life Sciences and Chemistry, Roskilde University, DK-4000 Roskilde, Denmark

Jacek Waluk
Department of Chemical Engineering, Colorado School of Mines, Golden, Colorado 80401; National Renewable Energy Laboratory, Golden, Colorado 80401; and Institute of Physical Chemistry, Polish Academy of Sciences, Kasprzaka 44, 01-224 Warsaw, Poland

J. George Radziszewski[a)]
Department of Chemical Engineering, Colorado School of Mines, Golden, Colorado 80401 and National Renewable Energy Laboratory, Golden, Colorado 80401

(Received 30 March 2001; accepted 10 May 2001)

Isotopically labeled nitrous oxide has been produced in solid nitrogen matrices using mixtures of nitrogen and water containing ^{14}N, ^{15}N, ^{16}O, ^{17}O, and ^{18}O. All twelve possible N_2O isotopomers have been obtained, and their fundamental, overtone and combination frequencies were assigned by the joint use of infrared spectroscopy and quantum chemical calculations (B3LYP/AUG-cc-pVTZ). Specific influence of the nitrogen matrix upon frequency and anharmonicity of the vibrations has been discussed. © *2001 American Institute of Physics.* [DOI: 10.1063/1.1383031]

I. INTRODUCTION

Nitrous oxide, N_2O, discovered by Priestley in 1793, and dubbed "laughing gas" by Davy shortly afterwards, is widely known for its anesthetic properties. More important, it is one of the greenhouse gases, with a capacity to trap heat in the atmosphere more than two orders of magnitude larger than that of CO_2.[1,2] Its IR absorption range fills the gap between the regions of absorption of water and CO_2. N_2O also participates in the stratospheric ozone cycle.[3,4] The concentration of N_2O in the atmosphere is increasing at a rate of 0.25%/year, mostly due to agricultural soil management and fuel combustion. The atmospheric residence time of N_2O is about 150 years; it is destroyed through photolysis (90%), yielding N_2 and O, and by photooxidation that leads either to two molecules of NO (6%) or to N_2 and O_2 (4%).

In spite of numerous studies,[5–17] the global budget of nitrous oxide and the mechanisms of its formation and decay are still not well understood. A powerful tool for identification of its sources and sinks is the isotopic characterization of N_2O collected from different locations (oceans, soils, atmosphere). When applied to atmospheric chemistry, this procedure led to divergent interpretations. Stratospheric N_2O is enriched in ^{15}N and ^{18}O.[5–8] On the basis of measurements of $^{15}N/^{14}N$, $^{18}O/^{16}O$, and $^{17}O/^{16}O$ ratios in atmospheric samples, some authors suggested the existence of a previously undefined atmospheric process.[6–8] An alternative explanation was proposed,[9] that assumed different yields of photolysis of various isotopomers. In particular, the $^{15}N^{14}N^{16}O$ and $^{14}N^{15}N^{16}O$ species were postulated to have very different isotopic fractionations in the atmosphere as a result of different ground state zero point vibrational energies (ZPEs). The experimental evidence supporting this hypothesis has been provided recently.[10,17–19]

It becomes obvious in the above context that a desired property of an analytical method used to study isotopic composition should be the ability to determine the intramolecular position of the nitrogen isotope in N_2O. This is not the case with conventional mass spectrometry, although a modified spectrometer, able to perform this task, has recently been described.[20] Laboratory procedures based on workup of field samples require attention, in order to avoid artifacts, such as surface reactions or contamination with CO_2. *In situ* measurements are evidently preferable, with infrared spectroscopy as an attractive choice. Fourier transform infrared (FTIR) (Refs. 21–25) and tunable diode laser[26–29] instruments have been described that are able to operate onboard a shuttle or aircraft. These measurements can use an extensive data basis of gas phase rovibrational N_2O spectra, accumulated over several decades.[30–83] High-resolution IR measurements for N_2O have been performed with great accuracy, and the obtained data serve as standards in wavenumber calibration tables.[62,73,80–83] Moreover, IR studies provide the ZPEs necessary for calculating fractionation factors for various isotopomers. Substantial effort has been devoted to the determination of the force field for N_2O.[84–94]

Much less is known about vibrational spectroscopy of

a)Author to whom correspondence should be addressed.

nitrous oxide in condensed phases. Cryogenic studies involving N_2O have been reported in several papers.[95–113] The spectra of the parent $^{14}N_2{}^{16}O$ species were obtained in solid N_2O,[95] argon,[97–101] nitrogen,[96,102–104] and xenon[101,105] matrices. Matrix-isolated N_2O has also been used as a source of molecular ions[106–110] and as a reagent with laser-ablated metal atoms.[111,112] The experimental data for isotopically substituted species are very scarce. IR frequencies have only been reported for the three fundamentals and several other bands of $^{15}N^{14}N^{16}O$, $^{14}N^{15}N^{16}O$, $^{15}N_2{}^{16}O$, $^{14}N_2{}^{18}O$, and $^{15}N^{14}N^{18}O$ in nitrogen and argon matrices.[96,98,99] No systematic investigation of all isotopomers has been performed so far. In this work, we present a vibrational study of matrix-isolated isotopomers of N_2O, obtained in a microwave discharge of water-containing mixtures with nitrogen. Using ^{15}N, ^{17}O, and ^{18}O isotopically labeled species resulted in the production of all possible twelve isotopomers. Combined use of matrix-isolation FTIR spectroscopy and quantum chemical computations enabled a complete characterization of vibrational patterns. It is hoped that the obtained results can contribute to practical applications, such as environmental control, and to further development of the theoretical investigation of this important molecule.

II. EXPERIMENTAL AND COMPUTATIONAL DETAILS

Various isotopically labeled oxides of nitrogen (nitrous oxide, N_2O; nitric oxide, NO; nitrogen dioxide, NO_2; and dinitrogen tetroxide, N_2O_4), as well as several isotopic compositions of ozone were prepared in the gas-phase by reacting atomic or molecular nitrogen with oxygen. The gaseous dinitrogen [$^{14}N_2$, $^{15}N_2$ (98+% ^{15}N, Cambridge Isotope Laboratories) or 1:1 mixture] was passed in the glass or quartz tube through a 2450 MHz microwave cavity. In some experiments we have used 30 kV electrical discharge between two electrodes attached to the deposition tube. The ^{18}O was introduced from 95%–98% ^{18}O-labeled water, while ^{17}O was added from 50% labeled water (Cambridge Isotope Laboratories). The reaction mixture was condensed onto a cold (6.5 K) salt window (CsI or BaF_2) attached to the tip of the closed-cycle helium refrigerator (DE-202A-N, APD-Cryogenics). The infrared spectra were measured on a Nicolet-560 FTIR spectrometer with 0.125 cm^{-1} resolution.

In some experiments, oxygen, neon, krypton or xenon were added to the deposition mixture, to check for the possible formation of complexes with oxygen and to determine spectral shifts in different matrices.

The molecular equilibrium geometry and harmonic force field[114,115] for N_2O were computed with the GAUSSIAN 94 and GAUSSIAN 98 software packages[116,117] by using B3LYP density functional theory[118,119] and the AUG-cc-pVTZ basis set.[120] Numerous structure and force field calculations reported for nitrous oxide[89–94,121–127] have shown that obtaining reliable results for both geometry and vibrational frequencies requires an extensive treatment of electron correlation and large basis sets. Our calculated values for N–N and N–O distances, 1.121 Å and 1.184 Å, respectively, are in excellent agreement with the experimental values of 1.127 Å and 1.185 Å.[87] Values of similar accuracy, 1.131 Å and 1.186 Å, were recently calculated using CASPT2(10,9)/cc-pVTZ level of theory.[121] Interestingly, it was shown in the same work that the computational results are significantly influenced by using only slightly smaller active space or basis set: The agreement with experiment was found to be much worse for CASPT2(10,9)/cc-pVDZ and CASPT2(10,8)/cc-pVDZ levels.

The dipole moment predicted with B3LYP/AUG-cc-pVTZ is 0.076 D, with the negative end pointing towards the oxygen atom; the experimental gas phase value is 0.166 D.[128] This theoretical prediction should be considered very satisfactory, given that the calculated value of the dipole moment of N_2O is very sensitive to the value of interatomic distances and the extent of electron correlation. It has been shown[126] that SCF and SDCI methods yield a correct sign, $^{+}NNO^{-}$, but the computed values are too large. On the other hand, MP2 produces a value close to the experimental one, but yields an incorrect sign.

III. RESULTS AND DISCUSSION

In the gas phase, the frequencies corresponding to the fundamental stretching (ν_3 and ν_1, Σ^+ symmetry species) and bending (ν_2, Π symmetry species) vibrations of N_2O are 2223.8, 1284.9, and 588.8 cm^{-1}, respectively.[41,42] Portions of the IR spectra recorded in corresponding spectral regions in nitrogen matrices at 10 K are presented in Figs. 1–3. Using equimolar mixtures of isotopomers of nitrogen led to practically the same intensities of the product bands. Hence, starting from a 1:1 mixture of $^{14}N_2$ and $^{15}N_2$ produced equal amounts of $^{14}N_2{}^{16}O$, $^{15}N^{14}N^{16}O$, $^{14}N^{15}N^{16}O$, and $^{15}N_2{}^{16}O$. This implicates that the isotope scrambling is complete, and thus, that the products are obtained from nitrogen atoms.

Assignments of vibrational bands to particular isotopomers were achieved by comparing patterns observed for samples of various isotopic compositions, by referring to previously reported matrix and gas phase data, and by comparing experimentally observed frequencies with the calculated ones. The results are compiled in Tables I–V. Our frequencies agree to within 0.2 cm^{-1} with those recently reported for nitrogen matrix.[103] With regard to the data obtained on a dispersive instrument with lower spectral resolution,[96] the largest differences, about 1–2 cm^{-1} are observed in the lower energy region (ν_2 fundamental) and for combination bands lying above 3000 cm^{-1}.

In the vicinity of the ν_1 and ν_3 bands, weak features are observed. The relative intensity of these features depends on the mode of sample preparation. In accordance with the results of recent work,[103,104] we assign these bands to complexes of N_2O with molecular oxygen. We have verified these assignments by performing experiments in which oxygen was being gradually added to the deposition mixture. This led to significant growth of satellite bands.

In an early study in a nitrogen matrix,[96] and in the investigation of solid N_2O, [95] the bands observed at 1885.9 cm^{-1} and at 1891 cm^{-1}, respectively, were assigned to $\nu_1 + \nu_2$ combination. In a recent paper, this assignment was made for a band at 1866.3 cm^{-1}.[103] We have observed both bands in this region, the former of much weaker intensity. We assign the $\nu_1 + \nu_2$ combination to the band detected at 1885.3 cm^{-1} (Table V), in accordance with the finding that,

TABLE I. Experimental and calculated frequencies for the ν_3 vibration and the isotopic shifts with respect to parent $^{14}N^{14}N^{16}O$.

	Frequency (cm^{-1})		Isotopic shift (cm^{-1})	
	Experiment[a]	Calculated[b]	Experiment[a]	Calculated[b]
$^{14}N^{14}N^{16}O$	2235.6 (2223.8)	2339.5	...	...
$^{15}N^{14}N^{16}O$	2212.9 (2201.6)	2314.7	22.7 (22.2)	24.8
$^{14}N^{15}N^{16}O$	2188.8 (2177.7)	2289.8	46.8 (46.1)	49.7
$^{15}N^{15}N^{16}O$	2165.6 (2154.7)	2264.2	70.0 (69.1)	75.3
$^{14}N^{14}N^{17}O$	2232.0 (2220.1)	2336.6	3.6 (3.7)	2.9
$^{15}N^{14}N^{17}O$	2209.4 (2197.6)	2311.2	26.2 (26.2)	28.3
$^{14}N^{15}N^{17}O$	2185.7 (2174.2)	2286.6	49.9 (49.6)	52.9
$^{15}N^{15}N^{17}O$	2162.4 (2150.9)	2260.7	73.2 (72.9)	78.8
$^{14}N^{14}N^{18}O$	2228.7 (2216.7)	2336.6	6.9 (7.1)	2.9
$^{15}N^{14}N^{18}O$	2205.9 (2194.0)	2308.4	29.7 (29.8)	31.1
$^{14}N^{15}N^{18}O$	2182.7 (2171.0)	2284.1	52.9 (52.8)	55.4
$^{15}N^{15}N^{18}O$	2159.1 (2147.6)	2257.9	76.5 (76.2)	81.6

[a]Gas phase values in parentheses (from Refs. 44, 51–54, 86).
[b]B3LYP/AUG-cc-pVTZ; see text.

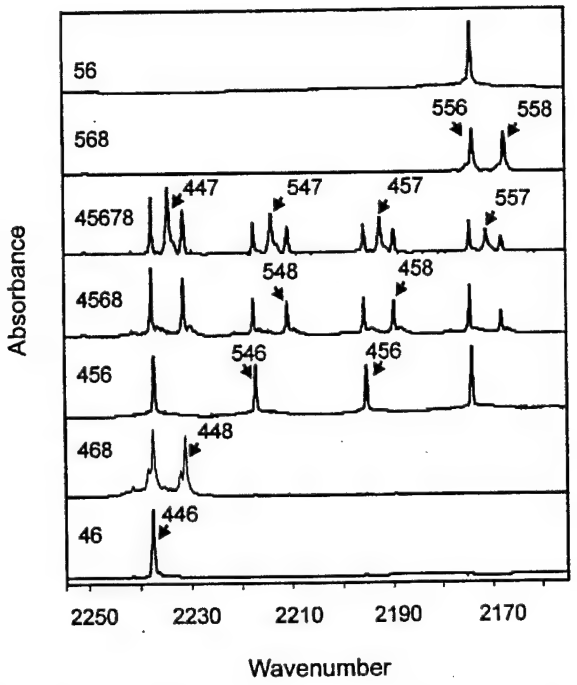

FIG. 1. Portions of IR spectra of N_2O isotopomers in the region of the ν_3 fundamental transition. The spectra were recorded in nitrogen matrices at 10 K. The labeling on the left indicates the isotopic composition of the mixture used in preparing the matrix. For instance, 456 denotes a mixture composed of equal fractions of ^{14}N and ^{15}N; 4568, a mixture composed of equal fractions of ^{14}N, ^{15}N, ^{16}O, and ^{18}O, and so forth. The symbols labeling individual species indicate their isotopic content, e.g., $^{14}N^{15}N^{18}O$ is labeled 458, and so on.

in nitrogen matrices, the values of the six combination bands involving ν_2 that we observed are always higher than the corresponding gas phase values (see Table V).

The intensity pattern for the three fundamental transitions is practically the same for all isotopomers. The strongest band, corresponding to ν_3, is about five times more intense than the band corresponding to ν_1 and about 35 times stronger than the ν_2 transition. The intensity ratios are similar to those observed in the gas phase,[61,73] and are consistent with the intensities predicted by B3LYP/AUG-cc-pVTZ: I = 396, 70, and 10 km/mol for ν_3, ν_1, and ν_2, respectively.

A. ν_3 vibration (Table I and Fig. 1)

The frequency for the parent $^{14}N_2{}^{16}O$ species is 2235.6 cm^{-1}; exactly the same value was previously reported for the nitrogen matrix.[103] Interestingly, a large blue shift with respect to the gas phase is observed, nearly constant for all isotopomers and ranging from 10.9 cm^{-1} for $^{15}N_2{}^{6}O$ to 12.0 cm^{-1} for $^{14}N_2{}^{18}O$. A blue shift was also encountered in solid $^{14}N_2O$, where the frequency is 2238 cm^{-1}.[95] This effect seems to be specific for the nitrogen-containing matrices: In argon[100] and xenon matrices[105] and xenon free-standing crystals[101] red shifts of 5.2, 9.3, and 9.0 cm^{-1}, respectively, have been detected. Adding krypton to deposition mixtures, we have observed several sites, of which the strongest was redshifted with respect to the gas phase by 4.9 cm^{-1}.

The shifts observed after an isotopic substitution at a particular position reflect the character of the vibration, which is essentially an N≡N stretch, with the amplitude of vibration of the central nitrogen atom much larger than that of the peripheral one, and a small contribution from the oxygen motion. Accordingly, $^{14}N \rightarrow {}^{15}N$ isotopic replacement of a central atom leads to the strongest shift. The observed values for $^{14}N^{15}N^{16}O$, $^{14}N^{15}N^{17}O$, and $^{14}N^{15}N^{18}O$ are 46.8, 46.3, and 46.0 cm^{-1}, respectively. Similarly, the shifts observed with regard to $^{15}N^{14}NO$ as a reference are 47.3, 47.0, and 46.8 cm^{-1} for $^{15}N^{15}N^{16}O$, $^{15}N^{15}N^{17}O$, and $^{15}N^{15}N^{18}O$, respectively. Upon substitution of the terminal nitrogen atom, the shifts are about half as large: 22.7, 22.6, and 22.8 cm^{-1} with respect to $^{15}N^{14}N^{16}O$, $^{15}N^{14}N^{17}O$, and $^{15}N^{14}N^{18}O$, respectively. Taking $^{14}N^{15}NO$ as a reference, the corresponding values are 23.2, 23.3, and 23.6 cm^{-1} for $^{15}N^{15}N^{16}O$, $^{15}N^{15}N^{17}O$, and $^{15}N^{15}N^{18}O$, respectively. Isotopic substitution of oxygen exerts only a minor effect, with shifts of 3.0–3.6 cm^{-1}.

The isotopic shifts in the matrix are usually somewhat larger than the corresponding values for the gas phase. This may be caused by a smaller anharmonicity in the solid phase, due to interaction with the environment.

B. ν_1 vibration (Table II and Fig. 2)

The frequency for the $^{14}N^{14}N^{16}O$ species is 1291.2 cm^{-1}, in excellent agreement with a previously reported value.[10] Similarly as for ν_3, a blue shift with respect to the gas phase is observed. It is very similar for all species and ranges from 5.4 cm^{-1} for $^{15}N^{14}N^{18}O$ to 6.5 cm^{-1} for

TABLE II. Experimental and calculated frequencies for the ν_1 vibration and the isotopic shifts with respect to parent $^{14}N^{14}N^{16}O$.

	Frequency (cm^{-1})		Isotopic shift (cm^{-1})	
	Experiment[a]	Calculated[b]	Experiment[a]	Calculated[b]
$^{14}N^{14}N^{16}O$	1291.2 (1284.9)	1323.6	...	...
$^{15}N^{14}N^{16}O$	1276.1 (1269.9)	1301.7	15.1 (15.0)	21.9
$^{14}N^{15}N^{16}O$	1286.9 (1280.4)	1321.4	4.3 (4.5)	2.2
$^{15}N^{15}N^{16}O$	1271.7 (1265.3)	1305.3	19.5 (19.6)	18.3
$^{14}N^{14}N^{17}O$	1270.6 (1264.7)	1300.4	20.6 (20.2)	23.2
$^{15}N^{14}N^{17}O$	1255.9 (1250.2)	1284.0	35.3 (34.7)	39.6
$^{14}N^{15}N^{17}O$	1265.4 (1259.3)	1297.8	25.8 (25.6)	25.8
$^{15}N^{15}N^{17}O$	1250.7 (1244.6)	1282.0	40.5 (40.3)	41.6
$^{14}N^{14}N^{18}O$	1252.5 (1246.9)	1279.1	38.7 (38.0)	44.5
$^{15}N^{14}N^{18}O$	1238.3 (1232.9)	1262.8	52.9 (52.0)	60.8
$^{14}N^{15}N^{18}O$	1246.4 (1240.3)	1276.2	44.8 (44.6)	47.4
$^{15}N^{15}N^{18}O$	1231.9 (1226.0)	1260.5	59.3 (58.9)	63.1

[a]Gas phase values in parentheses (from Refs. 45, 52, 86).
[b]B3LYP/AUG-cc-pVTZ; see text.

TABLE III. Experimental and calculated frequencies for the ν_2 vibration and the isotopic shifts with respect to parent $^{14}N^{14}N^{16}O$.

	Frequency (cm^{-1})		Isotopic shift (cm^{-1})	
	Experiment[a]	Calculated[b]	Experiment[a]	Calculated[b]
$^{14}N^{14}N^{16}O$	588.0 (588.8)	616.7	...	...
$^{15}N^{14}N^{16}O$	584.6 (585.3)	613.0	3.4 (3.5)	3.7
$^{14}N^{15}N^{16}O$	574.6 (575.4)	602.6	13.4 (13.4)	14.1
$^{15}N^{15}N^{16}O$	571.1 (571.9)	598.9	16.9 (16.9)	17.8
$^{14}N^{14}N^{17}O$	585.5 (586.4)	614.2	2.5 (2.4)	2.5
$^{15}N^{14}N^{17}O$	581.9	610.5	6.1	6.2
$^{14}N^{15}N^{17}O$	572.3	600.0	15.7	16.7
$^{15}N^{15}N^{17}O$	568.4	596.2	19.6	20.6
$^{14}N^{14}N^{18}O$	583.4 (584.2)	611.9	4.6 (4.6)	4.8
$^{15}N^{14}N^{18}O$	580.1 (580.7)	608.2	7.9 (8.1)	8.5
$^{14}N^{15}N^{18}O$	569.9 (570.8)	597.7	18.1 (18.0)	19.0
$^{15}N^{15}N^{18}O$	566.4 (567.2)	593.9	21.6 (21.6)	22.8

[a]Gas phase values in parentheses (from Refs. 52, 86).
[b]B3LYP/AUG-cc-pVTZ; see text.

$^{14}N^{15}N^{16}O$. In solid $^{14}N_2O$, the blue shift is even larger, the observed value for ν_1 is 1293.4 and that for $^{15}N^{14}N^{16}O$ is 1279.8 cm^{-1}. This is again in contrast to solid argon[97,100] and xenon,[101] where small red shifts of the order of 1–4 cm^{-1} were found. Our data for krypton are consistent with this trend, giving a red shift of about 7 cm^{-1}.

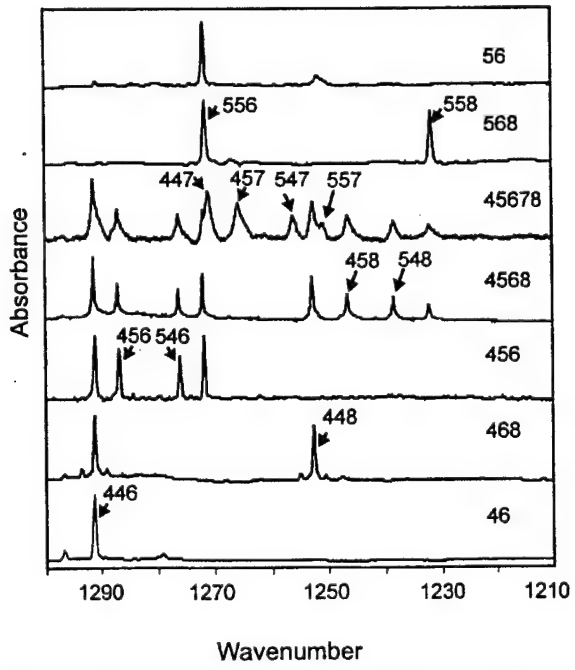

FIG. 2. Portions of IR spectra of N_2O isotopomers in the region of ν_1 fundamental transition. See caption to Fig. 1 for details.

This vibration has been often referred to as N^+-O^- stretching, but the calculated normal mode resembles more a symmetric stretch involving the whole molecule, with the amplitudes of motion of the two terminal atoms much larger than that of the central one. The largest amplitude corresponds to the oxygen atom. Indeed, the most prominent spectral shifts are observed for samples containing oxygen isotopes. $^{16}O\rightarrow{}^{17}O$ substitution leads to the shifts of 20.6, 20.2, 21.5, and 21.0 cm^{-1} for $^{14}N^{14}N^{17}O$, $^{15}N^{14}N^{17}O$, $^{14}N^{15}N^{17}O$, and $^{15}N^{15}N^{17}O$, respectively. Upon $^{16}O\rightarrow{}^{18}O$ replacement, the corresponding values are 38.7, 37.8, 40.5, and 39.8 cm^{-1} for $^{14}N^{14}N^{18}O$, $^{15}N^{14}N^{18}O$, $^{14}N^{15}N^{18}O$, and $^{15}N^{15}N^{18}O$, respectively. The shifts accompanying peripheral $^{14}N\rightarrow{}^{15}N$ substitution are also quite substantial and span a narrow range between 14.2 and 15.2 cm^{-1}. The smallest shifts, 4.3–6.4 cm^{-1} correspond to the $^{14}N\rightarrow{}^{15}N$ substitution of the central nitrogen atom.

Similarly as in the case of ν_3, we observe somewhat larger isotopic shifts in the matrix than in the gas phase. Again, this may mean that the vibration becomes more harmonic in the solid environment.

C. ν_2 vibration (Table III and Fig. 3)

The position of the band in a nitrogen matrix is redshifted by only 0.8 cm^{-1} with respect to the gas phase. In free-standing crystals of xenon the red shift is 4.9 cm^{-1}.[101] In argon matrices, a doublet at 589.4 and 588.7 cm^{-1} was observed, and assigned to splitting of the degeneracy of the ν_2 vibration due to a site effect.[99] We have not detected a similar splitting phenomenon in nitrogen matrices. The degen-

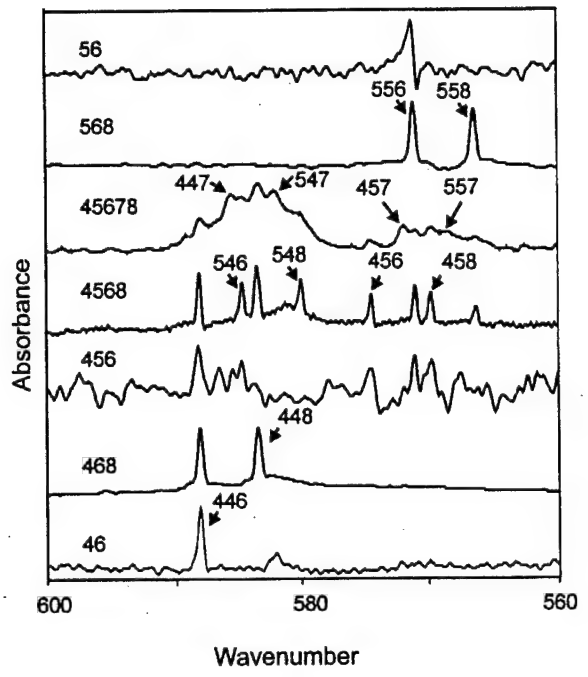

FIG. 3. Portions of IR spectra of N_2O isotopomers in the region of ν_2 fundamental transition. See caption to Fig. 1 for details.

TABLE IV. Observed frequencies of the overtone bands.

	Frequency[a] (cm^{-1})			
	$2\nu_1$	$3\nu_1$	$2\nu_2$	$2\nu_3$
$^{14}N^{14}N^{16}O$	2575.3	3853.7	1166.6	4471.6
	(2563.3)	(3836.4)	(1168.1)	(4417.4)
$^{15}N^{14}N^{16}O$	2546.3		1158.7	4426.9
	(2534.5)		(1160.0)	(4373.6)
$^{14}N^{15}N^{16}O$	2565.2		1142.3	4379.0
	(2552.4)		(1144.3)	(4326.6)
$^{15}N^{15}N^{16}O$	2534.7		1134.9	4332.7
	(2523.3)		(1136.5)	(4281.3)
$^{14}N^{14}N^{17}O$	2534.4		1160.2	4464.2
	(2524.7)		(1161.5)	
$^{15}N^{14}N^{17}O$	2507.8		1151.9	4419.2
	(2497.1)		(1153.0)	
$^{14}N^{15}N^{17}O$	2523.2		1135.9	4371.9
	(2511.2)		(1138.3)	
$^{15}N^{15}N^{17}O$	2494.5		1129.1	4325.3
	(2482.9)		(1130.2)	
$^{14}N^{14}N^{18}O$	2501.4		1154.1	4457.5
	(2491.2)		(1155.1)	(4403.0)
$^{15}N^{14}N^{18}O$	2474.7		1145.5	4412.1
	(2465.0)		(1146.2)	
$^{14}N^{15}N^{18}O$	2486.4		1128.3	4366.4
	(2474.7)		(1132.6)	
$^{15}N^{15}N^{18}O$	2457.4		1123.0	4318.8
	(2447.2)		(1124.3)	(4267.0)

[a]Gas phase values in parentheses (from Refs. 44, 51–54, 68, 86).

eracy of the ν_2 level is also maintained in solid N_2O.[95] In the latter case, the reported frequency is 591.0 cm^{-1}, and thus blueshifted with respect to the gas phase, in contrast to all matrix isolation data.

Since ν_2 is a bending vibration, with the largest amplitude of motion exhibited by the central nitrogen atom, the isotopic replacement of the latter should lead to largest shifts. This is indeed the case; the observed values are between 13.2 and 13.7 cm^{-1}. Replacement of a side ^{14}N atom by ^{15}N leads to shifts between 3.3 and 3.9 cm^{-1}. For $^{16}O \rightarrow {}^{17}O$ and $^{16}O \rightarrow {}^{18}O$ substitutions, the shifts fall between 2.3–2.7 cm^{-1} and 4.5–4.7 cm^{-1}, respectively.

Contrary to the cases of ν_1 and ν_3 vibrations, the observed matrix isotopic shifts are practically identical to those in the gas phase, in nice agreement with the observation that the ν_2 vibration is almost harmonic.[84]

D. Combinations and overtones

Tables IV and V contain the frequencies of overtone and combination bands, along with the corresponding gas phase data. These values contribute further evidence for the specific effects exerted by the nitrogen matrix upon the ν_1 and ν_3 stretches. For instance, the blue frequency shifts in N_2 matrix for the first overtones of ν_3 and ν_1 are above 50 cm^{-1} and about 12 cm^{-1}, respectively. In Ar matrices, red shifts of 3–4 cm^{-1} were observed for ν_1;[99] in xenon, the red shift is larger, 10.3 cm^{-1}.[101] The same is true for combination bands; the gas phase values are bracketed on the blue side by those obtained in nitrogen, and on the red side by those measured in argon or xenon.

Calculated frequencies for all isotopomers along with the experimental ones are presented in Tables I–III. The agreement is very good, especially when the isotopic shifts are compared. For a particular vibration, the ratio of experimental and calculated frequencies is constant within less than 0.4% along the series of all isotopomers. These ratios vary slightly for the three fundamentals, being 0.977, 0.953, and 0.956 for ν_1, ν_2, and ν_3, respectively. Figure 4 presents the correlation between calculated and observed spectral shifts. With the above ratios as scaling factors, the isotopic spectral shifts for ν_1, ν_2, and ν_3 could be reproduced with standard deviations of 2.99, 0.12, and 1.65 cm^{-1}, respectively. It is worth noticing that the best accuracy was obtained for the ν_2 vibration; it is known that the bending potential is almost harmonic.[84]

IV. SUMMARY AND CONCLUSIONS

Frequencies of fundamental, overtone and combination bands for all 12 isotopomers of N_2O have been obtained and compared with corresponding data for the gas phase and other matrices. Specific influence of the nitrogen matrix upon the shape of the potential energy surface has been discussed, resulting in a blue shift for the frequencies of both stretching vibrations. Since an analogous shift has been observed for solid N_2O,[95] one may postulate that the factor responsible for the blue shift has to do with a repulsive character of the N–N interaction potential, contrary to the case of the interactions with argon or xenon. In consequence, ν_1 and ν_3 vibrations become more harmonic in a nitrogen matrix.

Our data may serve as input to further refinement of the force field of nitrous oxide. It was previously attempted to

TABLE V. Observed frequencies of the combination bands.

	Frequency[a] (cm^{-1})					
	$\nu_1+\nu_2$	$\nu_1+\nu_3$	$\nu_2+\nu_3$	$\nu_1+2\nu_2$	$\nu_1+3\nu_2$	$2\nu_2+\nu_3$
$^{14}N^{14}N^{16}O$	1885.3	3499.3	2809.3	2466.5	3052.3	3374.5
	(1880.3)	(3480.8)	(2798.3)	(2462.0)	(3046.2)	(3364.0)
$^{15}N^{14}N^{16}O$		3461.9	2783.6	2444.4		
		(3443.7)	(2772.8)	(2431.3)		
$^{14}N^{15}N^{16}O$		3450.7	2750.4	2435.5		
		(3432.2)	(2739.6)			
$^{15}N^{15}N^{16}O$	1847.8	3411.0	2723.2	2413.8		3274.8
	(1842.4)	(3394.2)	(2713.1)			(3264.7)
$^{14}N^{14}N^{17}O$		3474.7	2802.5			
$^{15}N^{14}N^{17}O$		3440.4	2777.5			
$^{14}N^{15}N^{17}O$		3425.6	2746.5			
$^{15}N^{15}N^{17}O$		3391.8	2718.5			
$^{14}N^{14}N^{18}O$		3452.7	2798.2	2416.5		
		(3435.0)	(2787.0)			
$^{15}N^{14}N^{18}O$		3416.2	2772.1	2393.9		
		(3398.4)				
$^{14}N^{15}N^{18}O$		3403.4	2739.6	2385.3		
		(3385.2)	(2728.6)			
$^{15}N^{15}N^{18}O$		3363.8	2711.8			
		(3347.4)	(2701.6)			

[a]Gas phase values in parentheses (from Refs. 44, 52, 53, 66, 86).

build a force field for the N_2O molecule in the nitrogen matrix cage, basing exclusively on the values of vibrational frequencies measured in a matrix.[96] Five different N_2O isotopomers were used. However, due to insufficient number of experimental data points (32), the force constants could not be obtained without introducing additional constraints on the potential energy. With over 100 frequency values provided by this work, we believe such an endeavor is now feasible.

Finally, we would like to use our data for a kind of prediction that may be of importance in atmospheric chemistry. It has been postulated that the atmospheric enrichment in some N_2O isotopomers is related to various rates of photolysis of different isotopic species.[9] This, in turn, should be due to relatively small shifts in the electronic absorption spectrum of individual isotopomers in the 190–210 nm region. These shifts may be predicted on the basis of ZPE energies. Such an analysis has been previously presented for eight isotopomers.[9] We have repeated this procedure, adding an additional four species. The results are shown in Fig. 5. It is readily seen that the $^{15}N^{15}N^{17}O$ and $^{15}N^{15}N^{18}O$ species should exhibit the largest blue shift. This means that they should be the most difficult to photolyze, and one can therefore expect their presence in the atmosphere in larger than statistically dictated amounts.

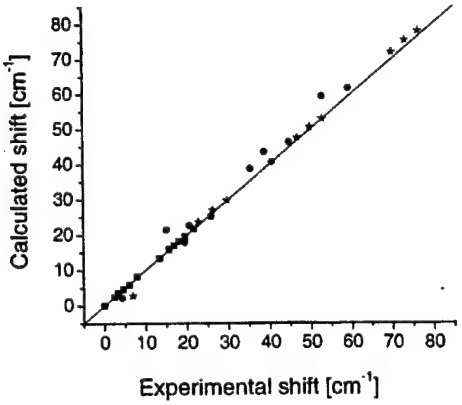

FIG. 4. Correlation between experimental and calculated (B3LYP/AUG-cc-pVTZ) frequency shifts upon isotopic substitution of N_2O. ν_1, circles; ν_2, squares; ν_3, stars. The calculated values have been scaled by the factors of 0,977, 0.953, and 0.956 for ν_1, ν_2, and ν_3, respectively (see text for details).

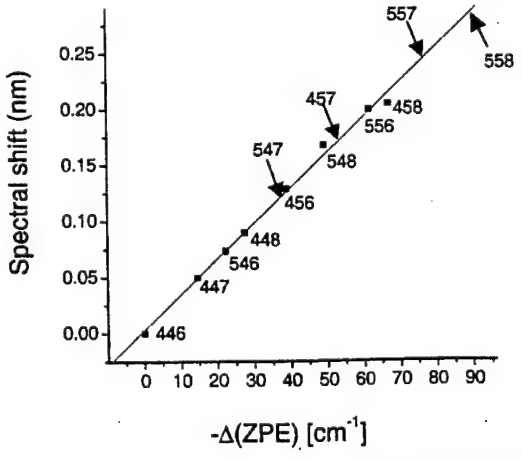

FIG. 5. Correlation between the changes in experimentally determined ZPEs with respect to $^{14}N_2{}^{16}O$ and the blue shift in the electronic spectrum. The spectral shifts for points indicated by squares were taken from Ref. 9. The arrows indicate predicted shifts for the four remaining isotopomers based on the results of this work.

ACKNOWLEDGMENTS

This project was supported by grants from the NREL DDRD program and from DARPA/AFOSR (F49620-98-1-0483). Part of the instrumentation used in this project was obtained by funds from a DURIP grant.

[1] W. C. Trogler, Coord. Chem. Rev. **187**, 303 (1999).
[2] A. A. Lacis, J. Hansen, P. Lee, T. Mitchell, and S. Lebedeff, Geophys. Res. Lett. **8**, 1035 (1981).
[3] P. J. Q. Crutzen, Q. J. R. Meteorol. Soc. **96**, 320 (1970); J. Geophys. Res. **76**, 7311 (1971).
[4] F. S. Rowland, Annu. Rev. Phys. Chem. **42**, 731 (1991).
[5] K. R. Kim and H. Craig, Science **262**, 1855 (1993).
[6] S. S. Cliff and M. Thimens, Science **278**, 1774 (1997).
[7] S. S. Cliff, C. A. M. Brenninkmeijer, and M. H. Thiemens, J. Geophys. Res., [Oceans] **104**, 16171 (1999).
[8] T. Rahn and M. Wahlen, Science **278**, 1776 (1997).
[9] Y. L. Yung and C. Miller, Science **278**, 1778 (1997).
[10] N. Yoshida and S. Toyoda, Nature (London) **405**, 330 (2000).
[11] N. Yoshida, Nature (London) **335**, 528 (1988).
[12] S. W. A. Naqvi, T. Yoshinari, D. A. Jayakumar, M. A. Altabet, P. V. Narvekar, A. H. Devol, J. A. Brandes, and L. A. Codispoti, Nature (London) **405**, 330 (2000).
[13] T. Yoshinari and M. Wahlen, Nature (London) **317**, 349 (1985); M. Wahlen and T. Yoshinari, *ibid.* **313**, 780 (1985).
[14] K.-R. Kim and H. Craig, Nature (London) **347**, 58 (1990).
[15] M. J. Prather, Science **279**, 1339 (1998).
[16] E. G. Estupiñán, R. E. Stickel, and P. H. Wine, Chem. Phys. Lett. **336**, 109 (2001).
[17] T. Rahn, H. Zhang, M. Wahlen, and G. A. Blake, Geophys. Res. Lett. **25**, 4489 (1998).
[18] H. Umemoto, Chem. Phys. Lett. **314**, 267 (1999).
[19] T. Röckmann, C. A. M. Brenninkmeijer, M. Wollenhaupt, J. N. Crowley, and P. J. Crutzen, Geophys. Res. Lett. **27**, 1399 (2000).
[20] S. Toyoda and N. Yoshida, Anal. Chem. **71**, 4711 (1999).
[21] D. W. T. Griffith and B. Galle, Atmos. Environ. **34**, 1087 (2000).
[22] D. K. Zhou, G. E. Bingham, B. K. Rezai, G. P. Anderson, D. R. Smith, and R. M. Nadile, J. Geophys. Res., [Oceans] **102**, 3559 (1997).
[23] B. Galle, L. Klemedtsson, and D. W. T. Griffith, J. Geophys. Res., [Oceans] **99**, 16575 (1994).
[24] J. Notholt, Geophys. Res. Lett. **21**, 2385 (1994).
[25] R. N. Horton and C. P. Rinsland, Appl. Opt. **30**, 389 (1991).
[26] I. Murata, N. Fukuma, Y. Ohtaki, H. Fukunishi, H. Kanazawa, H. Nakane, and K. Shibasaki, Adv. Space Res. **24**, 1623 (1999).
[27] D. C. Scott, R. L. Herman, C. R. Webster, R. D. May, G. J. Flesch, and E. J. Moyer, Appl. Opt. **38**, 4609 (1999).
[28] T. Güllük, F. Slemr, and B. Stauffer, J. Geophys. Res., [Oceans] **103**, 15971 (1998).
[29] C. B. Carlisle, H. Risis, and D. E. Cooper, Appl. Opt. **34**, 938 (1995).
[30] W. S. Richardson and E. B. Wilson, J. Chem. Phys. **18**, 694 (1950).
[31] G. Herzberg and L. Herzberg, J. Chem. Phys. **18**, 1551 (1950).
[32] J. Bigeleisen and L. Friedman, J. Chem. Phys. **18**, 1656 (1950).
[33] H. W. Thompson and R. L. Williams, Proc. R. Soc. London, Ser. A **208**, 326 (1951).
[34] H. J. Callomon, D. C. McKean, and H. W. Thompson, Proc. R. Soc. London, Ser. A **208**, 332 (1951).
[35] R. M. Goody and T. W. Wormell, Proc. R. Soc. London, Ser. A **209**, 178 (1951).
[36] D. F. Eggers and B. L. Crawford, J. Chem. Phys. **19**, 1554 (1951).
[37] K. Lakshmi, K. Narahari Rao, and H. H. Nielsen, J. Chem. Phys. **24**, 811 (1956).
[38] K. Narahari Rao and H. H. Nielsen, Can. J. Phys. **34**, 1147 (1956).
[39] M. Migeotte, L. Neven, and J. Swenson, Mem. Soc. R. Sci. Liège, Vol. Hors Ser. 2 (1957).
[40] G. M. Begun and W. H. Fletcher, J. Chem. Phys. **28**, 414 (1957).
[41] E. D. Tidwell, E. K. Plyler, and W. S. Benedict, J. Opt. Soc. Am. **50**, 1243 (1960).
[42] D. E. Burch and D. Williams, Appl. Opt. **1**, 473 (1960).
[43] P. E. Fraley, W. W. Brimm, and K. Narahari Rao, J. Mol. Spectrosc. **9**, 487 (1962).
[44] L. Plíva, J. Mol. Spectrosc. **12**, 360 (1964).
[45] R. P. Grosso and T. K. McCubbin, Jr., J. Mol. Spectrosc. **13**, 240 (1964).
[46] E. K. Plyler, E. D. Tidwell, and A. G. Maki, J. Res. Natl. Bur. Stand. **68A**, 79 (1964).
[47] H. Yamada and W. B. Person, J. Chem. Phys. **45**, 1861 (1966).
[48] J. Lemaire, J. Houriez, J. Thibault, and B. Maillard, J. Phys. (Paris) **32**, 35 (1971).
[49] J. Walrand, G. Blanquet, and C. P. Courtoy, Ann. Soc. Scient. Bruxelles **87**, 409 (1973).
[50] J. M. Krell and R. L. Sams, J. Mol. Spectrosc. **51**, 492 (1974).
[51] R. Farrenq and J. Dupre-Maquaire, J. Mol. Spectrosc. **49**, 268 (1974).
[52] C. Amiot and G. Guelachvili, J. Mol. Spectrosc. **51**, 475 (1974).
[53] C. Amiot and G. Guelachvili, J. Mol. Spectrosc. **59**, 171 (1976).
[54] C. Amiot, J. Mol. Spectrosc. **59**, 191 (1976); **59**, 380 (1976).
[55] B. G. Whitford, K. J. Siemsen, H. D. Riccius, and G. R. Hanes, Opt. Commun. **14**, 70 (1975).
[56] J. P. Boissy, A. Valentin, P. Cardinet, M. L. Claude, and A. Henry, J. Mol. Spectrosc. **57**, 391 (1975).
[57] B. G. Whitford, K. J. Siemsen, H. D. Riccius, and G. R. Hanes, Opt. Commun. **14**, 70 (1975).
[58] G. Blanquet, J. Walrand, and C. P. Courtoy, Ann. Soc. Scient. Bruxelles **89**, 93 (1975).
[59] J. Perrizo, L. A. Pugh, and K. Narahari Rao, J. Mol. Spectrosc. **57**, 397 (1975).
[60] J. Dupre-Maquaire and P. Pinson, J. Mol. Spectrosc. **58**, 239 (1975).
[61] R. H. Kagann, J. Mol. Spectrosc. **95**, 297 (1982).
[62] M. J. Reisfeld and H. Flicker, Appl. Opt. **18**, 1136 (1979).
[63] G. Guelachvili, Can. J. Phys. **60**, 1334 (1982).
[64] K. Jolma, J. Kauppinen, and V. M. Horneman, J. Mol. Spectrosc. **101**, 278 (1983).
[65] C. R. Pollock, F. R. Petersen, D. A. Jennings, J. S. Wells, and A. G. Maki, J. Mol. Spectrosc. **107**, 62 (1984).
[66] J. S. Wells, D. A. Jennings, A. Hinz, J. S. Murray, and A. G. Maki, J. Opt. Soc. Am. B **2**, 857 (1985).
[67] J. S. Wells, A. Hinz, and A. G. Maki, J. Mol. Spectrosc. **114**, 84 (1985).
[68] L. R. Zink, J. S. Wells, and A. G. Maki, J. Mol. Spectrosc. **123**, 426 (1987); Z. Phys. D: At., Mol. Clusters **5**, 351 (1987).
[69] M. P. Esplin, W. M. Barowy, R. J. Huppi, and G. A. Vanasse, Mikrochim. Acta (Wien) **2**, 403 (1988).
[70] M. D. Vanek, M. Schneider, J. S. Wells, and A. G. Maki, J. Mol. Spectrosc. **134**, 154 (1989).
[71] M. D. Vanek, D. A. Jennings, J. S. Wells, and A. G. Maki, J. Mol. Spectrosc. **138**, 79 (1989).
[72] A. G. Maki, J. S. Wells, and M. D. Vanek, J. Mol. Spectrosc. **138**, 84 (1989).
[73] R. A. Toth, J. Mol. Spectrosc. **40**, 588 (1971); **40**, 605 (1971); **197**, 158 (1999); Appl. Opt. **23**, 1825 (1984); **30**, 5289 (1991); **32**, 7326 (1993); J. Opt. Soc. Am. B **3**, 1263 (1986); **4**, 357 (1987); J. Quant. Spectrosc. Radiat. Transf. **66**, 285 (2000).
[74] T. L. Tan, E. C. Looi, and K. T. Lua, J. Mol. Spectrosc. **154**, 218 (1992).
[75] A. Campargue, D. Permogorov, M. Bach, M. A. Temsamani, J. V. Auwera, and M. Fujii, J. Chem. Phys. **103**, 5931 (1995).
[76] P. Jin, H. Wang, S. Oatis, G. E. Hall, and T. J. Sears, J. Mol. Spectrosc. **173**, 442 (1995).
[77] D. R. Willey, K. A. Ross, A. Mullin, S. Schowen, L. Zheng, and G. Flynn, J. Mol. Spectrosc. **169**, 66 (1995).
[78] Y. He, M. Hippler, and M. Quack, Chem. Phys. Lett. **289**, 527 (1998).
[79] M. Hippler and M. Quack, Chem. Phys. Lett. **314**, 273 (1999).
[80] L. B. Brown and R. A. Toth, J. Opt. Soc. Am. B **2**, 842 (1985).
[81] W. B. Olson, A. G. Maki, and W. J. Lafferty, J. Phys. Chem. Ref. Data **10**, 1065 (1981).
[82] G. Guelachvili and K. Narahari Rao, *Handbook of Infrared Standards* (Academic, New York, 1986).
[83] A. G. Maki and J. S. Wells, NIST Special Publication 821, Web Version 1.3, 1998, http://physics.nist.gov/PhysRefData/wavenum/html/contents.html.
[84] I. Suzuki, J. Mol. Spectrosc. **32**, 54 (1969).
[85] M. Kobayashi and I. Suzuki, J. Mol. Spectrosc. **125**, 24 (1987).
[86] A. Chédin, C. Amiot, and Z. Cihla, J. Mol. Spectrosc. **63**, 348 (1976).
[87] J.-L. Teffo and A. Chédin, J. Mol. Spectrosc. **135**, 389 (1989).
[88] M. Lacy and D. H. Whiffen, Mol. Phys. **45**, 241 (1982).
[89] A.-T. Wong and G. B. Bacskay, Chem. Phys. Lett. **207**, 360 (1993).
[90] J. M. L. Martin, P. R. Taylor, and T. J. Lee, Chem. Phys. Lett. **205**, 535 (1993).
[91] J. Zúñiga, M. Alacid, A. Bastida, and A. Requena, J. Chem. Phys. **105**, 6099 (1996).

[92] W. D. Allen, Y. Yamaguchi, A. G. Csaszar, D. A. Clabo, Jr., R. B. Remington, and H. Schaefer III, Chem. Phys. **145**, 427 (1990).
[93] W. D. Allen and A. G. Csaszar, J. Chem. Phys. **98**, 2983 (1993).
[94] A. G. Csaszar, J. Phys. Chem. **98**, 8823 (1994).
[95] D. A. Dows, J. Chem. Phys. **26**, 745 (1957).
[96] D. Foss Smith, Jr., J. Overend, R. C. Spiker, and L. Andrews, Spectrochim. Acta Part A **28A**, 87 (1972).
[97] L. Andrews and G. L. Johnson, J. Chem. Phys. **76**, 2875 (1982).
[98] J. N. Crowley and J. R. Sodeau, J. Phys. Chem. **91**, 2024 (1987).
[99] J. R. Sodeau and R. Withnall, J. Phys. Chem. **89**, 4484 (1985).
[100] H. Chabbi, P. R. Dahoo, B. Gauthier-Roy, A. M. Vasserot, and L. Abouaf-Marguin, J. Phys. Chem. A **104**, 1670 (2000).
[101] W. G. Lawrence and A. Apkarian, J. Chem. Phys. **97**, 2224 (1992).
[102] L. M. Nxumalo and T. A. Ford, J. Mol. Struct. **327**, 145 (1994).
[103] M. Bahou, L. Schriver-Mazzuoli, C. Camy-Peyret, A. Schiver, T. Chiavassa, and J. P. Aycard, Chem. Phys. Lett. **265**, 145 (1997).
[104] M. Bahou, L. Schriver-Mazzuoli, C. Camy-Peyret, and A. Schiver, J. Chem. Phys. **108**, 6884 (1998).
[105] H. Krueger and E. Weitz, J. Chem. Phys. **96**, 2846 (1992).
[106] M. E. Jacox, J. Chem. Phys. **93**, 7622 (1990).
[107] M. E. Jacox and W. E. Thompson, J. Chem. Phys. **93**, 7609 (1990).
[108] W. E. Thompson and M. E. Jacox, J. Chem. Phys. **93**, 3856 (1990).
[109] D. E. Milligan and M. E. Jacox, J. Chem. Phys. **55**, 3404 (1971).
[110] J. Hacaloglu, S. Suzer, and L. Andrews, J. Phys. Chem. **94**, 1759 (1990).
[111] G. P. Kushto, P. F. Souter, L. Andrews, and M. Neurock, J. Chem. Phys. **106**, 5894 (1997).
[112] L. Andrews, G. V. Chertihin, A. Citra, and M. Neurock, J. Phys. Chem. **100**, 11235 (1996).
[113] M. S. Gudipati, Chem. Phys. Lett. **248**, 452 (1996).
[114] J. B. Foresman and Æ. Frisch, *Exploring Chemistry with Electronic Structure Methods* (Gaussian, Inc., Pittsburgh, Pennsylvania, 1996).
[115] F. Jensen, *Introduction to Computational Chemistry* (Wiley, Chichester, 1999).
[116] M. J. Frisch, G. W. Trucks, H. B. Schlegel *et al.*, GAUSSIAN 94, Revision E.1, Gaussian, Inc. Pittsburgh, Pennsylvania, 1995.
[117] M. J. Frisch, G. W. Trucks, H. B. Schlegel *et al.*, GAUSSIAN 98, Revision A.7, Gaussian, Inc. Pittsburgh, Pennsylvania, 1998.
[118] A. D. Becke, J. Chem. Phys. **98**, 5648 (1993).
[119] C. Lee, W. Yang, and R. G. Parr, Phys. Rev. B **37**, 785 (1988).
[120] T. H. Dunning, Jr., J. Chem. Phys. **90**, 1007 (1989); R. A. Kendall, T. H. Dunning, Jr., and R. J. Harrison, *ibid.* **96**, 6796 (1992); A. K. Wilson, T. van Mourik, and T. H. Dunning, Jr., J. Mol. Struct. **388**, 339 (1996).
[121] H. Akagi, A. Yokoyama, Y. Fujimura, and T. Takayanagi, Chem. Phys. Lett. **324**, 423 (2000).
[122] D.-Y. Hwang and A. M. Mebel, Chem. Phys. **259**, 89 (2000).
[123] J. M. L. Martin and T. Lee, J. Chem. Phys. **98**, 7951 (1993).
[124] A. Brown, P. Jimeno, and G. G. Balint-Kurti, J. Phys. Chem. A **103**, 11089 (1999).
[125] A. H. H. Chang and D. R. Yarkony, J. Chem. Phys. **99**, 6824 (1993).
[126] K. Mogi, T. Komine, and K. Hirao, J. Chem. Phys. **95**, 8999 (1991).
[127] D. Feller, J. Comput. Chem. **17**, 1571 (1996).
[128] R. G. Shulman, B. P. Dailey, and C. H. Townes, Phys. Rev. **78**, 145 (1950).

Arylpentazoles Revisited: Experimental and Theoretical Studies of 4-Hydroxyphenylpentazole and 4-Oxophenylpentazole Anion

Vladimir Benin,[†,§] Piotr Kaszynski,[*,†] and J. George Radziszewski[‡,#]

Organic Materials Research Group Department of Chemistry, Vanderbilt University, Nashville, Tennessee 37235, Department of Chemistry, Colorado School of Mines, Golden, Colorado 80401, and National Renewable Energy Laboratory, Golden, Colorado 80401

piotr@ctrvax.vanderbilt.edu

Received November 14, 2001

Kinetic measurements for the degradation of 4-hydroxyphenylpentazole (**2a**) and its salt **2b**-NBu_4 in CD_3OD and in CD_2Cl_2 provided a set of activation parameters. The resulting free energies of activation in methanol ($\Delta G^{\ddagger}_{298}$ = 19.7 kcal/mol for **2a** and $\Delta G^{\ddagger}_{298}$ = 20.6 kcal/mol for **2b**-NBu_4) were compared with previous results for the 4-chloro derivative, **2c**, and collectively correlated with results of gas-phase calculations at the B3LYP/6-31+G(d,p) level of theory. This, and another linear correlation of the seven computed $\Delta G^{\ddagger}_{298}$ values with the previously reported kinetic data of Ugi and Huisgen, gave the basis for the estimation of the stability of pentazole anion (**1**) and its derivatives in solutions. Thus, $N_5(-)$ is predicted to have $t_{1/2}$ = 2.2 d, while the half-lifetime for HN_5 is expected to be only about 10 min in methanol at 0 °C. Controlled ozonolysis of **2b**-NBu_4 followed by ^1H and ^{15}N NMR spectroscopy shows a preferential destruction of the N_5 ring, which excludes it from possible methods for preparation of the parent pentazole.

Introduction

Current interest in allotropes of nitrogen[1−4] and nitrogen analogues of metallocenes[5,6] has identified pentazole $N_5(-)$ (**1**) as a possible precursor. Several gas-phase calculations predict anion **1** to be an isolable stable species separated by a barrier of at least 19 kcal/mol from the thermodynamically stable $N_3(-)$ and N_2.[5,7,8] Despite experimental efforts, the anion has remained elusive, and only arylpentazoles have been isolated and extensively characterized to date.[8,9]

In a simple scenario, the preparation of the parent pentazole anion **1** can be envisioned as a two-step process shown in Scheme 1. In the first step, a substituted pentazole **C** is formed by the reaction of $N_3(-)$ with an electrophilic two-nitrogen fragment as in **A** or **B**. Subsequently, the protecting group PG, such as carboxyl,[10] in pentazole **C** is removed to form **1**. Unfortunately, the choice of stable diazonium cation **A** appears to be limited to aryl derivatives, and our attempts to use other compounds with electrophilic two-nitrogen fragments such as azenes with a leaving group L (**B** in Scheme 1) have been discouraging thus far.[11−13]

Scheme 1

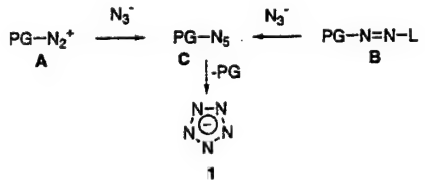

Removal of a benzene ring from **C** to form **1** was first attempted on 4-dimethylaminophenylpentazole by saturation of the solutions with ozone.[14] Mass spectrometric analysis of the reaction mixture did not find $N_5(-)$ among the products, but it is unclear whether a more controlled approach, with limited amounts of ozone, would be more successful.

We decided to reinvestigate the ozonolysis route to **1** and focused on two arylpentazoles, 4-hydroxyphenylpentazole (**2a**) and 4-oxophenylpentazole anion (**2b**), which were only briefly mentioned in the literature.[15−17] The

* To whom correspondence should be addressed. Piotr Kaszynski, Organic Materials Research Group, Department of Chemistry, Vanderbilt University, Box 1822 Station B, Nashville, TN 37235. Phone/fax: (615) 322-3458.
† Vanderbilt University.
‡ Colorado School of Mines.
# National Renewable Energy Laboratory.
§ Current address: Department of Chemistry, University of Dayton, 300 College Park, Dayton, OH 45469.

(1) Ferris, K. F.; Bartlett, R. J. *J. Am. Chem. Soc.* **1992**, *114*, 8302−8303.
(2) Glukhovtsev, M. N.; Jiao, H.; Schleyer, P. v. R. *Inorg. Chem.* **1996**, *35*, 7124−7133.
(3) Nguyen, M. T.; Ha, T.-K. *Chem. Phys. Lett.* **2001**, *335*, 311−320.
(4) Gagliardi, L.; Orlandi, G.; Evangelisti, S.; Roos, B. O. *J. Chem. Phys.* **2001**, *114*, 10733−10737.
(5) Nguyen, M. T.; McGinn, M. A.; Hegarty, A. F.; Elguéro, J. *Polyhedron* **1985**, *4*, 1721−1726.
(6) Lein, M.; Frunzke, J.; Timoshkin, A.; Frenking, G. *Chem. Eur. J.* **2001**, *7*, 4155−4163.
(7) Glukhovtsev, M. N.; Schleyer, P. v. R.; Maerker, C. *J. Phys. Chem.* **1993**, *97*, 8200−8206.
(8) Butler, R. N. In *Compehensive Heterocyclic Chemistry II*; Storr, R. C., Ed.; Elsevier Science Inc.: New York, 1996; Vol. 4; pp 897−911.
(9) Ugi, I. In *Hetarene III part 4*; Schaumann, E., Ed.; Georg Thieme Verlag: Stuttgart, 1994; Houben-Weyl Vol. E8d; pp 796−803.
(10) The pentazolecarboxylate anion could not be located on the potential energy surface as a stable species and spontaneously decomposes to **1** and CO_2, according to our calculations at the B3LYP/6-31+G(d) level. Thus, generation of the carboxylate anion would be one of the best routes to **1**.
(11) Benin, V.; Kaszynski, P.; Radziszewski, J. G. *J. Org. Chem.*, submitted.
(12) Benin, V.; Kaszynski, P.; Radziszewski, J. G. *Tetrahedron*, submitted.
(13) Benin, V.; Kaszynski, P.; Young, V. G., Jr.; Radziszewski, J. G., submitted.
(14) Ugi, I. *Angew. Chem.* **1961**, *73*, 172.
(15) Huisgen, R.; Ugi, I. *Chem. Ber.* **1957**, *90*, 2914−2927.
(16) Ugi, I.; Perlinger, H.; Behringer, L. *Chem. Ber.* **1958**, *91*, 2324−2329.

10.1021/jo0110754 CCC: $22.00
Published on Web 01/29/2002

Scheme 2

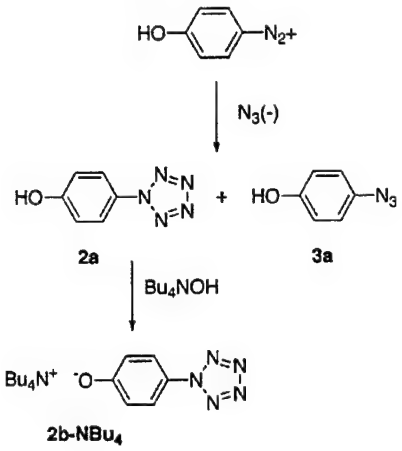

choice for anion **2b** was dictated by the reported high thermal stability of the pentazole ring,[17] and enhanced reactivity of the benzene ring toward ozone when substituted with an electron-donating group.

Here we report the synthesis of 4-hydroxyphenylpentazole (**2a**) and its O-anion **2b-NBu$_4$**, derive activation parameters for their thermal decomposition, and discuss the reaction of anion **2b** with ozone. The analysis of experimental results is aided with DFT calculations, which allow the prediction of the stability of **1** and other pentazole derivatives.

Results

Synthesis. 4-Hydroxyphenylpentazole (**2a**) was prepared in about 40% yield as shown in Scheme 2, according to a general procedure reported by Ugi and Huisgen.[16] For reasons of stability and handling, the 4-hydroxybenzenediazonium was prepared as the trifluoroacetate salt[18] rather than the chloride. Upon reaction of the salt with sodium azide at −25 °C, 4-hydroxyphenylpentazole (**2a**) preferentially precipitated, together with some of 4-hydroxyphenyl azide (**3a**). The latter was removed from the solid of **2a** by washing it with cold methanol. The solid pentazole **2a** was carefully dried in a vacuum at low temperature. The ^{15}N-labeled pentazole **2a-^{15}N** was prepared in an analogous manner using partially labeled sodium azide, Na^{15}N^{14}N^{14}N. On the basis of the proposed mechanism of the reaction,[15,19] the ^{15}N isotope is expected to be incorporated either in position 2 or 3 of the pentazole ring.

Careful ^{1}H NMR monitoring of the reaction between 4-hydroxyphenyldiazonium trifluoroacetate and sodium azide in a CD_3OD/D_2O mixture revealed that the formation of pentazole **2a** was very slow below −40 °C and accelerated only at higher temperatures. As reported before,[19] the parallel formation of aryl azide is inevitably observed. Interestingly, the ratio of pentazole **2a** to azide **3a** is temperature dependent and gradually changed from about 1:2.0 at −30 °C to about 1:1.3 at 0 °C.

4-Oxophenylpentazole anion (**2b**) was prepared by deprotonation of the hydroxyl group in **2a** with 1 equiv of tetrabutylammonium hydroxide, giving ion pair **2b-NBu$_4$** soluble in organic solvents (Scheme 2). Attempts at preparation of pentazole salt **2b-NBu$_4$** directly, by addition of azide anion to *p*-diazobenzoquinone (**4**), resulted in the formation of the aryl azide **3b-NBu$_4$** as the sole product (Scheme 3) as evident from ^{1}H NMR spectra of the reaction mixture.

Scheme 3

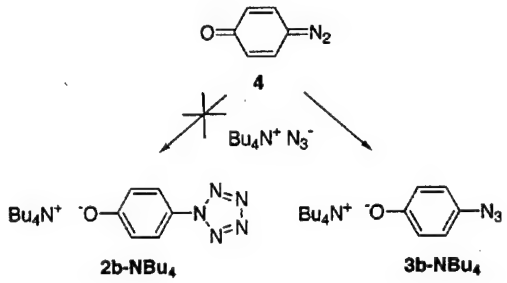

Scheme 4

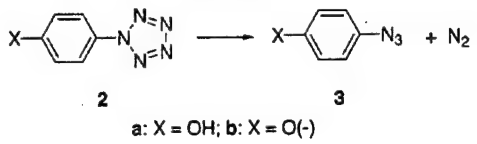

Table 1. Activation Parameters for Arylpentazoles 2

compound	solvent	$\Delta H^{\ddagger}$, [kcal/mol]	$\Delta S^{\ddagger}$, [cal/mol·K]	$\Delta G^{\ddagger}_{298}$, [kcal/mol]
4-OHC$_6$H$_4$N$_5$ (**2a**)	CD_3OD	28.4	29.1	19.7
4-(−)OC$_6$H$_4$N$_5$ (**2b**)	CD_3OD	24.1	11.8	20.6
	CD_2Cl_2	30.2	32.1	20.6
4-ClC$_6$H$_4$N$_5$ (**2c**)[a]	CD_3OD/D_2O[b]	20.3	4.1	19.1

[a] Data from ref 19. [b] 4:1 (v/v) ratio.

Stability of Pentazoles. Kinetic Studies. The thermal decomposition of arylpentazoles **2a** and **2b-NBu$_4$** to azides **3b** and **3b-NBu$_4$**, respectively (Scheme 4), was run in methanol at several temperatures and monitored by ^{1}H NMR spectroscopy. The kinetic results yielded activation parameters which are collected in Table 1 and compared to the recent results on 4-chlorophenylpentazole (**2c**).[19,20] For **2b-NBu$_4$** the kinetic measurements were also done in methylene chloride in order to establish a possible solvent effect on the pentazole ring stability. Unfortunately, 4-hydroxy derivative **2a** was insufficiently soluble in CD_2Cl_2 to conduct comparative kinetic measurements.

The order of free energy of activation $\Delta G^{\ddagger}_{298}$ for the three pentazoles in methanol follows the general trend of stability established by Ugi and Huisgen. As expected, the energy of 20.6 kcal/mol obtained for anion **2b** is the highest in the series. Plotting the three experimental activation energies against the Hammett constants gave the ρ_{expt} value of +0.87 (R^2 = 0.980) at 25 °C,[21] which compares to +1.00 obtained from rate constants[17] at 0 °C for eight derivatives **2**.

A comparison of results for **2b-NBu$_4$** obtained in methanol and methylene chloride shows the same $\Delta G^{\ddagger}_{298}$

(17) Ugi, I.; Huisgen, R. *Chem. Ber.* **1958**, *91*, 531−537.
(18) Colas, C.; Goeldner, M. *Eur. J. Org. Chem.* **1999**, 1357−1366.
(19) Butler, R. N.; Fox, A.; Collier, S.; Burke, L. A. *J. Chem. Soc., Perkin Trans. 2* **1998**, 2243−2247.
(20) Butler, R. N.; Collier, S.; Fleming, A. F. M. *J. Chem. Soc., Perkin Trans. 2* **1996**, 801−803.
(21) The value σ_p = −0.81 for the O(−) substituent is considered to be incorrect (Hansch, C.; Leo, A.; Taft, R. W. *Chem. Rev.* **1991**, *91*, 165). For the Hammett correlation of the experimental $\Delta G^{\ddagger}_{298}$ we used σ_p = −0.97 which was obtained from the Hammett plot of the original Ugi and Huisgen kinetic data from ref 17 for 8 other para-substituted phenylpentazoles.

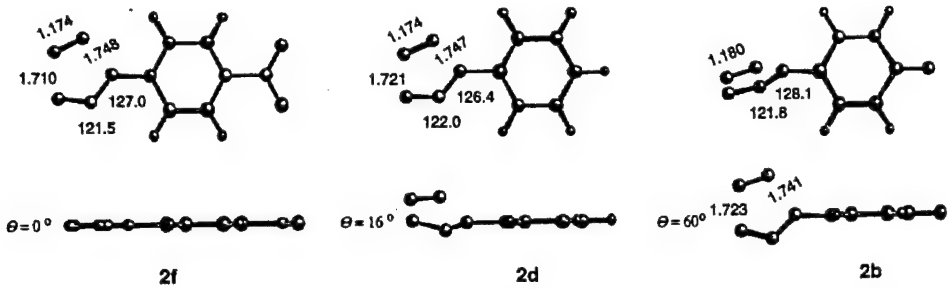

Figure 1. DFT-optimized transition structures for decomposition of (a) 4-nitrophenyl- (**2f**), (b) phenyl- (**2d**), (c) oxyphenylpentazole anion (**2b**). Distances are in Å and the angles for N(3)−N(2)−N(1) and N(2)−N(1)−C(1) in degrees. Θ is defined as the N(2)−N(1)−C(1)−C(2) dihedral angle.

for decomposition, within experimental error, but different kinetic parameters. The rate of decomposition of the salt in methanol at 5 °C increased 3-fold relative to that in CD_2Cl_2, which is reflected in lower E_a and lnA values by about 6 kcal/mol and 10, respectively. The observed solvent effect is consistent with the reported 1.1 times increase of the rate constant for phenylpentazole (**2d**) upon transition from chloroform to methanol at 0 °C.[16]

DFT Calculations. Gas-phase decomposition processes for several 4-substituted phenylpentazoles **2a−g** were modeled using the B3LYP/6-31+G(d,p) level of theory. All ground-state structures were found to be planar with C_{2v} symmetry except for **2a**, which has C_s molecular symmetry. In the transition state structures the aryl and N_5 rings are no longer coplanar (C_1 symmetry) except for the CN and NO_2 derivatives, **2e** and **2f** (Figure 1). The dihedral angle between the rings was found to correlate with the ability of the phenyl ring to accommodate a negative charge that develops on the N(1) atom in the TS as the dipolar azide is formed. Thus, the aryl and pentazole rings are coplanar (Θ = 0°) for strongly electron-withdrawing substituents such nitro (σ_p = +0.78), moderately twisted (Θ = 14°) for the parent phenylpentazole (σ_p = 0.0), and significantly twisted (Θ = 60°) for 4-oxyphenylpentazole (σ_p = −0.97).[21]

The calculated activation energies $\Delta G^{\ddagger}_{298}$ for the gas-phase decomposition processes of 4-substituted phenylpentazoles **2** increase in the expected order from the lowest for **2f** (X = NO_2) to the highest for **2b** (X = O^-). The calculated $\Delta G^{\ddagger}_{298}$ values correlate well with the Hammett σ parameters (ρ_{calcd} = +1.98, R^2 = 0.987), experimental solution activation energy for **2a−c**, and kinetic data[17] for a series of aryl derivatives measured at 0 °C. The last two correlations are shown in Figure 2.

^{15}N NMR Spectroscopy. The NMR spectrum of the ^{15}N-labeled 4-oxophenylpentazole anion (**2b-^{15}N-NBu$_4$**) shows two signals (Figure 3) whose chemical shifts are consistent with values reported for other arylpentazoles.[19,22,23] The results of DFT calculations differ from the experimental data by up to 17 ppm, but nevertheless they clearly support the structural assignment shown in Figure 3.[24] The predicted ^{15}N chemical shifts for pentazole

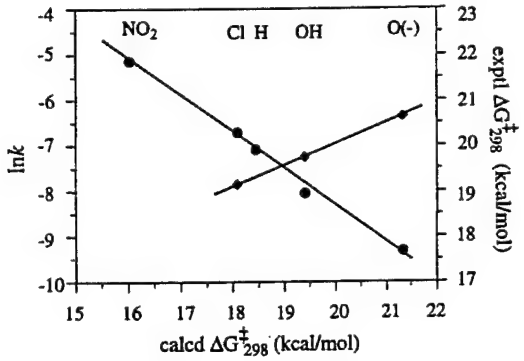

Figure 2. Plots of the calculated free energy of activation $\Delta G^{\ddagger}_{298}$ (calcd) vs experimental activation energy $\Delta G^{\ddagger}_{298}$ (exptl) (diamonds) and kinetic data from ref 17 (circles). Best fit functions: $\Delta G^{\ddagger}_{298}$ (exptl) = 0.462 × $\Delta G^{\ddagger}_{298}$ (calcd) + 10.75 (R^2 = 0.999, diamonds) and ln k = −0.799 × $\Delta G^{\ddagger}_{298}$ (calcd) + 7.65 (R^2 = 0.995, circles).

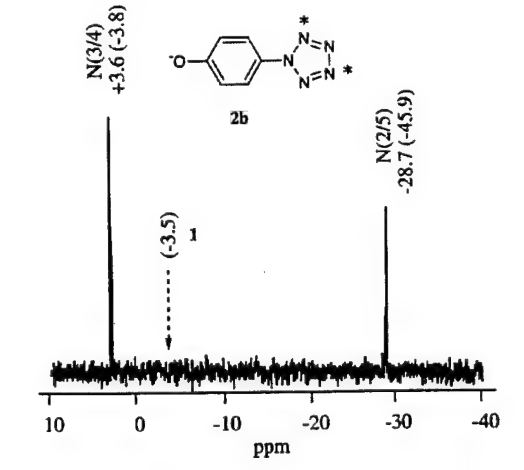

Figure 3. ^{15}N NMR spectrum for 4-oxyphenylpentazole anion (**2b-15N-NBu$_4$**) in CD_2Cl_2. The arrow shows the expected chemical shift for pentazole anion **1**. Experimental and calculated (in parentheses) chemical shifts are listed above the signals.

1 is −3.5 ppm, which is close to the N(3) resonance in arylpentazoles. Upon protonation, the N(1) and N(2/5) atoms in HN_5 are significantly shielded (−113.8 and −19.5 ppm, respectively), while the N(3/4) atoms are deshielded (+15.4 ppm). These results are consistent with the recently reported gas-phase chemical shifts obtained

(22) Müller, R.; Wallis, J. D.; von Philipsborn, W. *Angew. Chem., Int. Ed. Engl.* **1985**, *24*, 513−515.
(23) Burke, L. A.; Butler, R. N.; Stephens, J. C. *J. Chem. Soc., Perkin Trans. 2* **2001**, 1679−1684.
(24) ^{15}N NMR chemical shifts show a generally large solvent effect up to 40 ppm (ref 28), which partially accounts for the observed difference between the results obtained for gas phase and CH_2Cl_2 solutions. Nevertheless, these computational results appear to be significantly closer to the experiment than those obtained wth the IGLO method in ref 2.

for **1** and other pentazole derivatives at the B3LYP/6-311++G(2d,p) level of theory.[23]

Ozonolysis of 4-Oxophenylpentazole. The experiment was performed on an NMR scale sample of ^{15}N-labeled 4-oxophenylpentazole salt **2b-^{15}N-NBu$_4$**, in CD_2Cl_2 at −78 °C in the presence of excess NBu_4OH. After 3 min of passing ozone/air mixture through the solution, the ^1H NMR spectrum showed a virtually unaltered pattern, characteristic for 1,4-disubstituted benzenes, but considerably shifted, relative to the signals of the starting **2b-^{15}N-NBu$_4$**. ^{15}N NMR, however, clearly showed the complete absence of the two initial signals assigned to the pentazole moiety (Figure 3). In fact, there were no signals detected at all, indicating that no compound with labeled nitrogen remained in the solution. The latter result, combined with the possible distribution of labeled nitrogen in the pentazole unit, led to the conclusion that the remaining material contained most likely only the nitrogen directly bound to the aromatic ring. The nature of this new aromatic product remains unclear. By comparison with authentic samples, we excluded 4-nitrophenol or its anion as possible products.

Discussion and Conclusions

The calculated activation energies $\Delta G^{\ddagger}$ (but not $\Delta H^{\ddagger}$) for arylpentazoles show excellent correlation with experimental data (Figure 2), which validates the computational results. The significant difference between the observed and theoretical values is presumably largely due to the difference between the gas phase and the polar and protic environment of methanol. The slope of 0.462 for the $\Delta G^{\ddagger}$ (calcd)/$\Delta G^{\ddagger}$ (exptl) correlation in Figure 2 and the ratio of $\rho_{exptl}/\rho_{calcd} = 0.44$ suggest that arylpentazoles are generally stabilized in methanol solution relative to gas phase except for those with strongly electron-donating substituents. This is consistent with the calculated polarity of the ground and transition structures **2**. Thus, polarity of the ground state increases for derivatives with substituent of increasing electron-donating ability (e.g., **2f**: μ_{GS} = 0.35 D and **2a**: μ_{GS} = 6.16 D). Also the transition state is more polar than the ground state for derivatives with electron-withdrawing substituents and less polar for derivatives with electron-donating substituents (e.g., **2f**: $\mu_{TS} - \mu_{GS} = +1.56$ D and **2a**: $\mu_{TS} - \mu_{GS} = -1.32$ D). More experimental datapoints, especially for electron-deficient derivatives such as **2e** and **2f**, would be helpful to extend the correlation of free energies of activation. It should be pointed out, however, that the excellent correlation for ln*k* with the computed $\Delta G^{\ddagger}$ over a broad range of σ_p values strongly suggests a cogency of the free energy correlation in Figure 2.

Assuming that the correlations in Figure 2 are general, one can estimate the stability of other pentazole derivatives and the parent pentazole **1**. Some of the results are shown in Table 2. Not surprisingly, 4-thiophenylpentazole anion (**2g**), with the very negative σ_p value of −1.21, is expected to be more stable than the oxo anion **2b**. Its rate of decomposition in MeOH at 0 °C can be estimated to be 1.2 times lower than that for **2b**, the most stable pentazole derivative known. The same correlations allow estimation of the stability of pentazole anion **1** in methanol solution, which is a likely medium for its generation and study. Thus, the estimated half-lifetime $t_{1/2}$ for **1** is about 2.2 days in methanol at 0 °C, which offers encouragement for future experimental work. The parent hydrogen pentazole, HN_5, is predicted to be as stable as 4-chlorophenylpentazole (**2c**), while 1-aminopentazole[1] has a predicted half-lifetime $t_{1/2}$ of less than 1 min at 0 °C.

Table 2. Calculated Free Energy of Activation for Selected Pentazole Derivatives and Predicted Stability in Methanol[a]

	calculated[b]	predicted[a]	
compound	$\Delta G^{\ddagger}_{298}$, [kcal/mol]	$\Delta G^{\ddagger}_{298}$, [kcal/mol]	$k\cdot10^4$ at 0 °C, [s^{-1}]
4-(−)$SC_6H_4N_5$ (**2g**)	21.43	20.65	0.77
N_5(−) (**1**)	25.25	22.42	0.036
N_5H	17.95	19.04	12.4
1-NH_2N_5	14.90	17.63	142.0

[a] Predictions made based on correlations in Figure 2. [b] At the B3LYP/6-31+G(d,p) level of theory.

The results from ozonolysis of **2b** suggest that O_3 reacts much faster with pentazole than with the benzene ring, which eliminates this method from possible routes to **1**. Other precursors need to be considered, especially those that lead to the N_5-COO(−), silicon or sulfur derivatives of **1**. This approach hinges, however, upon the ability to construct a linear or cyclic array of nitrogen atoms by methods such as those shown in Figure 1.

Computational Details

Quantum-mechanical calculations were carried out at the B3LYP/6-31+G(d,p)[25] level of theory using the Linda-Gaussian 98 package[26] on a Beowulf cluster of 16 processors. Geometry optimizations were undertaken using appropriate symmetry constraints and default convergence limits. Transition structures were located using the QST2 keyword. Vibrational frequencies were used to characterize the nature of the stationary points and to obtain thermodynamic parameters. Zero-point energy (ZPE) corrections were scaled by 0.9806.[27]

Nuclear magnetic shielding tensors were calulated for molecules at ground-state geometry using the NMR keyword and the default GIAO method at the B3LYP/6-31+G(d,p) level of theory. The resulting energies and absolute shielding tensors are listed in the Supporting Information.

Experimental Section

^1H NMR spectra were recorded at 400 MHz and referenced to the solvent. ^{15}N NMR spectra were recorded at 40.56 MHz in CD_2Cl_2, and externally referenced to the ^{15}N signals of doubly labeled $^{15}NH_4{}^{15}NO_3$ ($^{15}NH_4$ δ −360.4, $^{15}NO_3$ δ −4.00) which was indirectly referenced to neat CH_3NO_2 (δ = 0.0

(25) Becke, A. D. *Phys. Rev. A*, **1988**, *38*, 3098−3100. Lee, C.; Yang, W.; Parr, R. G. *Phys. Rev. B*, **1988**, *37*, 785−789. Frisch, M. J.; Pople, J. A.; Binkley, J. S. *J. Chem. Phys.* **1984**, *80*, 3265−3269.

(26) Gaussian 98, Revision A.9, M. J. Frisch, G. W. Trucks, H. B. Schlegel, G. E. Scuseria, M. A. Robb, J. R. Cheeseman, V. G. Zakrzewski, J. A. Montgomery, Jr., R. E. Stratmann, J. C. Burant, S. Dapprich, J. M. Millam, A. D. Daniels, K. N. Kudin, M. C. Strain, O. Farkas, J. Tomasi, V. Barone, M. Cossi, R. Cammi, B. Mennucci, C. Pomelli, C. Adamo, S. Clifford, J. Ochterski, G. A. Petersson, P. Y. Ayala, Q. Cui, K. Morokuma, D. K. Malick, A. D. Rabuck, K. Raghavachari, J. B. Foresman, J. Cioslowski, J. V. Ortiz, A. G. Baboul, B. B. Stefanov, G. Liu, A. Liashenko, P. Piskorz, I. Komaromi, R. Gomperts, R. L. Martin, D. J. Fox, T. Keith, M. A. Al-Laham, C. Y. Peng, A. Nanayakkara, M. Challacombe, P. M. W. Gill, B. Johnson, W. Chen, M. W. Wong, J. L. Andres, C. Gonzalez, M. Head-Gordon, E. S. Replogle, and J. A. Pople, Gaussian, Inc., Pittsburgh, PA, 1998.

(27) Scott, A. P.; Radom, L. *J. Phys. Chem.* **1996**, *100*, 16502−16513.

ppm).[28] Labeled sodium azide was purchased from Cambridge Isotope Laboratories. Ozone was generated using a Griffin Ozonia G-TC-0.5 instrument.

Thermolysis of 2. Kinetic Measurements. Pentazole **2a** or **2b-NBu$_4$** (approximately 0.06 mmol) was dissolved in deuterated solvent (0.5 mL) and transferred into an NMR tube at low temperature. The sample was kept at a constant temperature, and ^{1}H NMR spectra were taken at regular time intervals, until the virtual disappearance of the starting material. A ratio of intensities of the signals of the aromatic hydrogens in the starting material (**2a**: (CD_3OD) δ 7.04 and 8.01 ppm; **2b-NBu$_4$** (CD_2Cl_2) δ 6.58 and 7.69 ppm, (CD_3OD) δ 6.74 and 7.79 ppm) to that in the forming azide (**3a**: (CD_3OD) δ 6.78 and 6.90 ppm; **3b-NBu$_4$** (CD_2Cl_2) δ 6.47 and 6.65 ppm, (CD_3OD) δ 6.59 and 6.69 ppm) was used to calculate the rate constants. Four kinetic measurements were done in the range of temperatures between −10 to +20 °C. Full kinetic data is listed in the Supporting Information.

4-Hydroxybenzenediazonium Trifluoroacetate.[18] The salt was prepared in 65% yield as a 1:1 complex with trifluoroacetic acid according to a general literature procedure.[18] ^{1}H NMR (CD_3CN) δ 7.16 (d, J = 9.4 Hz, 2H), 8.17 (d, J = 9.4 Hz, 2H), 8.70 (bs, 2H).

4-Hydroxyphenylpentazole (2a). 4-Hydroxybenzenediazonium trifluoroacetate (0.42 g, 1.26 mmol) was dissolved in methanol (3.40 mL) at −23 °C (dry ice−carbon tetrachloride bath) and petroleum ether (3.40 mL) was added to the solution. Sodium azide (0.16 g, 2.46 mmol), in water (0.65 mL), was added dropwise and the stirring continued for about 0.5 h at the same temperature. The solid material was separated using a jacketed funnel for low temperature filtration and carefully washed with a small amount of cold methanol. The remaining solid was collected at low temperature and vacuum-dried to give 0.08 g (40% yield) of the product as a gray solid, which was 90% pure by NMR: ^{1}H NMR (CD_3OD) δ 7.04 (d, J = 6.4 Hz, 2H), 8.01 (d, J = 6.5 Hz, 2H).

The second major product was identified as 4-hydroxyphenyl azide (**3a**): ^{1}H NMR (CD_3OD) δ 6.78 (d, J = 8.8 Hz, 2H), 6.90 (d, J = 8.8 Hz, 2H); ($CDCl_3$) δ 6.83 (d, J = 8.9 Hz, 2H), 6.92 (d, J = 8.9 Hz, 2H). Lit.[29] ($CDCl_3$) δ 6.83 (d, J = 9 Hz, 2H), 6.92 (d, J = 9 Hz, 2H).

4-Oxophenylpentazole, Tetrabutylammonium Salt (2b-NBu$_4$). Pentazole **2a** (0.01 g, 0.06 mmol) was suspended in a solution of tetrabutylammonium hydroxide (0.02 g, 0.08 mmol) in deuterated dichloromethane (0.5 mL) at − 78 °C. Temperature was raised to − 35 °C and stirring continued until the full dissolution of the solid and formation of **2b**: ^{1}H NMR (CD_2Cl_2) δ 0.92 (t, J = 7.2 Hz, 12H), 1.24−1.34 (m, 8H), 1.41−1.52 (m, 8H), 2.99−3.06 (m, 8H), 6.58 (d, J = 6.8 Hz, 2H), 7.69 (d, J = 6.8 Hz, 2H); ^{15}N NMR (CD_2Cl_2) δ −28.7 (s, 1N), 3.2 (s, 1N).

Attempted Preparation of 4-Oxophenylpentazole, Tetrabutylammonium Salt (2b-NBu$_4$). *p*-Diazobenzoquinone[18,30] (**4**, 10 mg, 0.09 mmol) was dissolved in CD_3OD (0.25 mL) and the solution cooled to −78 °C. A solution of tetrabutylammonium azide (30 mg, 0.10 mmol) in CD_3OD (0.25 mL) was added dropwise and the temperature gradually raised to 0 °C during 1 h period. The solution was transferred to an NMR tube and a spectrum was accumulated immediately at ambient temperature. The spectral data were consistent with the sole presence of azide **3b-NBu$_4$**.

Ozonolysis of 4-Oxophenylpentazole, Tetrabutylammonium Salt (2b-NBu$_4$). A solution of ^{15}N-labeled 4-oxophenylpentazole salt **2b-15N-NBu$_4$** (30 mg, 0.07 mmol) and Bu_4NOH (35 mg, 0.14 mmol) in deuterated dichloromethane was cooled to −78 °C. A slow stream of ozone was passed through the solution for 3 min after which both ^{1}H and ^{15}N NMR spectra were measured. A new set of peaks in the ^{1}H NMR spectrum: ^{1}H NMR (CD_2Cl_2) δ 7.15 (d, 2H), 7.87 (d, 2H). No signals were detected in the ^{15}N NMR spectrum. The data were compared with measurements on CD_2Cl_2 solutions of original samples of *p*-nitrophenol (δ 6.95 (d, 2H), 8.16 (d, 2H)) and tetrabutyammonium *p*-nitrophenolate (δ 6.21 (d, 2H), 7.87 (d, 2H)).

4-Oxophenyl Azide, Tetrabutylammonium Salt (3b-NBu$_4$). ^{1}H NMR (CD_3OD) δ 6.59 (d, J = 9.0 Hz, 2H), 6.69 (d, J = 9.0 Hz, 2H); (CD_2Cl_2) δ 6.47 (d, J = 8.8 Hz, 2H), 6.65 (d, J = 8.8 Hz, 2H); ^{15}N NMR (CD_2Cl_2) δ −148.4 (s, 1N), −131.7 (s, 1N).

Acknowledgment. This project has been supported by DARPA/AFOSR F49620-98-1-0483.

Supporting Information Available: Listing of full kinetic data and computational results including isotropic shielding tensors are available. This material is available free of charge via the Internet at http://pubs.acs.org.

JO0110754

(28) Witanowski, M.; Stefaniak, L.; Webb, G. A. In *Annual Reports on NMR Spectroscopy*; Webb, G. A., Ed.; Academic Press: London, 1993; Vol. 25; pp 86−87.

(29) Dunkin, I. R.; ElAyeb, A. A.; Gallivan, S. L.; Lynch, M. A. *J. Chem. Soc., Perkin Trans. 2* **1997**, 1419−1427.

(30) Puza, M.; Doetschman, D. *Synthesis* **1971**, 481−482.

Pergamon

Tetrahedron 58 (2002) 2085–2090

TETRAHEDRON

N-Chloro-*N*,*N*′,*N*′-tris(ethoxycarbonyl)hydrazine and *N*,*N*-dichloro-*N*′,*N*′-bis(ethoxycarbonyl)hydrazine: synthesis, stability and reactions with nucleophiles

Vladimir Benin,[a,†] Piotr Kaszynski[a,*] and J. George Radziszewski[b,c]

[a]*Organic Materials Research Group, Department of Chemistry, Vanderbilt University, Nashville, TN 37235, USA*
[b]*Department of Chemistry, Colorado School of Mines, Golden, CO 80401, USA*
[c]*National Renewable Energy Laboratory, Golden, CO 80401, USA*

Received 4 October 2001; accepted 22 January 2002

Abstract—*N*-Chloro-*N*,*N*′,*N*′-tris(ethoxycarbonyl)hydrazine (**1b**) was prepared in 27% yield by chlorination of *N*,*N*,*N*′-tris(ethoxycarbonyl)hydrazine anion with *t*-BuOCl. The reaction of **1b** with CN(−) gave the product of *N*-substitution. Attempts at chlorination of *N*,*N*-bis(ethoxycarbonyl)hydrazine (**2a**) with *t*-BuOCl did not yield the expected *N*,*N*-dichloro-*N*′,*N*′-bis(ethoxycarbonyl)hydrazine (**1a**), and led to the exclusive formation of ClCOOEt. The mechanism of the decomposition and the relative stability of **1a** and **1b** are assessed using DFT calculations and compared to those for the parent chlorohydrazine (**3**).

1. Introduction

N-Chlorohydrazines are rare compounds and only a handful of them have been isolated as stable species.[1–3] The main reason for their observed instability is the enhanced reactivity of the N–Cl bond. This results from the $n_{N'}$–σ_{NCl}^* interaction in which the lone pair of the N′ atom populates the antibonding N–Cl orbital, facilitating the departure of the Cl(−) anion. Thus some chlorohydrazines exist in solution as ion pairs, while many others eliminate a proton, if possible, to form imines.[1] The in-depth analysis done by Shustov et al.[1] and supported by quantum mechanical calculations,[4] led to the conclusion that stable chlorohydrazines with a covalent N–Cl bond can be obtained if the donor capabilities of the N′ nitrogen lone pair are significantly reduced either by placing a strong π acceptor or imposing conformational constraints. Also substitution at the nitrogen atom bonded to the halogen with an electron withdrawing group is predicted to increase the stability of the chlorohydrazine.

With this in mind, and in the context of our interest in new heterocycles, we designed two tetrasubstituted chlorohydrazines, **1a** and **1b**, containing ester groups and two or one chlorine atoms, respectively.

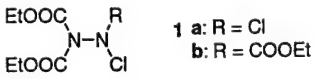

1 a: R = Cl
b: R = COOEt

The ester groups in **1** are intended to stabilize the chlorohydrazines by acting as π acceptors for the nitrogen lone pairs, and to provide means for further functional group transformations including deprotection of the nitrogen centers. Chlorine atoms are expected to undergo nucleophilic displacement analogous to the well documented substitution at the N-centers in *N*-chloroamides with a variety of carbon-,[5] nitrogen-,[6] sulfur-,[7–11] phosphorus-,[12] and oxygen-centered[13,14] nucleophiles. There is also a single report of nucleophilic substitution on an *N*-halohydrazine.[15] According to the report, an *N*-chloro derivative of 1,6-diazabicyclo[3.1.0]hexane-5-carboxamide reacted with the methoxide anion to give the *N*-methoxy derivative in 37% yield. However, another chlorohydrazine, *N*-chloro-2-azaquinuclidone, acts as a chlorine donor in the reaction with dimethylamine.[1]

Here we report our efforts at preparation of chlorohydrazines **1**, evaluate their thermal stabilities with the aid of DFT calculations, and investigate reactions of **1b** with several nucleophiles.

2. Results and discussion

2.1. Chlorination of *N*,*N*-bis- and *N*,*N*,*N*′-tris(ethoxycarbonyl)hydrazine

Both the di- and trisubstituted hydrazines **2a** and **2b** were

Keywords: hydrazines; halogenation; mechanisms; computer-assisted methods; substitution.
* Corresponding author. Tel.: +1-615-322-3458; fax: +1-615-322-4936; e-mail: piotr@ctrvax.vanderbilt.edu
† Present address: Department of Chemistry, University of Dayton, 300 College Park Dayton, OH 45469-2357, USA.

0040–4020/02/$ - see front matter
PII: S0040-4020(02)00101-1

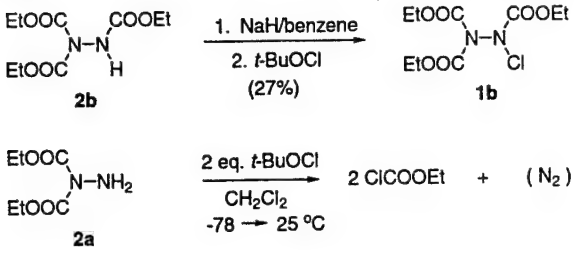

Scheme 1.

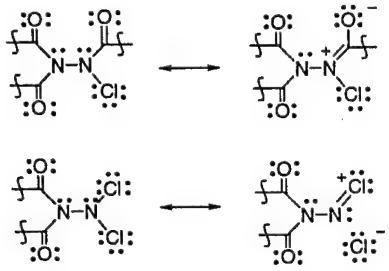

Figure 1. Selected resonance structures for **1a** and **1b**.

reacted with *t*-BuOCl under the general conditions used for preparation of *N*-chloroamides[16] and some *N*-chlorohydrazides.[1] While the disubstituted hydrazine **2a** reacted rapidly with the hypochlorite, **2b** was recovered unchanged. To increase its reactivity, **2b** was deprotonated with NaH and subsequently treated with *t*-BuOCl. The expected *N*-chloro-*N*,*N*′,*N*′-tris(ethoxycarbonyl)hydrazine (**1b**) was isolated in 27% yield as a stable oil (Scheme 1).

Despite the rapid reaction of *N*,*N*-bis(ethoxycarbonyl)-hydrazine (**2a**) with *t*-BuOCl, none of the desired *N*,*N*-dichloro-*N*′,*N*′-bis(ethoxycarbonyl)hydrazine (**1a**) was isolated and no residue was obtained upon removal of solvent from the reaction mixture. To investigate this unexpected result, the reaction was carried out in a NMR tube. After 10 min at −50°C, all **2a** was converted into a single compound whose ^{1}H and ^{13}C NMR spectra matched those obtained for an authentic sample of ethyl chloroformate (Scheme 1).

2.2. Stability of the chlorohydrazines

The difference in thermal stability of the two chlorohydrazines is significant. Compound **1b** is an isolable stable oil, while **1a**, presumably formed as the initial product of chlorination (vide infra), apparently decomposes rapidly to ClCOOEt and N_2 below ambient temperature. In contrast, no traces of decomposition of **1b** were detected by ^{1}H NMR analysis of a benzene solution heated at 80°C for 3 days in a sealed NMR tube.

The observed difference in stability of the two hydrazines can be rationalized in terms of a previous discussion on the subject.[1] Thus, the main factor causing instability of chlorohydrazines, the $n_{N'}-\sigma_{NCl}^{*}$ interaction, is largely eliminated in **1** since the two *geminal* carbonyl groups on N′ act as strong π acceptors for the $n_{N'}$ lone pair. The stability of the N–Cl covalent bond is enhanced further in **1b** by the presence of another carboxyl group *geminal* to chlorine and strong $n_{N}-\pi_{CO}^{*}$ interactions. Placement of a second chlorine atom in **1a** has the opposite effect. Now, through the $n_{Cl'}-\sigma_{NCl}^{*}$ interactions, the lone pair of the second chlorine populates the N–Cl antibonding orbital and activates departure of Cl(−) as shown in Fig. 1. This results in an electronegative chlorine in **1a**, while in **1b** the halogen is electropositive.

The presence of the destabilizing $n_{Cl'}-\sigma_{NCl}^{*}$ interactions suggests that the decomposition pathway for **1a** may be analogous to that of other chlorohydrazines[1,4] and involve heterolytic dissociation of the halide and the formation of an ion pair. The subsequent attack of the chloride anion on the carbonyl group leads to the formation of ethyl chloroformate and molecular nitrogen. Decomposition of **1a** through the HERON mechanism[4] is unlikely since neither diethyl azodicarboxylate nor tetrazine, the expected products, have been observed experimentally.

The above qualitative considerations are largely supported

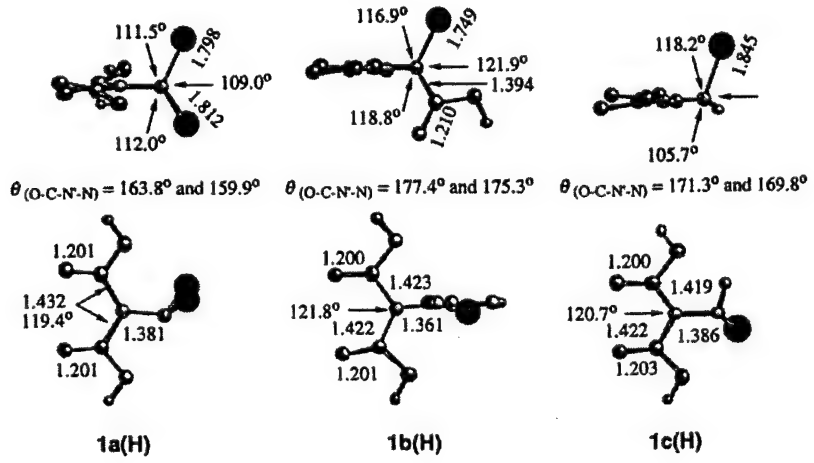

Figure 2. Ball and Stick models for DFT-optimized chlorohydrazines with selected bond lengths and angles.

Table 1. Calculated molecular parameters and gas-phase dissociation energies for selected hydrazines

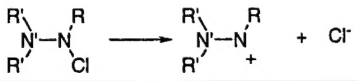

Compound	R′	R	N–Cl (Å)	BO[a]	θ (deg)[b]	Q_{Cl}[c]	ΔH_{298}	ΔG_{298}
1a(H)	COOH	Cl	1.800/1.810	0.51/0.49	35	0.12/0.13	133.6	124.9
1b(H)	COOH	COOH	1.743	0.55	9.6	0.17	148.7	139.9
1c(H)	COOH	H	1.845	0.47	36	0.01	143.9	135.3
3	H	H	1.969	0.37	37	−0.18	138.8	131.1

B3LYP/6-31+G(d)//B3LYP/6-31G(d) level calculations. Energies in kcal/mol.
[a] Total of atom–atom overlap-weighted NAO bond order for chlorine atom.
[b] Pyramidalization of the nitrogen atom measured as the dihedral angle defined by N–N′–Cl–R atoms.
[c] Natural charge on chlorine atom.

by computational results for three related chlorohydrazines **1(H)**, in which the ester ethyl groups were replaced with hydrogen atoms (Fig. 2), and parent chlorohydrazine (**3**). The *syn* pseudocoplanar orientation of the two *geminal* carboxyl groups was found to be most favorable energetically in derivatives **1** and **2**. The diazenium ions derived from chlorohydrazines **1(H)** can be described as the corresponding *trans* azocarboxylic acids with a carboxyl cation coordinated to nitrogen atom lone pair.

Generally, the lone pairs of the two nitrogen atoms are orthogonal to each other, which leads to two distinct molecular subunits in **1** and **2**. The nitrogen N′ bearing two carboxyl groups is almost planar and the dihedral angle θ defined by N′–N–R′–R′ atoms, ranges from 0.0° in **2a(H)** to 4.8° in **2b(H)**. The pyramidalization of the other nitrogen atom N is significantly higher, about 36°, except for the tricarboxy derivatives **1b(H)** and **2b(H)** for which the n_N–π_{CO}^* interactions result in low pyramidalization of about 10 and 14°, respectively. The planar structures represent low energy transition states (about 0.5 kcal/mol) for inversion at the nitrogen atom.

The variation in the pyramidalization angle can be rationalized using either electrostatic interaction arguments or the Hückel MO model. In the latter, the planar O=C–N′–C=O, O=C–N–Cl and Cl–N–Cl can be viewed as a 6π electron pentadienyl, butadiene and allyl system, respectively. The first π system is energetically favorable and expected to remain planar. In contrast, the presence of an electron pair on the antibonding orbital of butadiene and allyl destabilizes the planar structures and results in pyramidalization to avoid unfavorable π conjugation.

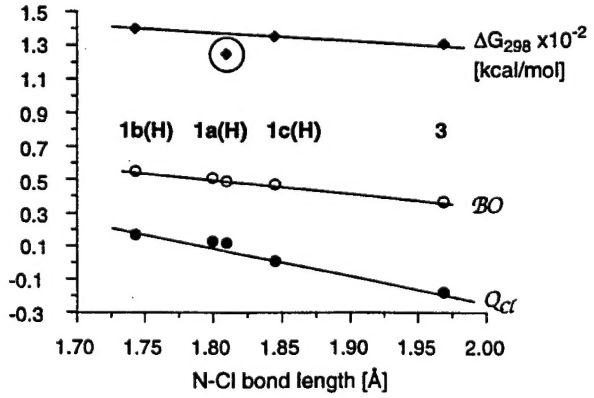

Figure 3. Correlation between the N–Cl bond length $\mathscr{L}$ and bond order BO (open circles), natural charge Q_{Cl} on Cl (full circles) and bond heterolytic dissociation energy ΔG_{298} (diamonds). The best fit functions: BO=−0.80$\mathscr{L}$+1.94 ($\mathscr{R}^2$=0.996); Q_{Cl}=−1.65$\mathscr{L}$+3.08 ($\mathscr{R}$=0.963); ΔG_{298}=−38.8$\mathscr{L}$+207.2 ($\mathscr{R}$=0.993, for three points; **1a(H)** is excluded).

The bond lengths, bond orders and atomic charges calculated for **1(H)** are shown in Table 1. The chlorine–nitrogen distance in **1b(H)** (d_{NCl}=1.743 Å) is typical for *N*-chloroamines (e.g.[17] 1.736(3) Å) and *N*-chloroamides (e.g.[18] 1.683(3)–1.713(2) Å). This distance is longer by about 0.1 Å in **1c(H)**, and it reaches d_{NCl}=1.969 Å in chlorohydrazine (**3**) indicating a significantly weakened N–Cl bond. The increase in the bond length in the chlorohydrazines is paralleled by the proportional decrease of bond order (BO) and increase of the negative charge Q on the halogen (Table 1). Correlations in Fig. 3 show that the N–Cl bond vanishes (BO=0) at a distance of 2.43 Å, at which the chlorine carries a charge of −0.92.

The bond length also correlates well with the ability of chlorohydrazines, except for **1a(H)**, to form ion pairs in gas phase. Thus, results in Table 1 show that introduction of three carboxyl groups into chlorohydrazine (**3**) to form **1b(H)** disfavors heterolytic dissociation by about 10 kcal/mol. As a consequence, the dissociative pathway for decomposition is practically shut down, as is experimentally observed for **1b**. Results also suggest that the dicarboxyl derivative **1c** also may be sufficiently stable for isolation.

The data in Table 1 show that dichlorohydrazine **1a(H)** is exceptional. With a pyramidalized nitrogen center, a slightly elongated N–Cl bond, and a positive charge on the halogens, **1a(H)** resembles monochlorohydrazine **1c(H)** and fits well to the series of other chlorohydrazines (Fig. 3). However, dichlorohydrazine **1a(H)** has a significantly lower heterolytic dissociation energy than **1c(H)**, even lower than parent chlorohydrazine (**3**). This suggests that **1a** undergoes decomposition more readily than chlorotrialkylhydrazines, which are known to form ion pairs as the first step in decomposition in solutions.[1,4]

It can be estimated that the calculated dissociation energy is 12.3 kcal/mol lower than that expected from the correlation in Fig. 3. Since the molecular parameters of **1a(H)** fit the other three chlorohydrazines well (Fig. 3), it is likely that the difference in the dissociation energies is due to the

Table 2. Calculated gas-phase energies for elimination reactions of selected hydrazines

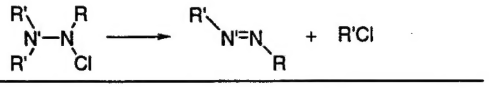

Compound	R′	R	ΔH_{298}	ΔG_{298}
1a(H)	COOH	Cl	−21.9	−35.1
1b(H)	COOH	COOH	+2.0	−12.0
1c(H)	COOH	H	+0.3	−12.6
3	H	H	−4.6	−14.1

B3LYP/6-31+G(d)//B3LYP/6-31G(d) level calculations. Energies in kcal/mol.

unusually high relative stability of the corresponding diazenium ion. Indeed, the $(HOOC)_2NNCl(+)$ cation is unique among the carboxyldiazenium cations. Analysis of its molecular structure shows a nearly planar HOOC–N=N–Cl fragment ($\theta_{(O-C-N-N)}$=174.1°). The natural bond order (NBO) calculations indicate that the BO of Cl–N increases from 0.51 to 0.68 upon ionization of **1a(H)**, while the BO for the C=O group in the cation is 1.35, the lowest for all carbonyl groups in the series of the diazenium cations. This suggests π conjugation and weak donor–acceptor interactions in the cation,[19] which additionally stabilizes the cation and facilitates the dissociation process.

The unusually high propensity of **1a** to form ion pairs is paralleled by the high exothermicity of the elimination reaction to form the chloride R′–Cl and azene (Table 2). While for **1b(H)**, **1c(H)** and **3** the process is almost thermoneutral, the first step in the decomposition of **1a(H)** is exothermic by almost −22 kcal/mol. The subsequent step, elimination of chloroformate from chloroazocarboxylate and formation of molecular nitrogen, is even more exothermic. Thus the total change of enthalpy is −86.5 kcal/mol which provides a significant driving force for decomposition.

The computational results in Tables 1 and 2 strongly suggest that the formation of ethyl chloroformate upon chlorination of **2a** proceeds through dichlorohydrazine **1a** (path a in Scheme 2), rather than through monochlorohydrazine **1c** (path b in Scheme 2). Both the dissociation energy and the exothermicity of the formation of the azene appear to be much more favorable for **1a** than for **1c**. Path b would also involve the formation of ethyl formate, which could undergo subsequent chlorination. This is not supported by ^{1}H NMR analysis of the reaction mixture since no signals other that those for ethyl chloroformate and *t*-butanol were detected.

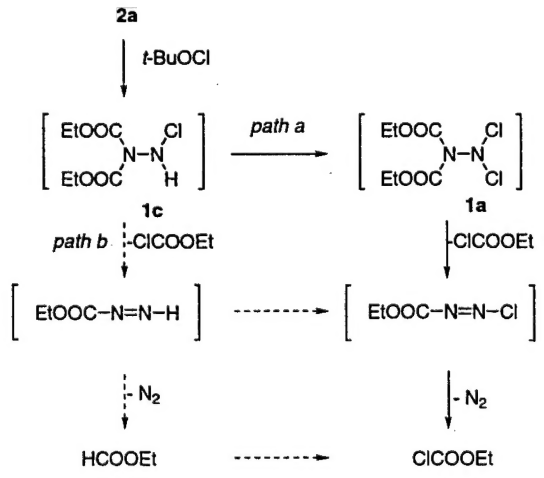

Scheme 2.

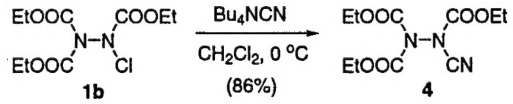

Scheme 3.

2.3. Reactions of *N*-chloro-*N*,*N*′,*N*′-tris(ethoxycarbonyl)-hydrazine with nucleophiles

N-Chlorohydrazine **1b** was reacted with several typical nucleophiles. The *N*-substituted product was obtained only in a reaction with the cyanide anion (Scheme 3) which gave the *N*-cyano derivative **4** isolated in high yield. The formal substitution product **4** could be formed however, by initial chlorine transfer from **1b** to CN(−) and subsequent reaction of the resulting cyanogen chloride with the N-anion of **2b**. A similar mechanism (inverse nucleophilic substitution) was postulated for an analogous reaction of 1-chlorobenzotriazole.[20]

Reactions of **1b** with other nucleophiles gave hydrazine **2b**, a reduction product of **1b**, accompanied by various amounts of tetrakis(ethoxycarbonyl)hydrazine (**5**).[21] No *N*-substitution products were observed. For instance, a reaction of **1b** with *n*-C_3H_7SH in Et_3N/benzene, conducted according to a literature procedure,[9] and 4-$CH_3C_6H_4S^-Me_4N^+$ in MeCN led to the formation of the corresponding disulfides in quantitative yields and a mixture of **2b** and **5**. In the former case **2b** was isolated in 67%, while the reaction with the thiocresolate salt gave **2b** and **5** in 1:9 ratio, according to GC–MS. A similar mixture of hydrazine tri- and tetraesters, **2b** and **5**, was also obtained from the reaction of **1b** with the acetate anion, an oxygen-centered nucleophile, used for the preparation of an *N*-acetoxy urea.[13] The reaction of **1b** with morpholine led to the predominant formation of *N*,*N*,*N*′-tris(ethoxycarbonyl)hydrazine (**2b**), isolated in 60% yield, accompanied by about 30% of unidentified product derived from **1b**.[22]

Reaction of **1b** with ethanol in the presence of equimolar amount of AgOTf also resulted in the formation of the hydrazine **2b** as the sole product.

These results demonstrate that *N*-chloro-*N*,*N*′,*N*′-tris-(ethoxycarbonyl)hydrazine (**1b**) is a powerful donor of electrophilic chlorine. The DFT calculations show significant positive charge density on the chlorine atom in **1b(H)** (+0.17) which is very similar to that calculated for NCS. Further analysis of computational results shows that chlorohydrazine **1b(H)** is a more potent donor of Cl^+ than NCS

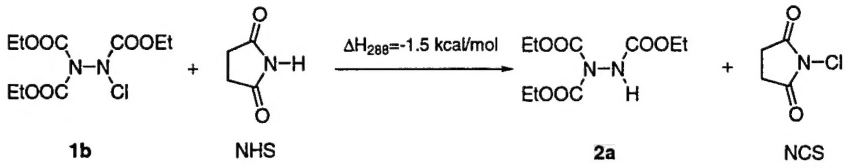

Scheme 4.

since the chlorination of succinimide (NHS) with **1b(H)** is moderately exothermic (Scheme 4).

3. Conclusions

Chlorination of two ethoxycarbonylhydrazines, **2a** and **2b**, gave an exceptionally stable chlorohydrazine **1b** and a particularly unstable dichlorohydrazine **1a** postulated as a transient species. The presence of the carbonyl groups generally stabilizes the covalent N–Cl bond in chlorohydrazines through n_N–π_{CO}^* interactions, which effectively compete with the detrimental $n_{N'}$–σ_{NCl}^* interactions. In contrast, the presence of a *geminal* halogen has a strong destabilizing effect on the N–Cl bond in **1a**, which appears to be less stable to heterolytic dissociation than the parent chlorohydrazine (**3**). The results of DFT calculations suggest that the instability of **1a** is related to the relatively high stability of the corresponding diazenium ion rather than to the destabilizing $n_{Cl'}$–σ_{NCl}^* interactions.

The experimental and computational results suggest that the two *geminal* carbonyl groups are sufficient to stabilize chlorohydrazines against dissociative decomposition pathways. Thus, some *N*-alkyl derivatives of **1c** may be sufficiently stable for isolation, which would significantly expand the small number of known halohydrazines. In addition, the chlorine atom in such *N*-alkyl-*N*-chloro derivatives should be less electropositive than that in **1b** and should more readily undergo nucleophilic displacement giving a variety of N-substituted hydrazines and heterocycles.

4. Computational details

Quantum-mechanical calculations were carried out at the B3LYP/6-31G(d) level of theory using the Linda–Gaussian 98 package[23] on a Beowulf cluster of 16 processors. Geometry optimizations were undertaken without symmetry constraints, except for NCS and NHS, and default convergence limits. Global conformational minima for **1**, **2** and the ions were located at the B3LYP/3-21G(d) and subsequently on the B3LYP/6-31G(d) level of theory by systematic changes of orientation for the COOH groups. Vibrational frequencies were used to characterize the nature of the stationary points and to obtain thermodynamic parameters. Zero-point energy (ZPE) corrections were scaled by 0.9806.[24] Following general recommendations,[25] dissociation energies of chlorohydrazines were derived as the differences of SCF energies of individual species computed using the diffuse function-augmented 6-31+G(d) basis set at the geometries obtained with the 6-31G(d) basis set (single point calculations). Thermodynamic corrections were obtained using the 6-31G(d) basis set. Atom–atom overlap-weighted NAO bond order and natural atomic charges were calculated using the NBO method in Gaussian 98.[26]

5. Experimental

5.1. General

^{1}H and ^{13}C NMR spectra were recorded at 300 and 75.4 MHz, respectively, on Bruker instruments in $CDCl_3$ and referenced to the solvent unless specified otherwise. IR spectra were recorded using an ATI Mattson Genesis FT-IR by deposition of a thin film onto sodium chloride disks. HRMS analysis was performed at the Mass Spectrometry facilities of the University of Notre Dame. Elemental analysis was provided by Atlantic Microlab in Norcross, GA. Liquid chromatography separations were carried out on Silica Gel 60 (230–400 mesh). Bu_4NCN was purchased from Fluka.

5.1.1. *N*-Chloro-*N*,*N*′,*N*′-tris(ethoxycarbonyl)hydrazine (1b). *N*,*N*,*N*′-tris(ethoxycarbonyl)hydrazine (**2b**, 400 mg, 1.61 mmol) was dissolved in dry benzene (5 mL) and added to a stirred suspension of NaH (50 mg, 1.93 mmol) in dry benzene (2 mL). The mixture was cooled to 5°C and *t*-BuOCl (170 mg, 1.61 mmol, 170 μL) was added. Stirring continued for 1 h at 5°C, followed by 24 h at ambient temperature. The mixture was washed with water and dried (Na_2SO_4). Solvent was removed and the residue was separated on a silica gel column (eluent: CH_2Cl_2). Evaporation of the solvent gave 120 mg (27% yield) of a colorless oil: ^{1}H NMR δ 1.32 (t, J=7.1 Hz, 3H), 1.37 (t, J=7.1 Hz, 6H), 4.27 (q, J=7.1 Hz, 2H), 4.35 (q, J=7.2 Hz, 4H); ^{13}C NMR δ 14.0, 14.2, 64.7, 65.4, 150.3; IR ν_{max} 1776 cm^{-1}. Anal. Calcd for $C_9H_{15}ClN_2O_6$: C, 38.24; H, 5.35; N, 9.91. Found: C, 38.77; H, 5.40; N, 10.03.

5.1.2. *N*,*N*-Bis(ethoxycarbonyl)hydrazine (2a).[27] The hydrazine was obtained according to a general literature procedure in 88% yield.[27,28] ^{1}H NMR[29] (CD_2Cl_2) δ 1.31 (t, J=7.1 Hz, 6H), 4.25 (q, J=7.1 Hz, 4H), 4.30 (bs, 2H); (C_6D_6) δ 0.99 (t, J=7.1 Hz, 6H), 4.00 (q, J=7.1 Hz, 4H), 4.00 (bs, 2H); ^{13}C NMR (C_6D_6) δ 14.2, 63.2, 154.1; MS *m/e* 176 (M, 10), 76 (100).

5.1.3. *N*,*N*′,*N*′-Tris(ethoxycarbonyl)hydrazine (2b).[27] The hydrazine was obtained according to literature procedure[27] in 69% yield starting from **2a**. Alternatively, triester **2b** was prepared in 30% yield by ethoxycarbonylation of *N*,*N*′-bis(ethoxycarbonyl)hydrazine sodium salt (NaH) with ClCOOEt in THF, followed by chromatographic separation (eluent: CH_2Cl_2 followed by MeCN) of the

resulting mixture of starting material, byproduct **5** and product **2b**: ^{1}H NMR[29] δ 1.26 (t, J=7.1 Hz, 3H), 1.30 (t, J=7.1 Hz, 6H), 4.19 (q, J=7.0 Hz, 2H), 4.28 (q, J=7.1 Hz, 4H), 7.04 (bs, 1H); ^{13}C NMR ($CDCl_3$) δ 14.0, 14.3, 62.4, 64.1, 152.2, 155.2; MS *m/e* 249 (M+1, 1), 59 (100).

5.1.4. *N*-Cyano-*N*,*N'*,*N'*-tris(ethoxycarbonyl)hydrazine (4). *N*-Chloro-*N*,*N'*,*N'*-tris(ethoxycarbonyl)hydrazine (**1b**, 40 mg, 0.13 mmol) was dissolved in methylene chloride (2 mL) and the solution cooled to 0°C. Bu_4NCN (40 mg, 0.13 mmol) in methylene chloride (1 mL) was added dropwise and the stirring continued at the same temperature for 0.5 h, followed by 2 h at ambient temperature. The mixture was then washed with water, dried (Na_2SO_4) and passed through a short silica gel pad. The solvent was removed and the residue was separated on a silica gel column (eluent: CH_2Cl_2). Removal of the solvent gave 30 mg (86% yield) of the product as a colorless oil: ^{1}H NMR δ 1.32 (t, J=7.1 Hz, 3H), 1.38 (t, J=7.1 Hz, 6H), 4.32 (q, J=7.1 Hz, 2H), 4.39 (q, J=7.1 Hz, 4H); ^{13}C NMR δ 14.0, 64.2, 65.4, 66.6, 106.0, 149.4, 150.6; IR ν_{max} 2252, 1790 cm^{-1}. HRMS (FAB$^+$) *m/e* Calcd for $C_{10}H_{16}N_3O_6$: 274.1039. Found: 274.1026.

5.1.5. Tetrakis(ethoxycarbonyl)hydrazine (5).[27] ^{1}H NMR[30] δ 1.31 (t, J=7.1 Hz, 12H), 4.31 (q, J=7.1 Hz, 8H); ^{13}C NMR ($CDCl_3$) δ 14.0, 64.2, 150.5; MS *m/e* 321 ((M+1)$^+$, 3), 176 (100).

Acknowledgements

This project has been supported by DARPA/AFOSR F49620-98-1-0483.

References

1. Shustov, G. V.; Tavakalyan, N. B.; Kostyanovskii, R. G. *Tetrahedron* **1985**, *41*, 575–584.
2. Shustov, G. V.; Tavakalyan, N. B.; Kostyanovskii, R. G. *Izv. Akad. Nauk SSSR, Ser. Khim.* **1981**, 1677–1678.
3. Davies, J. W.; Malpass, J. R.; Moss, R. E. *Tetrahedron Lett.* **1985**, *26*, 4533–4536.
4. Buccigross, J. M.; Glover, S. A. *J. Chem. Soc., Perkin Trans. 2* **1995**, 595–603.
5. De Rosa, M.; Nieto, G. C.; Gago, F. F. *J. Org. Chem.* **1989**, *54*, 5347–5350.
6. Vassiliades, M. C. *Bull. Soc. Chim. Fr.* **1936**, *3*, 160–163.
7. Zimin, M. G.; Fomakhin, E. V.; Pudovik, A. N.; Zheleznova, L. V.; Gol'dfarb, E. I. *J. Gen. Chem. USSR* **1986**, *56*, 667–673.
8. Mizuta, M.; Katada, T.; Itoh, E.; Kato, S.; Miyagawa, K. *Synthesis* **1980**, 721–722.
9. Carmona, O.; Greenhouse, R.; Landeros, R.; Muchowski, J. M. *J. Org. Chem.* **1980**, *45*, 5336–5339.
10. Back, T. G.; Brunner, K. *J. Chem. Soc., Chem. Commun.* **1987**, 1233–1235.
11. Boberg, F.; Paetz, A.; Bruchmann, B.; Garming, A. *Phosphorus Sulfur* **1987**, *33*, 99–107.
12. Ketari, R.; Foucaud, A. *Synthesis* **1982**, 844–846.
13. Shtamburg, V. G.; Pleshkova, A. P.; Serdyuk, V. N.; Ivonin, S. P. *Russ. J. Org. Chem.* **1999**, *35*, 1549–1550.
14. Rudchenko, V. F.; Shevchenko, V. I.; Ignatov, S. M.; Kostyanovskii, R. G. *Bull. Acad. Sci. USSR, Div. Chem. Sci.* **1983**, 2174.
15. Shustov, G. V.; Starovoitov, V. V.; Kostyanovskii, R. G. *Bull. Acad. Sci. USSR, Div. Chem. Sci.* **1986**, 1096–1097.
16. Cottrell, S. C.; Abrams, C.; Swern, D. *Org. Prep. Proced. Int.* **1976**, *8*, 25–32.
17. Pfafferott, G.; Oberhammer, H.; Boggs, J. E. *J. Am. Chem. Soc.* **1985**, *107*, 2309–2313.
18. Roszak, A. W.; Brunner, K.; Back, T. G.; Codding, P. W. *Acta Crystallogr.* **1991**, *B47*, 383–389.
19. Suresh, C. H.; Koga, N. *Inorg. Chem.* **2000**, *39*, 3718–3721.
20. Hughes, T. V.; Hammond, S. D.; Cava, M. P. *J. Org. Chem.* **1998**, *63*, 401–402.
21. The presence of tetraester **5** in the reaction mixture can be accounted for by facile disproportionation of the triester **2b** in the presence of a base. Such a process was reported before for the potassium salt of **2b** anion (Ref. 27) and frequently observed in reactions involving hydrazine carboxylate esters e.g.: Ingold, C. K.; Weaver, S. D. *J. Chem. Soc.* **1925**, *127*, 378–387.
22. The unknown has the following spectral characteristics: ^{1}H NMR ($CDCl_3$) δ 1.26 (t, J=7.1 Hz, 3H), 1.29 (t, J=7.1 Hz, 3H), 4.17 (q, J=7.1 Hz, 2H), 4.28 (q, J=7.1 Hz, 2H), 6.47 (bs, 1H).
23. Frisch, M. J.; Trucks, G. W.; Schlegel, H. B.; Scuseria, G. E.; Robb, M. A.; Cheeseman, J. R.; Zakrzewski, V. G.; Montgomery, Jr., J. A.; Stratmann, R. E.; Burant, J. C.; Dapprich, S.; Millam, J. M.; Daniels, A. D.; Kudin, K. N.; Strain, M. C.; Farkas, O.; Tomasi, J.; Barone, V.; Cossi, M.; Cammi, R.; Mennucci, B.; Pomelli, C.; Adamo, C.; Clifford, S.; Ochterski, J.; Petersson, G. A.; Ayala, P. Y.; Cui, Q.; Morokuma, K.; Malick, D. K.; Rabuck, A. D.; Raghavachari, K.; Foresman, J. B.; Cioslowski, J.; Ortiz, J. V.; Baboul, A. G.; Stefanov, B. B.; Liu, G.; Liashenko, A.; Piskorz, P.; Komaromi, I.; Gomperts, R.; Martin, R. L.; Fox, D. J.; Keith, T.; Al-Laham, M. A.; Peng, C. Y.; Nanayakkara, A.; Challacombe, M.; Gill, P. M. W.; Johnson, B.; Chen, W.; Wong, M. W.; Andres, J. L.; Gonzalez, C.; Head-Gordon, M.; Replogle, E. S.; Pople, J. A. *Gaussian 98, Revision A.9*; Gaussian, Inc.: Pittsburgh PA, 1998.
24. Scott, A. P.; Radom, L. *J. Phys. Chem.* **1996**, *100*, 16502–16513.
25. Clark, T.; Chandrasekhar, J.; Spitznagel, G. W.; Schleyer, P. v. R. *J. Comput. Chem.* **1983**, *4*, 294–301.
26. Glendening, E. D.; Reed, A. E.; Carpenter, J. E.; Weinhold, F. NBO version 3.1.
27. Diels, O.; Borgwardt, E. *Chem. Ber.* **1920**, *53*, 150–158.
28. Milcent, R.; Guevrekian-Soghomoniantz, M.; Barbier, G. *J. Heterocycl. Chem.* **1986**, *23*, 1845–1848.
29. Previously reported by Seyferth, D.; Shih, H. *J. Org. Chem.* **1974**, *39*, 2329–2335.
30. Previously reported by Brunn, E.; Funke, E.; Gotthardt, H.; Huisgen, R. *Chem. Ber.* **1971**, *104*, 1562–1572.